Design and Analysis of Wireless Positioning System in an Indoor Environment and Its Application to Mobile Robot

(室内環境での無線測位システムの設計および解析と移動ロボットへの応用)

January, 2017

Doctor of Engineering

Abdul Halim Bin Ismail

アブドゥル　ハリム　ビン　イスマイル

Toyohashi University of Technology

Design and Analysis of Wireless Positioning System in an Indoor Environment and Its Application to Mobile Robot

(室内環境での無線測位システムの設計および解析と移動ロボットへの応用)

This dissertation is dedicated to my lovely family, who always stay by my side through ups and downs, and to my dear mother and my late father, al-fatihah.

اَللهُمَّ اغْفِرْلَهُمْ وَارْحَمْهُمْ وَعَافِهِمْ وَاعْفُ عَنْهُم

Masyitoh Yusoff
Aysar Muhaimin Abdul Halim
Affan Mustaqeem Abdul Halim

Acknowledgements

بِسۡمِ ٱللَّهِ ٱلرَّحۡمَٰنِ ٱلرَّحِيمِ

Syukur Alhamdulillah, I praised the Almighty Allah S.W.T for giving me the strength and agility to write this doctoral thesis. With His hidayah I am able to complete my studies here in Japan.

I am very lucky to have Prof. Kazuhiko Terashima as my doctoral supervisor. Terashima-sensei is not only a supervisor, but also a mentor, advisor, and even a father to me who always giving me continuous support of my research and care for me and my family in living abroad, for his patience, motivation, and immense knowledge. His guidance helped me in all the time of research and writing of this thesis. I could not have imagined having a better advisor and mentor other than Terashima-sensei.

I would like to thank the rest of my thesis committees: Prof. Hideyuki Uehara, Prof. Tetsuo Miyake, as well as Prof. Takanori Miyoshi for their insightful comments and encouragement, which incented me to widen my research from various perspectives. I am also indebted to Prof. Hideo Kitagawa, Asst. Prof. Ryosuke Tasaki, Asst. Prof. Ryo Saegusa as well as Asst. Prof. Yuichi Miyaji for their valuable suggestions for my researches.

I also would like to express my gratitude to the Ministry of Higher Education of Malaysia and Universiti Malaysia Perlis (UniMAP) for giving me financial support during my studentship here.

My sincere thanks also go to SYSCON laboratory member, Mr. Tatsuro Toyama, Mr. Yuki Mizushiri for helping me conducting the experiments for the mobile robot Terapio. And also to other SYSCON members Yamamoto-san, Yamashita-san, Ueno-san, Wisnu-san, Sago-san, Sakurai-san, Sato-san, Ho Duc Tho, Benjamin, Philips, Alex and all other members for being my good friends here. Special thanks go to my friend Mr. Atsushi Ito who always there to help since the first day we rolled into doctor course together.

It is a blessed to have friends with various languages, background, and cultures. We in SYSCON enjoyed many precious and joyful times both in our researches and lives.

My gratitude also goes to Ms. Toyama Masae and Ms. Sasaki for always assisting and handling my messy documents in attending conferences. Thank you for being patient whenever I had issues with the documents. I can never repay that.

Lastly, I am bestowed with wonderful family; my wife Masyitoh Yusoff and my two kids Aysar Muhaimin and Affan Mustaqeem, my mother and my in-laws family who always there by my side. Also to the Malaysian community at Toyohashi and Toyohashi Muslim Community for supporting me spiritually throughout writing this thesis and our life in general.

Thank you.

-Abdul Halim Ismail-
Toyohashi, Japan.
February 2017.

Design and Analysis of Wireless Positioning System in an Indoor Environment and Its Application to Mobile Robot

Abdul Halim Bin Ismail
System and Control Laboratory, Department of Mechanical Engineering,
Toyohashi University of Technology
Jan. 13th, 2017

Abstract

The wireless positioning system (WPS) has gaining respectful attentions in the recent years. There are promising applications of WPS especially in today's modern world where everything requires wireless connectivity. The information received from the wireless transmitter is not only useful for communication and networking, but also it can be manipulated for computing the whereabouts of the receiver i.e. the position of the receiver. A mobile robot for example could employ the WPS system for its localization algorithm. Since such systems use the information received from the outside sensing element, then the use of on-board sensing elements such as the exorbitant laser range finder (LRF) can be reduced. Therefore, the WPS system is cost effective.

The round robot Terapio development has been phenomenal especially in the medical industries where Terapio could greatly assist medical practitioners in their daily works. The functionality of Terapio is indeed plentiful including the human tracking and following, simultaneous localization and mapping system, power assists system, medical record databases, dynamic eye systems, patients monitoring system, etc. In order to increase the functionality of Terapio, this dissertation proposed to employ the WPS system for Terapio positioning which can reduce the development cost. In addition, the WPS system is also a convenient approach for Terapio mobility tracking.

This dissertation focuses on three parts for employing the WPS system. The 2.4GHz Wireless Fidelity (WiFi) signal were used in this work. WiFi signal is chosen due to the fact that the signal is ubiquitous i.e. available everywhere as well as cheap implementation. It is as a matter of fact suitable since its application could reduce the development cost of the mobile robot.

The first part of the research considers the optimal placement of the wireless transmitter that could yield in minimum positioning accuracy while maximizing the signal coverage. In order to achieve these objectives, an algorithm called the Grid Greedy Search Logic (GGLS) is proposed with the combination of Tree Hierarchy and the formulation of the cost function. The finding from this research suggests that the

placement of the wireless transmitter is not necessarily in symmetrical form when the initial placement location is taken into consideration.

The second part of this work is redirected into the assessment of WiFi signal using the Design of Experiment (DoE) method. Two essential parameters were studied i.e. the antenna heights of the transmitter and the separation distance between the transmitter and receiver (Tx-Rx). The hypothesis was made, and then the experiments were conducted in the manner of replicated randomization. The ANalysis Of Variance (ANOVA) results suggested that the antenna heights of the transmitter are not significant when fingerprinting technique is used for position estimation. This finding then is later validated using the actual positioning system using fingerprinting technique where the spatial signal fingerprint database is made and positioned using the state-of-the-art Weighted K-Nearest Neighbor (WKNN) positioning system.

The third part of this research is emphasizes on the WPS using the fingerprinting technique. Since the fingerprinting technique requires the signal fingerprint database which is rather costly to build, interpolation is proposed. Three interpolation methods are experimented, namely the Inverse Distance Weighting (IDW), the geo-spatial Kriging algorithm and the firstly ever used interpolation method for wireless signal; the Modified Shepard's Method (MSM). The finding from this experiment suggested that the proposed method i.e. MSM scored the lowest positioning error despite the popularity of Kriging algorithm as the wireless interpolation method. Subsequently, a novel method of wireless signal interpolation to automatically construct the fingerprinting database is proposed, known as the Signal Propagated Modified Shepard's Method (SP-MSM). This new technique considers the wireless signal properties such as the close-in distance and the path loss exponent. The signal properties were firstly estimate using the Euclidean simplex method and later included in the MSM interpolation algorithm. The accuracy is then evaluated defining four distinctive stationary locations. Afterwards, signal filtering using three different methods i.e. the Moving Average Digital Filter (MADF), Low Pass Filter (LPF) and Linear Kalman Filter (LKF) are used to improve the positioning accuracy by eliminating the noisy and fluctuative online WiFi signal. The Kalman filter as expected performs prominently improving the positioning accuracy. In addition, the comparisons of the different positioning techniques such as the trilateration are also discussed in the effort of improving the accuracy of the WPS system.

Finally, this dissertation is concluded and some future works are delineated. The WPS systems in the sense of the two frameworks were proposed for Terapio. The first framework is finding the optimal location to place the WiFi transmitters, and the second framework is the interpolation of WiFi signal to construct the fingerprinting database. The use of appropriate filter could yield in reasonable accuracy for indoor positioning system for a mobile robot application. In addition, the WPS architecture can be adapted into various other systems such as the multi-agents systems, the Internet-of-Thing (IoT) as well as cloud computing systems.

Table of Contents

List of Figures

List of Tables

Chapter 1 INTRODUCTION

"*The important thing is not to stop questioning. Curiosity has its own reason for existence.*"

- Albert Einstein, 1950s

Autonomous mobile robot is not a new thing. It is seventeen year since millennium passed and so, mobile robot is now almost 100 years old since it first coined by Karek Capek in his famous play of R.U.R Rossum's Universal Robot [1]. An earliest form of mobile robots was demonstrated by Grey Walter in 1950s, where two turtle-like mobile robots, code-named *Machina Speculatrix* were used for environment exploration [2][3]. These mobile robots, namely Elmer and Elsie, each had a light sensor, propulsion and steering motors, and two vacuum tubes analog computer. With this simple design, these mobile robots exhibited complex behavior and speculative tendency to explore nearby environments. Over time, humans are fascinated by mobile robots, and many forms of mobile robots were developed, demonstrated, and filmed. The recent exploration mobile robot, being autonomous and alone in planet Mars, the NASA's Mars exploration rovers [4] proved human capacity in developing mobile robots.

In general, mobile robots are built to benefit human being as a whole. That being said, mobile robots are developed in order to ease human daily affairs in many environments, in our case the hospital environments. In short, our laboratory has developed a medical assisting round-shaped mobile robot whose primary function is to assist medical practitioners and patients in a nursing ward. This mobile robot, has been given a name – Terapio – was developed since 2010 in System and Control Laboratory (SYSCON) at Toyohashi University of Technology, Japan [5][6]. Terapio have advanced technologies, such as omni-directional drives using the novel omniwheel called the Differential Drive Steering System (DDSS) [7][8], multiple laser range finder sensors (LRF), tactile and force sensors to name a few. Recently, Terapio has been featured in the children educational book on artificial intelligence where the main purposed is to introduce artificial intelligence application field to the youngsters [9].

In this thesis, the main works are to introduce the wireless positioning approach for Terapio. By employing such methods, the development cost of Terapio, or multiple Terapio in the future could be

decrease significantly since the use of costly sensors can be reduced while adding more functionality and capabilities to the mobile robot. The wireless positioning technique is also a convenient approach for Terapio mobility tracking and self-positioned system with reasonable accuracy.

1.1 Wireless Positioning System

The wireless positioning is known with many notations in multiple literatures due to inexistence of standard taxonomy such in Global Positioning System (GPS) [10]. It is often used interchange with notations such as Indoor Positioning System (IPS), Wireless Positioning System (WPS), Location-Based Service (LBS), Indoor Location Based Services (ILBS) among many others. However, they use common method in order to position or tracking an object [11], peoples [12][13], pervasive computing [14][15] , environmental monitoring [16][17][18], as well as mobile robots [19][20][21]. In this section, the overview of this system is introduced for general understanding.

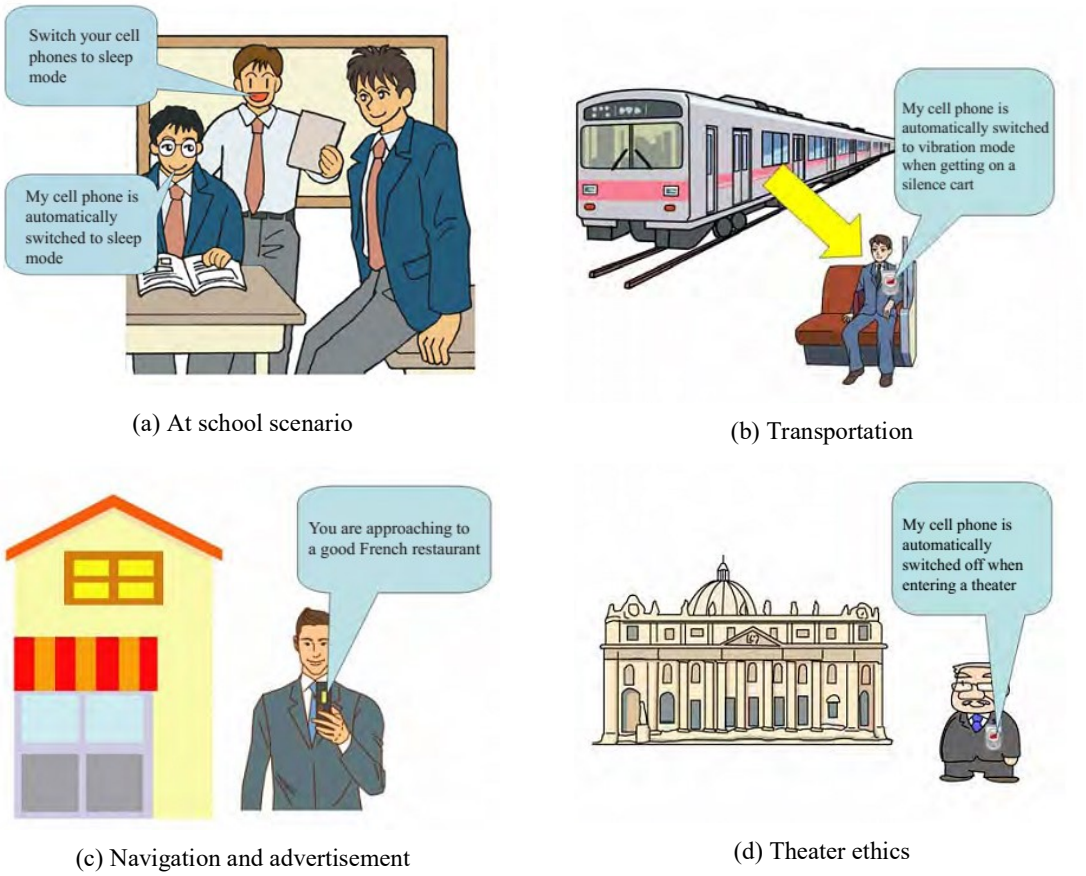

(a) At school scenario

(b) Transportation

(c) Navigation and advertisement

(d) Theater ethics

Figure 1.1: Example of WPS applications in working scenarios [22]

1.1.1 Overview

It is predicted that the market value of WPS system to be increased to over US$10 billion by the year 2020 [23]. The indoor location technology represents the next wave of opportunity in the location industry particularly in shopping and retails industries, infrastructural service, customer analytics, mobile advertising, local search, and hyperlocal offers [24][25]. There are also possible applications in major tourist attraction places such as museums, zoo and botanical gardens, and other related places. Figure 1.1 for example show applications of WPS in multiple scenarios [22]. In these applications, the mobility of a user detected by using the user's smartphone as sensor are tracked by the WPS, thus alerting the user location. In addition, such system also can be vigorous input to the location applications for other usage. Hence the conveniences. Albeit the easiness of applications, it is however still a long way before this kind of system became a standard such as in the GPS system.

It is known that the signals of GPS systems are practically non-usable in an indoor environment. This is due to the fact that the GPS signals from the satellites are attenuated and scattered by roofs, walls and other objects in the receiving space. Moreover, the error range of GPS system can be larger than the indoor space itself. Therefore, using GPS for indoor positioning system is nonetheless impractical. Since GPS and their standard cannot be used indoors, there is a need to find other means to provide solution for indoor positioning system. One attractive option is to use readily available wireless system utilizing microwave spectrum and the like such as Radio Frequency Identification (RFID), Bluetooth®, UWMB spectrum band and more popular Wireless Fidelity (WiFi) system. In this thesis, the commonly used 2.4GHz WiFi is chosen in order to design and develop the WPS for a mobile robot, or specifically Terapio.

1.1.2 General Methods in WPS

This section describes the general methods in WPS, which falls in two categories, the triangulation/trilateration technique and fingerprinting technique. WPS employing WiFi for example can be realized using these two techniques [26][27]. The more conventional technique, often known as triangulation or trilateration which both conveys difference meaning is an imitative concept of GPS system. The estimated position of the mobile robot is computed such as shown in Figure 1.2(a), normally known as Angle-of-Arrival (AoA) computation [28]. More related methods have been also revised, such as the Time-of-Arrival (ToA) [29], Time-Difference-of-Arrival (TDoA) [27][30] and many others. In this graphical example, the angle of receiving signal or receiving time is acknowledged by the mobile robot and also the locations of the transmitting devices such as WiFi Access Point (WiFi AP) are known. By relating these two parameters, the estimated location can be computed. However, this technique requires modification of the WiFi AP to transmit angular information and the time synchronization between the receiver and transmitter must in in

atomic level similar to the standard in the GPS system. Therefore, it can be tedious and requires expensive transmitter's modification.

Figure 1.2(b) on the other hand shows the WPS system employing the trilateration technique. The parameter that is normally required from the WiFi AP is their Received Signal Strength (RSS) in decibels (dB) or decibel meter (dBm). With the knowledge of the transmitting devices locations, the distance d_i of the mobile robot receiver can be estimated from signal propagation models. Later, geometrical computation in triangular form can be derived in order to estimate the final position of the mobile robot. However, accurate modeling of the signal propagations is too challenging to be developed due to the complex and unusual behavior of the wireless signal itself.

The third yet most popular method in WPS is known as fingerprinting technique [31][32]. This method in general works by matching an unknown signal to the signals recorded and stored earlier in the radio database. It typically operates on two stages; offline and online stage, depicted in Figure 1.3. In the offline stage, the wireless received signal strength (RSS) received from k number of WiFi Access Point is collected at n-th predefined locations over some required sampling period. This collected data can be stored in the form of a database tuple consisting of the information of the predefined locations and the RSS. Afterwards in the online stage, the RSS signal measured by the mobile robot at an unknown location will be match to those in the database. The matched signals will then return back in locations stored earlier.

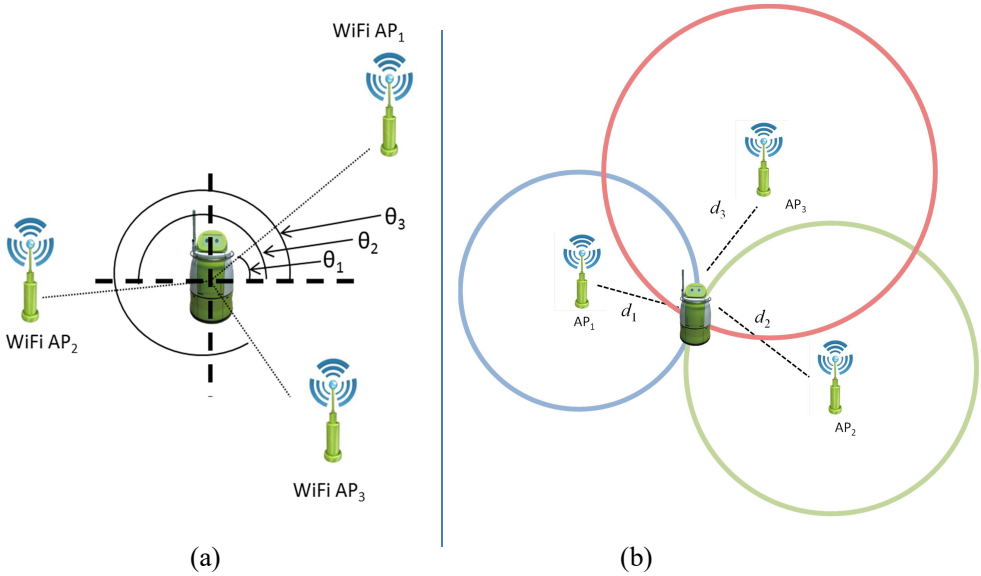

Figure 1.2: A positioning approach using (a) triangulation, and (b) trilateration technique

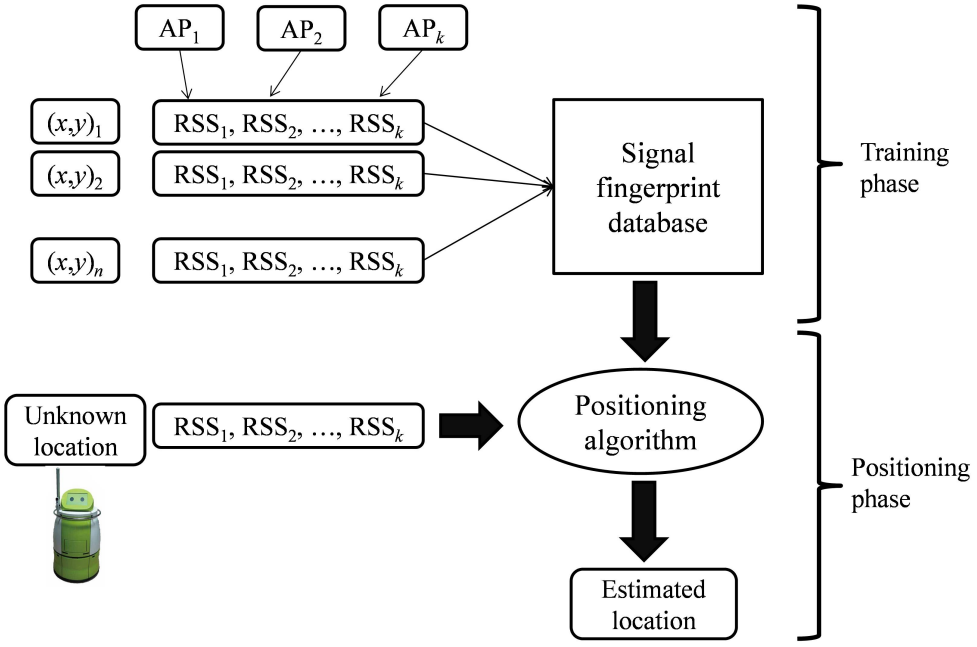

Figure 1.3: The WPS system utilizing fingerprinting technique

1.2 Research Motivation

The works in this research is originated by the round robot Terapio. Terapio is a special dedicated mobile robot developed by the team at Toyohashi University of Technology (TUT) with cooperation of Fukushima Medical University with the main task of assisting the healthcare services [5][6]. The first generation of Terapio is shown in Figure 1.4. It was green colored, round-shape, equipped with multiple sensors and functions. The core function of Terapio is an autonomous assistant for medical doctor and nurses while they were performing medical routine check of the warded patients. Terapio is also useful for the patients as therapy and rehabilitation robot, as well as a convenient mobile patient's database.

The development of Terapio has been particularly successful with many prospective medical industries have uttered their intentions to support Terapio. Terapio has been also praised as next-gen medical mobile robot by many organizations and corporations. As a matter of fact, Terapio has been premiered in numerous number of Japanese TV shows demonstrating its' usefulness.

In the recent years, there have been expectation that Terapio autonomous system can be extended into multi-agent systems (multiple Terapio) while reducing the development costs. Since the first generation of Terapio was developed as the research platform, then the development costs were indeed unquestionable.

Therefore, there is a need to adapt and extending Terapio functions into the multi-agent environment. In any cases, wireless system is more favorable for seamless communication between the agents (robots).

Therefore motivated by this factor, the initial step towards greater multi-agent system is anticipated. Considering the facts that there will be wireless system involve, with the aim to reducing the mobile robot development costs, the Wireless Positioning System (WPS) for the round robot Terapio is proposed. The wireless core in the WPS could be a framework for later multi-agent communication systems and also benefits in reducing the use of exorbitant sensors. In the current Terapio, a lot of costly sensors such as multiple laser range finders (LRF) were used in order to develop the Simultaneous Localization and Mapping (SLAM) algorithms. WPS on the other hand relies on the transmitting anchors in order to localize the robot position and the map is pre-defined in the mobile robot memory. Hence, the LRFs are least needed. Moreover, the tracking of the mobile robot can also be realized on the server level and monitored by human personnel for added security values.

Figure 1.4: The first generation of round robot Terapio and its conceptual usage by medical practitioners

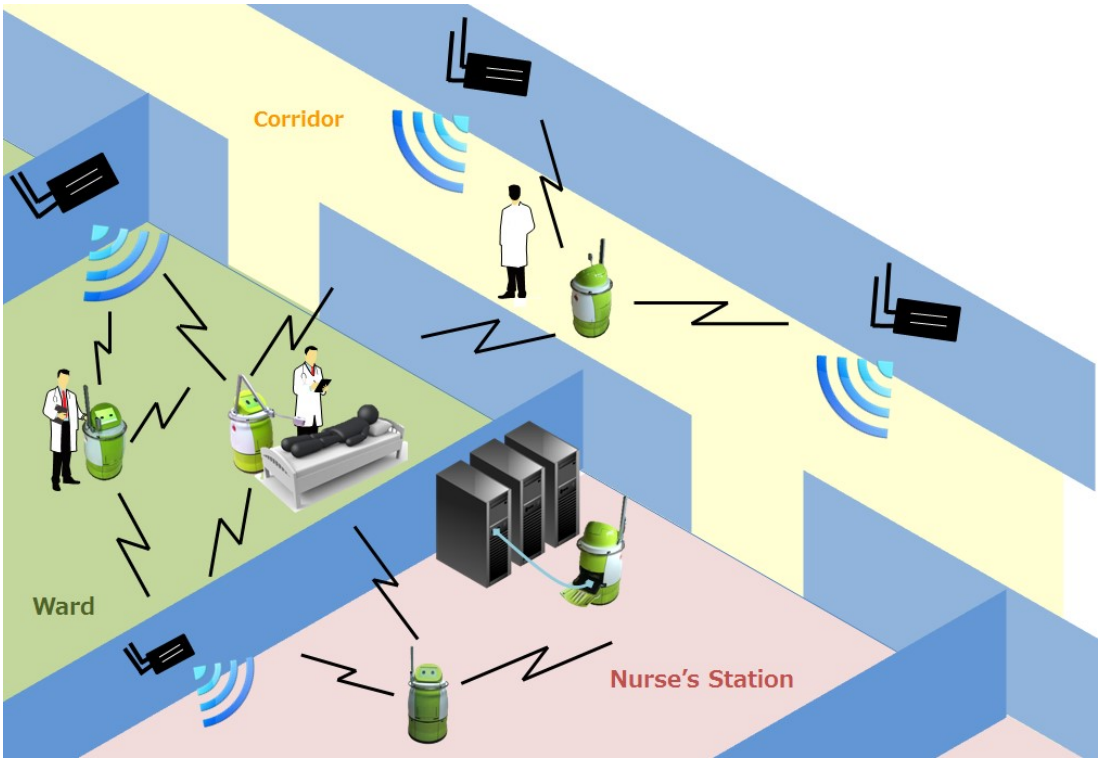

Figure 1.5: Concept and scenario of Wireless Positioning System for multiple Terapio in the warded hospital indoor environment

The conceptual application of WPS system employed by multiple round robots Terapio is depicted in Figure 1.5 as multi-agent systems. Ideally, all the mobile robots are connected to at least three WiFi APs in order to position itself in the environment. In the usual, Terapio were functioned as medical assistance mobile robots such as following medical practitioners while the other assisting in patient's treatment. By using the wireless positioning algorithm, each mobile robot could acknowledge its own location continuously as so the monitoring server, which mean an operator could always track the position of each agent (mobile robot). This matter will increase the security system of the environments. In addition, wireless system also offers seemless intra-communication between the mobile robots, with the promising perspective on master-slave control systems. Therefore, it can be stated that the WPS system is a convenience technique to be used especially in a known environment. Moreover, the system can be extended into cloud computing system, otherwise generally abbreviated as Internet-Of-Thing (IoT) or in the Ambient Intelligent field.

1.3 Problem Statement

In the outdoor environment, the localization or positioning of a mobile robot and human users are typically geo-localized by the global navigation satellite system (GNSS) since the 70s. GNSS provides geo-location and time information to a GPS receiver in all weather conditions, anywhere on or near the Earth where there is an unobstructed line of sight to four or more GPS satellites [33]. This system however, does not work very well in the indoor environment due to some issues.

The first issue is the Line-Of-Sight (LOS). The GPS system works accurately when the receiver has LOS with four or more GPS satellites from the sky. However, when the user going inside the building, then there is no direct line from the satellite to the receiver. The GPS signal weakens or distorts as it travels through the building to the receiver, resulting in inaccurate operation. The construction materials of buildings often are the major issues restricting the GPS signal inside the building. The GPS signal is badly absorbed by thick, solid materials such as brick, metal, stone or wood. Moreover, the GPS signal is also reflected by the shiny rooftop of the buildings.

In general, since GPS signal does not work in indoor environments, many researches resort to use the availability of indoor signals from indoor beacons to act similarly as GPS systems such as the ultrasound [34], FM radios [35], RFID [36], Bluetooth [37] and even overhead light [38] as reference inputs to the positioning system. The WiFi system has however attracted numerous researches since it is ubiquitous and the environment does not need any extensive modifications. Moreover, intensive and cheap WiFi-enable devices are readily available with the advance of the IEEE 802.11 standards. The range of applications using WiFi system is ever evolving such as the IoT and smart grids that signify the growing number of WiFi applications [39]. In fact, the IEEE has described that WiFi will be the pioneering sensing element for indoor environments where numerous big players such as Google Inc. and Apples Inc. are in the field [40].

The positioning using WiFi system was firstly introduced by Microsoft's RADAR team in the 2000s [31]. The focus of Wireless Positioning System (WPS) for mobile robot however is trending in this field where there is no exact focus of research direction. Moreover, the wireless signal propagation is heavily influences by the indoor environments arrangements and therefore, there is no generic solution as per GNSS system yet. For instance, the works in [41] discussed the experimental application of WiFi and ultrasound sensor which is a major difference as in [42] where the WiFi navigation system has been developed fusioning with odometry data. The research in [21] on the other hand presents the mobile robot SLAM in the Wireless Sensor Network (WSN) topology.

The WPS using WiFi system for mobile robot application also offers many open problems, such as the non-deterministic behavior of the wireless signal propagation, the effects of orientation of the mobile robot, detection of frontal obstacles, wireless noises and interferences and many other challenging problem.

Since there are countless open problems as well as the absence of mutual research focus, a particular research direction needed to be investigated. Hence, it can be summarize that the problem statement in this dissertation is to study, design and analyzed a suitable WPS architecture for mobile robot application specifically Terapio.

1.4 Research Aim, Objective and Scope of Works

The ultimate goal in this research is to develop a positioning algorithm for Terapio employing only the wireless signals that are available from transmitting wireless devices. Added function such as tracking and navigation system could be also achieved with the aid from digital compass and proximity sensors provided that developed positioning system are robust enough. Therefore, in order to achieved this aim, several objectives is delineated as per below;

(1) To develop an algorithm in order to find the most optimal locations for the wireless transmitting device placement such as the WiFi Access Point (AP),
(2) To find the suitable strategy for measurement of the WiFi signal, and lastly
(3) To develop a robust positioning algorithm, with minimum positioning error as much as possible.

In real world implementation, there are a lot of uncertainty involves, such as parametric and non-parametric uncertainties. To ensure this matter, a research scope must be resolute in order to conduct proper experiments. In this works, the scope of research is as follows;

(1) using the WiFi Receive Signal Strength (RSS) as the source data and system input,
(2) the system will assumed to be used at only the single-floor building, whereby the multi-floor building is not in the context in this works,
(3) the experimental area of the proposed WPS system is in 11×8.4 meter with the ceiling height at about 2.3 meter, and lastly,
(4) prior to use the system on the real Terapio, the experiments are firstly conducted using the mobile computer in order to measure the RSS from the WiFi AP.

1.5 Thesis Outline

The flow of this thesis is simplified and depicted in Figure 1.6. The brief overview of each chapter and the thesis is organized as following;

Chapter 1 has described the introduction of this thesis including the two general methods in the Wireless Positioning System as well as the research aims and objectives.

Chapter 2 on the other hand discusses about the wireless signal. The discussion includes the basic of wireless signal spectrum, the wireless signal properties and propagation mechanisms. Later topic will formulate the mathematical modeling of the wireless signal propagation starting with the most basic form of free space propagation, and empirical models such as the Log-Distance Path Loss model, Log-Normal Path Loss, Log-Normal Shadowing model and a discussion of the ITU-R P.1238 Multi Wall and Floor Model where the floor and wall obstruction are taken into consideration. A simple approach to calculate how many wall obstructed between the transmitter and receiver are also formulated in this section.

Chapter 3 illustrates the simulation works on finding the optimal location to install the WiFi Access Points (AP) in a given environment. The proposed algorithm is a modified version of the brute search algorithm called the Grid Greedy Logic Search (GGLS) and the combinatory of Tree Hierarchy searching method in order to satisfy the cost function. The resulting placement is compared with the conventional placement i.e. the symmetrical placement proposed by many literatures. This chapter also presents a method of digitization of the floor map blueprint using image processing technique.

On **Chapter 4**, the 2.4GHz WiFi signal is accessed and examined using the Design of Experiment (DoE) method. The WiFi signal assessment using DoE is the first in its category ever conducted around the globe. The measurement order is introduced and the resulting signals are hypothesized using ANalysis Of Variance (ANOVA) and later validated using the fingerprinting positioning technique.

The subsequent **Chapter 5** presents the WPS using the fingerprinting technique. The discussion start on the problem of signal fingerprints creation where tremendous amount of effort and time is required. Then the database interpolation is proposed to solve such problem. Several existing interpolation methods are employed such as the Inverse Distance Weighting (IDW), the geo-spatial Kriging algorithm and the proposed method using the Modified Shepard's Method (MSM). In addition, a novel method is afterwards proposed and developed using the integration of MSM and estimation of signal propagation model's parameter, namely the Signal-Propagated Modified Shepard's Method (SP-MSM). The positioning accuracies are evaluated at stationary test position in four different distinctive locations.

With the problem of unpredicted behavior of wireless signal even at stationary position, an improvement of such signal is required. This matter is emphasized on **Chapter 6**. The WiFi signal is filtered using methods such as the Moving Average Digital Filter (MADF), the Low Pass Filter (LPF) and Linear Kalman Filter (LKF) in order to improvise the positioning at stationary position. Afterward, the comparison between fingerprinting method and trilateration technique based on path loss model and empirical measurement fitting is also presented.

Chapter 7 draws the conclusion of this thesis that includes the academic and industrial contribution yielding from this works. The future perspectives with respect to this dissertation are also discussed in this chapter.

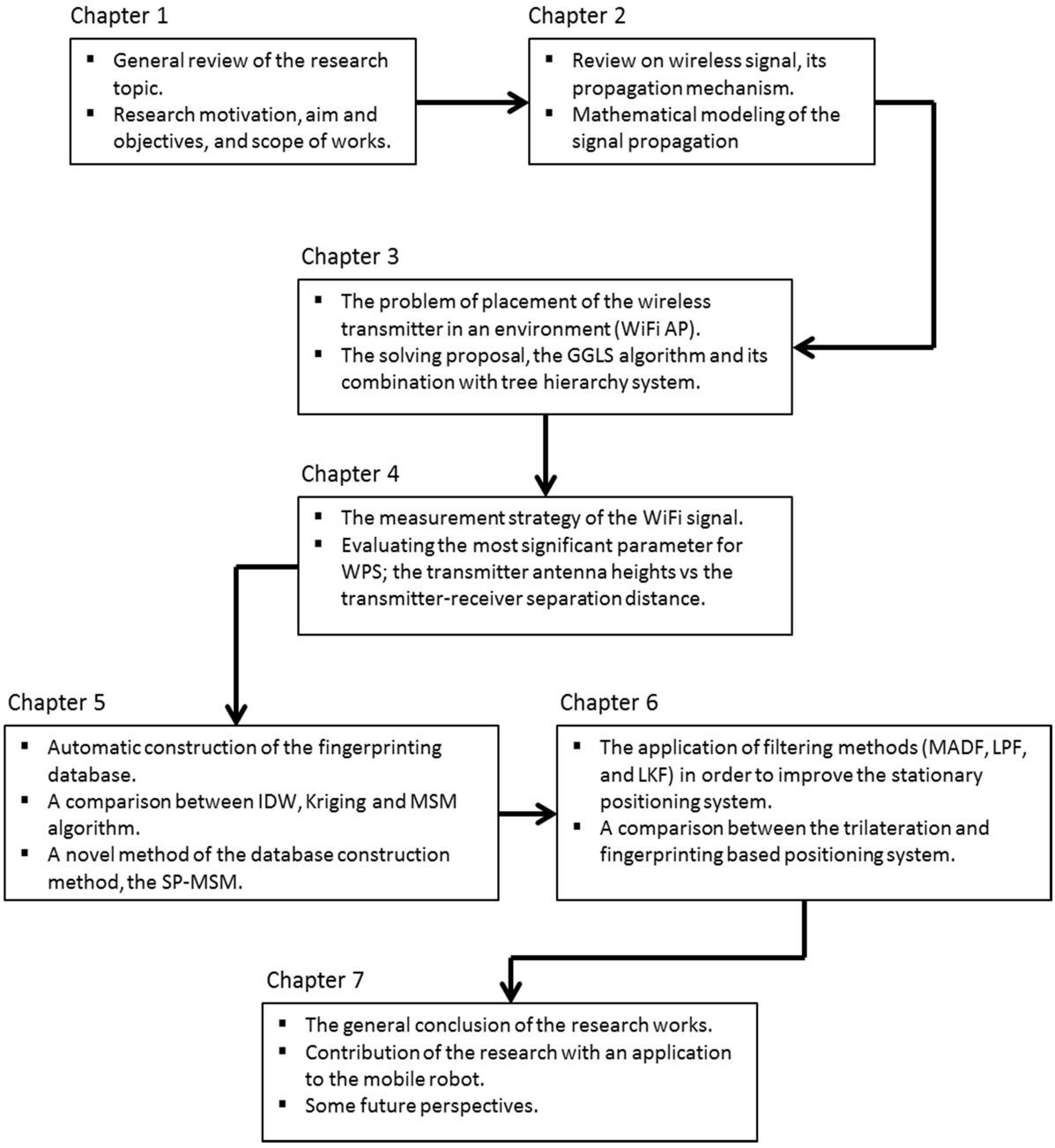

Figure 1.6: The flow of this doctoral dissertation

Chapter 2 WiFi SIGNAL PROPAGATION

"*Success is no accident. It is hard work, perseverance, learning, studying, sacrifice and most of all, love of what you are doing or learning to do*"

- Pele, 1980s

2.1 Introduction

It is essential to understand the characteristic of a wireless signal before digging into positioning details. Wireless signal can be regarded as one of human best creation in this technological world. Imagining a world without wireless solution is a total disaster; our spaces will be occupied with lots of wires here and there. Hence this chapter will describe the basic of wireless spectrum band, followed by the mechanism of wireless signal propagation and finally the mathematical modeling of the wireless signal propagation models.

2.2 Wireless Signal

Figure 2.1 shows the signal electromagnetic spectrum which are discovered by James Clerk Maxwell (1831–1879) and Heinrich Hertz (1857–1894). It is typically categorizes in six bands which are gamma rays, X-rays, ultraviolet (UV) rays, the visible spectrum that allows human to perceived colors, infrared (IR) spectrum, microwave and lastly radio spectrum. The signal frequency is inversely proportion to the signal wavelength accordingly to the Maxwell's $c = f\lambda$. The wireless signal that is normally used for communication and networking purpose is fall in the range of microwave and radio frequency spectrum.

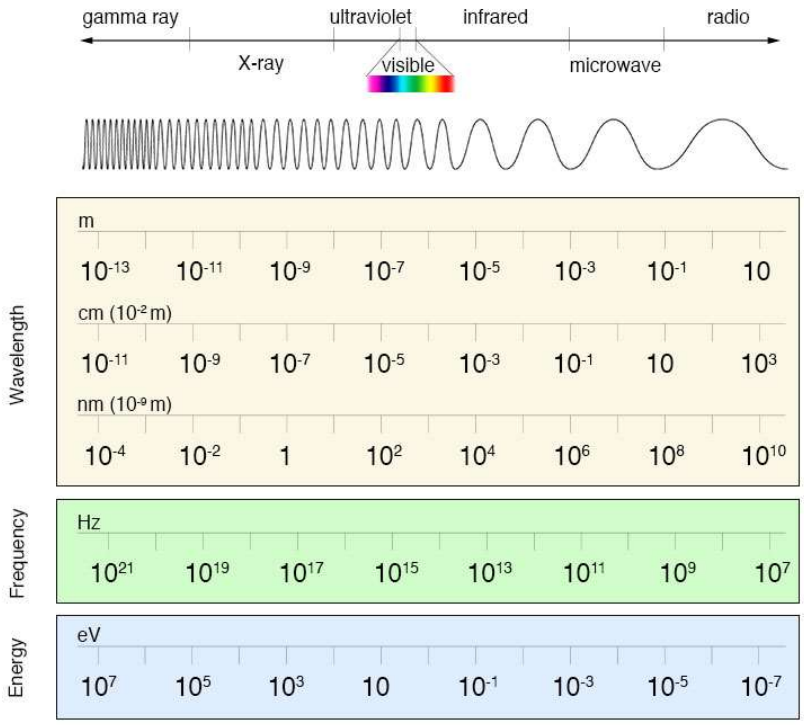

Figure 2.1: Conversion between wavelength, frequency and energy for the electromagnetic spectrum [43]

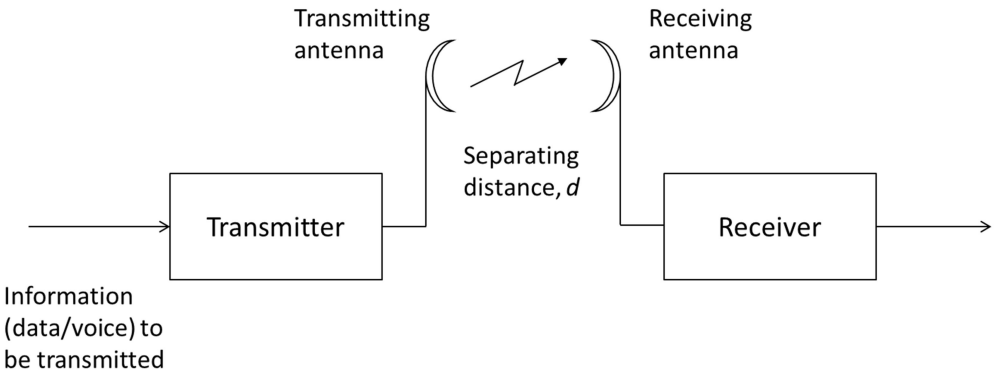

Figure 2.2: A typical wireless radio system

A typical wireless radio system architecture is shown in Figure 2.2. A radio system transmits information to the transmitting device source. The information is transmitted through an antenna which converts the radio frequency signal (RF) into an electromagnetic wave. The transmission medium for electromagnetic wave propagation in this context is the free air. Then, the electromagnetic wave is intercepted by the receiving antenna which converts it back to an RF signal. Ideally, this RF signal is the same as that originally generated by the transmitter. The original information is then demodulated back to its original form. When a straight line can be drawn connecting the transmitting antenna to the receiving antenna, this condition is known as Line-Of-Sight (LOS) scenario. In practice, the LOS condition is very hard to achieve for instance the medium is obstructed by multiple objects and boards, the presents of human between the transmitter and receiver, other interferences source and so on. However, the signal can still be detected by the receiver since the capability of electromagnetic wave to penetrate into living and non-living bodies. Such condition is normally attributes as Non Line-Of-Sight (NLOS) condition.

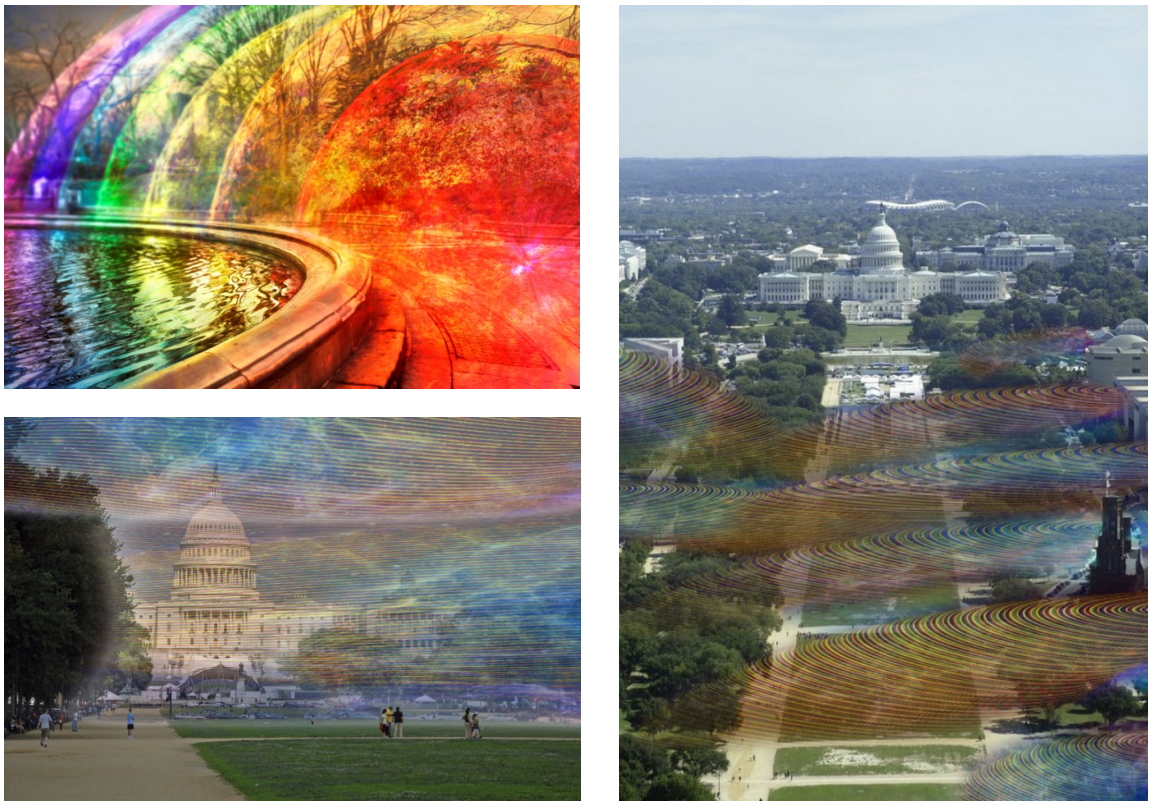

Figure 2.3: Artist illustrations - “if we can see WiFi” [44]

The IEEE 802.11 Wireless Fidelity (WiFi, or Wi-Fi for short) is operated in the 2.4GHz since it is one of the Industrial, Scientific and Medical (ISM) radio bands, which make it easier to certify the wireless equipment by legal organization such as the Federal Communications Commission (FCC) of the United States. It is also have long history of such bands in the sense of social and technical dimension, which can be refer in [45].

Wireless signal such as WiFi transmit over a certain distance caused by the complex integration of the signal propagation mechanism. The mechanisms made the wireless signal weak or fade over distances. Hence, the signal is strong when the receiver is close to the transmitting devices and vice versa if it is far away. Figure 2.3 illustrates the hobbyist graphic artists, Nickolay Lamn who try to imagines how WiFi looks if human could see them [44]. The artist portrayed vibrant color on the region near to the transmitting source and fading color when it is becoming further than the source. In any case, we have to realize that we are living in between of electromagnetic waves.

2.3 Wireless Signal Propagation and Mechanisms

The wireless signal travels in space when the connection between the transmitter and receiver is established. Such space or environment is also occupied by everything else. The space however is often dynamics caused by people walking around, the closing and opening of doors, windows, and even moving the furniture. Hence, the indoor radio signal can be especially difficult to model because of the dynamically changed environments. The wireless signal depends heavily on environmental factors which include building structure, layout of rooms, and the type of construction materials used. In order to understand the effects of these factors on electromagnetic wave propagation, it is necessary to understand the basic mechanisms of wireless signal propagation [46]. Figure 2.4 shows the illustration of the dominant signal propagation mechanisms as a physical encounter between the signal rays and the contact surfaces.

Reflection occurs when a wave impacts an object having larger dimensions than the wavelength. During reflection, part of the wave may be transmitted into the object with which the wave has collided. The remainder of the wave may be reflected back into the medium through which the wave was originally traveling. In the outdoor environment, the signal transmitted for example from the communication tower is reflected by many objects such as the surface of the earth, buildings and their walls. In an indoor environment, objects such as walls, floors, overhead ceiling and even furniture can cause reflection.

When the path between transmitter and receiver is obstructed by a surface with sharp irregularities oe edges, the transmitted waves undergo diffraction. Diffraction allows waves to bend around the obstacle even when there is no Line-Of-Sight (LOS) path between the transmitter and receiver. Diffraction relies heavily

on the geometry of the incident objects. Examples of objects that cause diffraction in an indoor environment include furniture and large appliances.

The third mechanism which contributes to electromagnetic wave propagation is scattering. Scattering occurs when the medium through which the wave travels consists of objects with dimensions that are small compared to the wavelength. It also happens where the number of obstacles per unit volume is larger. Scattered waves produced by rough surfaces, small objects as well as other irregularities in the channel. IN the outdoor environment, the signal are scattered by the means of foliage, street sign, lamp post, and even the trees and their leaves. On the other hand, the objects such as electronic appliances and room equipment i.e. computers, chairs and even the hair of walking person can cause scattering. As a consequence, modeling the signal propagation is indeed a challenging works due to the present of these three dominant mechanisms.

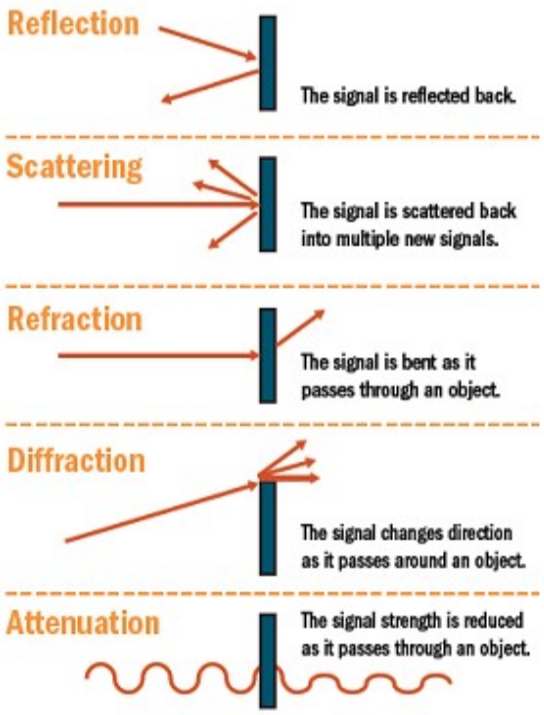

Figure 2.4: The illustration of the wireless signal propagation mechanism

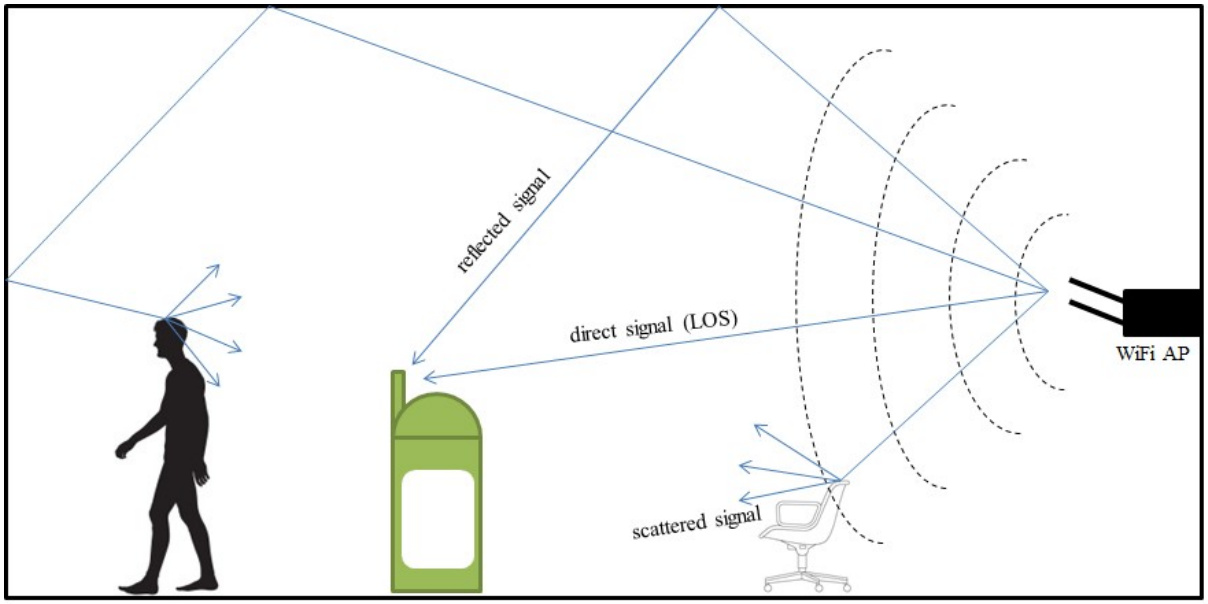

Figure 2.5: An illustration of multipath effect perceived by the mobile robot

The combined effects of reflection, diffraction, and scattering can cause multipath. Multipath results when the transmitted signal arrives at the receiver by more than one path. The multipath signal components combine at the receiver to form a distorted version of the transmitted waveform. The multipath components can combine constructively or destructively depending on phase variations of the component signals. The destructive combination of the multipath components can result in a severely attenuated received signal. Figure 2.5 illustrate the multipath effects as perceived by the mobile robot Terapio, where the LOS and NLOS are taking place by the combination of the reflection, scattering and diffraction mechanisms.

2.4 Signal Propagation Model

Modeling the wireless signal propagation, especially in an indoor environment has been a foremost topic in the communication engineering field. Over the years, numerous propagation models have been presented by the academia [47][48][49], standard organization [50] as well as industries [51][52][53]. However, still, there is no trivial model that is suitable for all environments. An empirical site-specific measurement is often the oblivious choice in order to obtain the most suitable model in the area of interest. In this section, several propagation models are presented.

2.4.1 Free Space Signal Propagation Model

The basic signal propagation model could be derived from the inverse power law function which stated that as the signal radiated from a source, the power is then dissipated inversely proportional to the square of distance travelled. If we assume the transmitter and receiver has a clear, unobstructed LOS between them, then the local area is given as $4\pi d^2$ with d being the distance from the transmitting source. Including the transmitter and receiver gain, the free space power received by a receiving antenna which separated from a radiating transmitting antenna by a distance d, is given by Friis [46] as in

$$P_r(d) = \frac{P_t G_t G_r \lambda^2}{(4\pi)^2 d^2 L}, \qquad \text{(Eq. 2-1)}$$

where P_r is the received power, P_t is the transmitted power, G_t and G_r are the transmitter and receiver gains respectively and L is the system loss factor not related to propagation ($L \geq 1$). The antenna gain is given by

$$G = \frac{4\pi A_e}{\lambda^2}, \qquad \text{(Eq. 2-2)}$$

where A_e is the effective aperture related to the size of antenna, and λ is related to the carrier frequency given by $c/f = 2\pi c/\omega_c$. For the WiFi signal, the communal frequency is 2.4GHz and c is the speed of light at approximately 3×10^8 ms^{-1}. However, it is perturbing to express the received power in such terms since the value is literally small. Instead, expressing them in *path loss* is much more feasible. Path loss represents the signal attenuation as a positive quantity measured in decibels between the transmitted powers over received power. Then (Eq. 2-1) becomes

$$\mathrm{PL(dB)} = 10\log_{10}\frac{P_t}{P_r} = -10\log_{10}\left[\frac{G_t G_r \lambda^2}{(4\pi)^2 d^2}\right] \qquad \text{(Eq. 2-3)}$$

Table 2.1: The relation between constant η and path loss units

η	Unit of f	Unit of d
- 147.55	Hertz	Meter
- 87.55	Kilohertz	Meter
- 27.55	Megahertz	Meter
32.45	Megahertz	Kilometer
92.45	Gigahertz	Kilometer

Assuming antennae unity gains of the transmitter and receiver, a convenient way to express the free space path loss model has been derived in [54] which is useful for the known units of *f* and *d*. This familiar expression is given in

$$\mathrm{PL(dB)} = 20\log_{10}(d) + 20\log_{10}(f) + \eta\,, \qquad \text{(Eq. 2-4)}$$

where the constant η is dependable to the units of carrier frequency *f* and separation distance *d*. The constant η value is tabulated in Table 2.1. In addition, this form of free space signal propagation model is the foundation model in many advances model describe in many literatures.

2.4.2 Log-Distance Path Loss Model

The free space path loss (FSPL) model is not practical to be used in real world applications since in 'free space' did not exist. FSPL however can be relatively useful when dealing with LOS condition, but most of the time it is not. Therefore, other realistic model must be sought. The empirical modeling of the signal propagation by fitting the measurement curve is an interesting modeling technique. Rappaport described many empirical modeling as practical link budget designs [46]. Since both theoretical and measurement-based models indicate that the average received signal power decreases logarithmically with distance, the average path loss for an arbitrary transmitter-receiver separation can then be expressed as a function of distance using the path loss exponent *n*, stated in

$$\overline{\mathrm{PL}}(d) \propto \left(\frac{d}{d_0}\right)^n \qquad \text{(Eq. 2-5)}$$

, where d_0 represent the arbitrary close-in reference distance, for instance the close-in reference distance for a 2.4 GHz WiFi signal is at 1 meter radius. The data is empirical where manufacturers do not provide them, and therefore it is normally obtained by experiments and measurements. Similarly as FSPL, logarithmic function can be used to simplify (Eq. 2-5), which now becomes

$$\overline{\mathrm{PL}}\,(\mathrm{dB}) = \overline{PL}(d_0) + 10\log_{10} n\left[\frac{d}{d_0}\right] \qquad \text{(Eq. 2-6)}$$

Table 2.2 shows the suggested value of the path loss exponent *n* in the different environments as suggested by [46]. Higher value of path loss exponent means that the larger signal is lost, usually in more cluttered and highly obstructed environments.

Table 2.2: Path loss component for different environments suggested by [46]

Environment	Path loss exponent, *n*
Free Space	2
Urban area cellular radio	2.7 to 3.5
Shadowed urban cellular radio	3 to 5
In building line-of-sight	1.6 to 1.8
Obstructed in building	4 to 6
Obstructed in factories	2 to 3

2.4.3 Log-Normal Shadowing Model

The large-scale variations of the wireless signal caused by shadowing of obstacle follow a log-normal distribution, which practically means that the measurements are in Gaussian distribution. It is also due to the fact that the cluttered environment may be vastly different at two different locations having the same Tx-Rx separation. Consequently shadowing effects are usually incorporated into path loss estimates by the addition of a *zero-mean* Gaussian random variable, with standard deviation σ: $N(0,\sigma)$, where σ is often estimated empirically by measurements.

Measurement shown that at any value d having PL(d) at a particular location, is random and distributed log-normally. Therefore, the generic equation of the Log-Normal Shadowing (LNS) path loss model is given as (Eq. 2-7),

$$PL(d)[dB] = \overline{PL}(d) + X_\sigma = \overline{PL}(d_0) + 10\log n\left[\frac{d}{d_0}\right] + X_\sigma \qquad \text{(Eq. 2-7)}$$

, where X_σ is the *zero-mean* Gaussian distributed random variable with the standard deviation of σ. Figure 2.6 shows the graphical meaning of (Eq. 2-7).

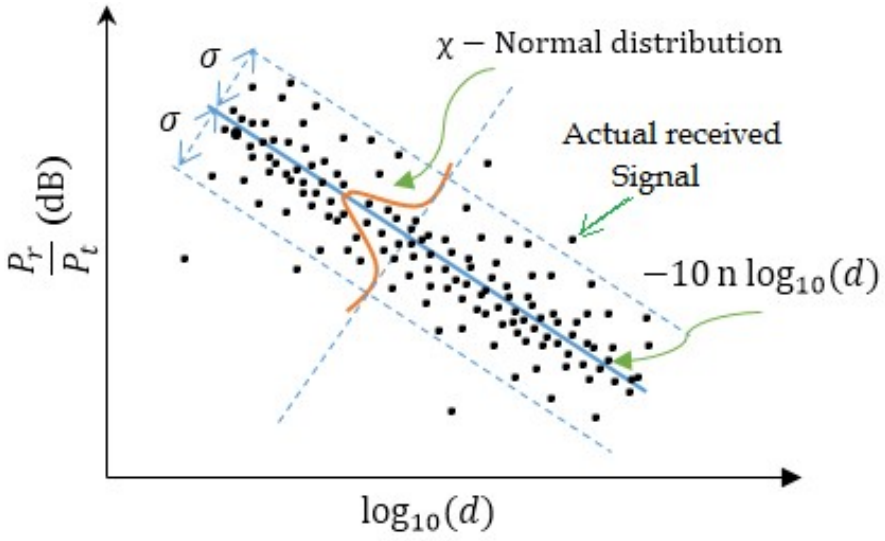

Figure 2.6: A graphical meaning of LNS path loss model [55]

2.4.4 ITU-R P.1238 Multi Wall and Floor Model

The previous models were empirical with unobstructed LOS, therefore the effects of wall and floor absorption are not taken into account. Thus, the coverage simulation may respond in a circular pattern, which is not realistic. The Multi Wall and Floor model (MWF) described in [49] with the aid of the documentation of the European ITU-R P.1238 [50] are used in this dissertation. This model is chosen since it considers the empirical relation of the signal with the addition of loss factors relating to the number of traversed floors and walls. The MWF model is given as (Eq. 2-8),

$$\mathrm{PL(dB)} = L_0 + 10n\log_{10}(d) + \sum_{i=1}^{I}\sum_{k=1}^{K_{wi}} L_{wik} + \sum_{j=1}^{J}\sum_{k=1}^{K_{fj}} L_{fjk} \qquad \text{(Eq. 2-8)}$$

, where

L_0 = path loss at d_0
n = power loss index
d = distance between transmitter and receiver
L_{wik} = attenuation due to wall type i and k-th traversed wall
L_{fjk} = attenuation due to floor type j and k-th traversed wall
I = number of wall types
J = number of floor types
K_{wi} = number of traversed walls of category i
K_{fj} = number of traversed floors of category j

As explained in [50], similarly with (Eq. 2-8), the number of wall and floor traverses by the signal is required in order to compute how much of the signal losses. For example, given the signal ray transmitted from point A and the receiver is at point B, and the wall is drawn from point C to point D, we would like to inspect whether the signal ray AB crossed the wall CD. This problem can be simplified as 'does a ray segment cross a line segment'.

A conventional approach to solve this matter is by using the intersection between the two. Two linear equations can be solving simultaneously to inspect the intersections. It is however slightly cumbersome if more than two drawn walls are between the signal rays. Therefore, a simple mathematical method based on rotational is developed to solve this problem elegantly.

A formal definition is as follows,

If we have an AB ray, we could check either the AB ray crossing a CD wall by using condition,

$$\mathrm{ccw(ABC)} \neq \mathrm{ccw(ABD)} \wedge \mathrm{ccw(ACD)} \neq \mathrm{ccw(BCD)},$$

for which ccw(ABC) represents the counter-clock-wise turning of a ABC triangular, similarly for ACD triangular. If both side are *true*, then the ray AB crossed the wall CD and vice versa. ABC is ccw if the slope of AB is smaller than the slope of AC, shown as

$$\mathrm{ccw(ABC)} = (\mathrm{C}_y - \mathrm{A}_y)(\mathrm{B}_x - \mathrm{A}_x) > (\mathrm{B}_y - \mathrm{A}_y)(\mathrm{C}_x - \mathrm{A}_x)$$

, where ABC have an individual Cartesian coordinates at (x,y).

2.5 Summary

In this chapter, a brief discussion on the wireless signal specifically the IEEE 802.11 WiFi signal characteristic and modeling is presented. The wireless signal is strong when the receiver is close with the transmitting source, and fades over distances corresponding to the fading effects.

The complex propagation of the wireless signal is dominantly caused by the reflection, diffraction and scattering mechanisms of the signal. In addition, other affecting mechanisms such as the refraction and attenuation are also contributes to the signal losses. The combination of the mechanisms yielding in the multipath effects where the receiver obtains the signal from several paths, at the same and different time stamp. It can be destructive or constructive or destructively interrupt the original signal transmission.

Despite the conveniences of using the WiFi signal, modeling them is not. In this chapter, the fundamental model known as the free space path loss model is introduced, along with the empirical models such as the log-distance path loss and log-normal shadowing model. In addition, while considering the obstruction factors such as the walls and floors, the MWF model is choose in this works, with the variables adapted from the European ITU-R P.1238 model. Since wall crossing detection is an important parameter, then a simple yet elegant mathematical solution is developed using the rotational i.e. the counter-clock-wise (ccw) method. This solution is convenience since solving multiple linear equations can be avoided.

Chapter 3 OPTIMIZATION OF WiFi ACCESS POINT PLACEMENT

"*There are many ways of going forward, but only one way of standing still*"

- Franklin D. Roosevelt, 1930s

3.1 Introduction

The works on finding the optimal location to install the wireless transmitters is the initial research in this thesis. It is crucial part of the research in order to ensure that the mobile robot is receiving enough signals from respective access points. While the main focus is for mobile robot application field, it is also extensible to communication engineering field such as for information technology work personnel i.e. to install the WiFi access point at their most optimal locations where maximum coverage are guaranteed.

3.2 Problem Statements

In today's modern society, the wireless signal typically the IEEE 802.11 Wireless Fidelity (WiFi) operating at nominal 2.4 GHz bands is nearly ubiquitous i.e. the WiFi signal is available almost everywhere [56]. This wireless signals are commonly transmitted by dedicated transmitting devices (transmitter) for instance the WiFi Access Point (AP). Usually, these WiFi APs were placed at locations to benefit human users in the area of interests. Notably, the WiFi APs were deployed in close proximity either in carefully managed environments or in an unplanned or unmanaged scenario [57][58]. As a matter of fact, such deployment of the WiFi APs placements for positioning system has never been of concerns. Hence, many of resulting positioning errors were debatable. Motivated by this problem, this research take initiatives to develop an algorithm which could yield in optimal locations to install the WiFi APS while maximizing the wireless signal coverage and minimizing the positioning error especially for positioning using fingerprinting approach. The details on fingerprinting methodology can be found in later Section 5.2. In this works, a new

technique is proposed in order to find the optimum location to place the WiFi AP that not only maximizes the need of total wireless connectivity for human use, but is also suitable for mobile robot fingerprinting database in an indoor environment. The proposed technique is much more generic and does not need deployment patterns. It can be also be said that this work is the work of killing two birds with one stone [56].

A formal definition is as follows;

Given a bounded spatial area of *MN*, it can be divided equally at *q* spacing, horizontally and vertically. The intersections of these grids can be nominated as candidates for placement locations. Then the discretized *MN* area with a set of location nodes *W* is obtained, as well as a set of *N* number of placement candidates. With signal coverage relative to the square distance *D* according to the inverse power law in meters, as well as the positioning accuracy of *Le*, the optimal placement of wireless nodes is to find a deployment *R* of a set of wireless nodes *N* of relative distance *D*, such that it's;

(i). guaranteed full coverage,
(ii). minimum number of *N*, and
(iii). minimum localization error.

The goal of this problem is to place *N* as minimum as possible (condition ii) that also maximizes the signal coverage for the end user (condition i) while achieving relatively satisfactory mobile robot positioning accuracy (condition iii). For each possible placement $j \in N$, the coverage could compute using the signal propagation models described in previous chapter. To ease the computation, the binary variable y_j is defined as the coverage output matrix. At any location on the map i.e. P_{mn}, the binary variable $y_j = 1$ if the signal is detected from the AP *k* and 0 if vice versa.

The core objective of this works is illustrated in Figure 3.1. In this case, the placement should be able to provide sufficient measurement data, such as the WiFi received signal strength (RSS), to a mobile robot so that accurate positioning can be computed. In this figure, we could observe that at the specific location, the mobile robot should receive strong signal from AP_1, moderate signal from AP_2, perceivable signal from AP_3 and perhaps no signal at all from AP_4. Moreover, the placement should also guarantee that all area in the particular indoor environments receive reasonable signal for human users.

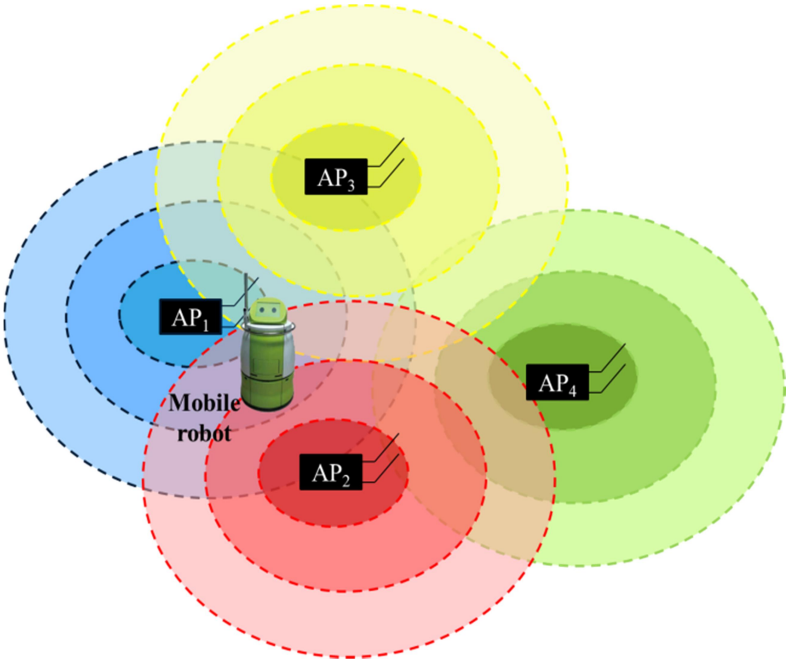

Figure 3.1: The placement objective so that the particular arrangement could provide enough signal data to the mobile robot

3.3 Related Works

Finding the placement strategy of the wireless access point has recently begun with the concern in improving the positioning accuracy. It is in fact many placement algorithms has been published in the last decades, especially with the successful wireless positioning pioneering works by Microsoft's RADAR [31]. However, the problem remains non-trivial, where each solution does not hold for others. Hence, there is necessity to develop owns' method.

The impact of positioning accuracy with respect to different APs placement strategy has been investigated in [59] and serve as deployment benchmark in many literatures. In this study, six principle configurations of the WiFi AP placements were suggested that could be deployed in a sample floor building. These six configurations consider different number of APs as well as different location of AP placement, as depicted in Figure 3.2. At the end, the researchers suggested that the symmetrical placement such as those in *Configuration 5* is a better choice for positioning system.

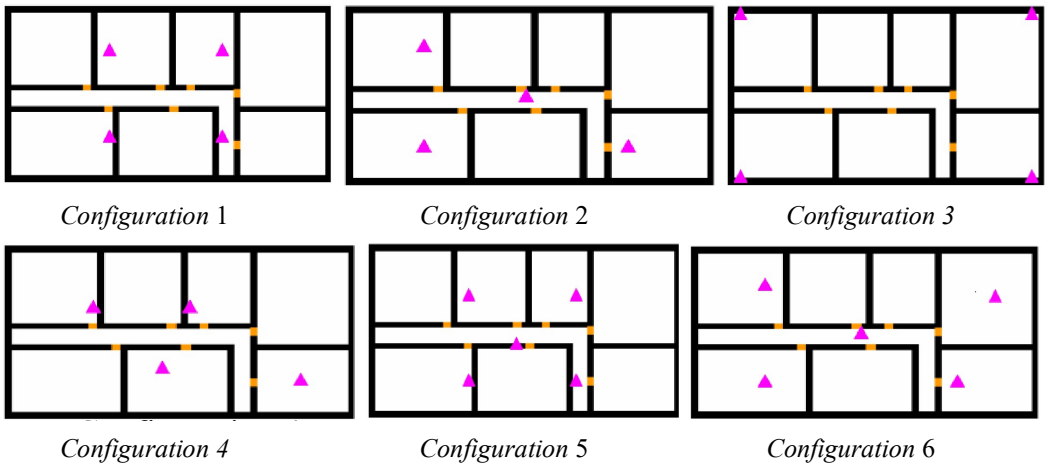

Figure 3.2: Six WiFi AP placement configuration by [59]

The theory of symmetrical placements were further investigated in [60][61]. Several deployment patterns such as equilateral triangle, square of 4 APs, square of 4 APs plus one center of mass and several more nested propositions are presented in [60]. This research works tried to fit the said deployments patterns onto a floor map and observed the results from trilateration positioning point of view. The works examined the signal coverage by means of Linear Least Squares (LLS). The LLS algorithms try to find which deployments patterns suit to an environment. The findings of this works proved that the symmetrical placements yield the maximum coverage on a floor in the cost of negative impact on the positioning performance. Hence, a work through of equal trade between the two is necessary. In [61], the investigation of the symmetrical placement is further investigated. The research works compared the square and cross deployments patterns with the method of maximizing the Signal-to-Noise Ratio (SNR) algorithm. Actual experiments using WKNN fingerprinting method were used, and proposed algorithm scored loosely with the symmetrical placements.

The WiFi AP placement optimization is also a discussion topic in [62] where the Differential Evolution (DE) function is proposed to solve an optimization function. The optimization function was formulated using the wireless signal propagation models namely the log-normal shadowing, where maximization is the cost function given in

$$
\begin{aligned}
&\text{Maximize}: f = \sum_{i=1}^{N} \sum_{j \in D_i} r_{ij} \\
&\qquad D_i = \{ j \mid \text{distance}(i, j) \le d \} \\
&\qquad r_{ij} = \sqrt{\sum_{k=1}^{M} [rss_i(k) - rss_j(k)]} \\
&rss_i(k) = p_0 - 10 \cdot n \cdot \log\left(\sqrt{(px_i - x_k)^2 - (py_i - y_k)^2} \right) \\
&\qquad \text{Subject to}: (x_k, y_k) \in S
\end{aligned}
\qquad \text{(Eq. 3-1)}
$$

, where the parameter rss_i is the Euclidean-inspired signal model. The details of other variables can be found in [62]. This optimization method i.e. the differential evolution is an iterative computation where hefty amount of computing time and metaheuristic measure such as the RSS is considered. The final results of the placement yield by the DE algorithm are remarkably improved compared to usual placements. It is however, since DE requires a lot of time and measurement data, only a small numbers of sampling points were taken in their experiments. Therefore, generality can be debated.

A Simulated Annealing (SA) algorithm is proposed in [63][64] in order to optimize the WLAN access point placement for indoor positioning system. These researchers employed the trilateration positioning system, thus the main requirement of SA is to keep at least three access point in the area of interest. A tree-graph is modeled with respect to the territory map with the area size of 106×102 meter. Then the SA algorithm try to find the tree branch that has the longest path. However, finding the longest path is the classical problem in NP-complete problem where multiple solutions can be found [65]. Therefore, each iterative will result in different solutions.

3.4 Map Digitization

The floor map blueprint is usually desired in order to understand the architecture as well as the environments for instance the location of the walls, windows, doors etc. It is also importance for the mobile robot application where the spatial location of the fingerprinting data is stored. However, the map blueprint is always in printed hardcopy. Therefore, the printed hardcopy is needed to be scan and digitized. This section describes the simple method that is used to digitize the floor map blueprint.

A typical floor map blueprint such as the 2nd floor of Center for Human-Robot Symbiosis Research at Toyohashi University of Technology (TUT) is depicted in Appendix A. It is usually enclosed with highly cluttered background and unnecessary information for placement purposed. For further works in this dissertation, a clean-up version of such map is required. Therefore, a simple image processing method, the

color overlay technique is used in order to digitize this map. The image processing methodology is illustrated in the flowchart shown in Figure 3.3. The original image of the scanned blueprint is manually overlayed with respective color for instance red color for the walls, blue for the doors and so on. Figure 3.4 shows an example of color overlayed onto the floor map blueprint.

When the floor map blueprint has been overlayed by the selective colors, the 'luminance' component of the image can be computed, pixel by pixel, using the generalized color conversion equation given as

$$L(i,j) = \begin{bmatrix} 0.2989 & 0.5870 & 0.1140 \end{bmatrix} \times \begin{bmatrix} R(i,j) \\ G(i,j) \\ B(i,j) \end{bmatrix}, \qquad \text{(Eq. 3-2)}$$

where $L(i,j)$ represent the luminance component and $R(i,j)$, $G(i,j)$ and $B(i,j)$ are the red, green and blue components of the image at pixel (i,j). Afterwards, the image subtraction is made correspondingly to the colors associated in the earlier overlayed. The subtraction equations are given as

$$\begin{aligned} Walls &= R(i,j) - L(i,j) \\ Doors &= B(i,j) - L(i,j) \end{aligned}. \qquad \text{(Eq. 3-3)}$$

The masking binary matrix, in this case the 5×5 matrixes are chosen in order to extract the information of the resulting images. The matrixes in the form of vertical, horizontal, and diagonal are used to identify the location of the walls and doors before normalizing them into the spatial Cartesian coordinates for later works. Figure 3.5 shows the final resulting image where the walls and doors location were identified and the angle associated with them area assigned, i.e. 0° and 90° correspondingly.

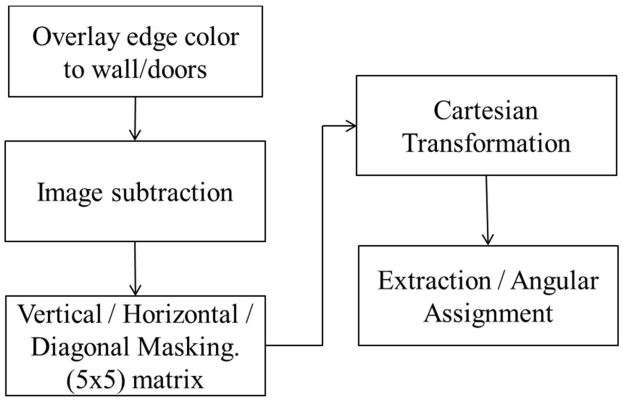

Figure 3.3: The flowchart of image processing method used for floor map digitization

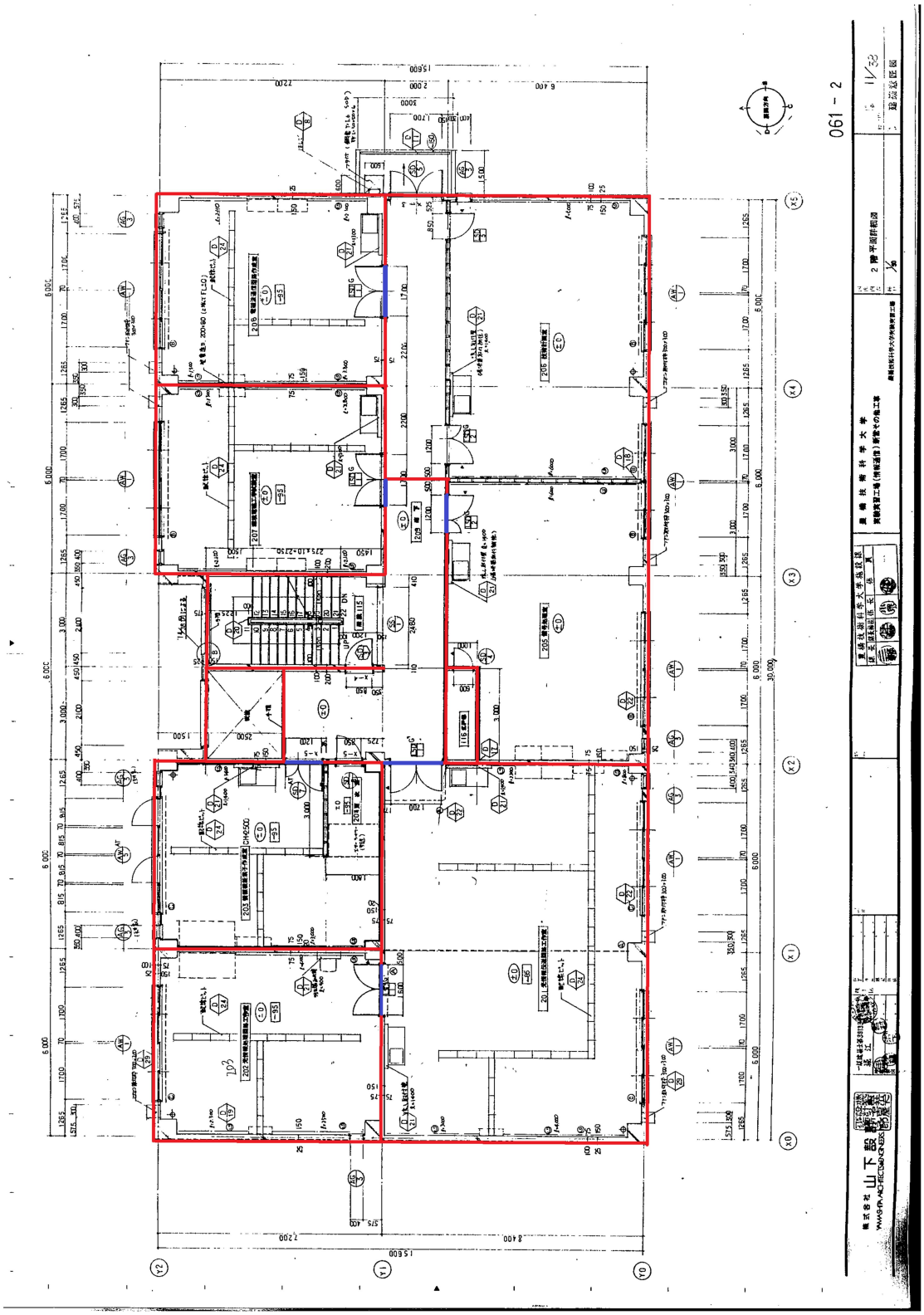

Figure 3.4: Color overlayed on the floor map blueprint

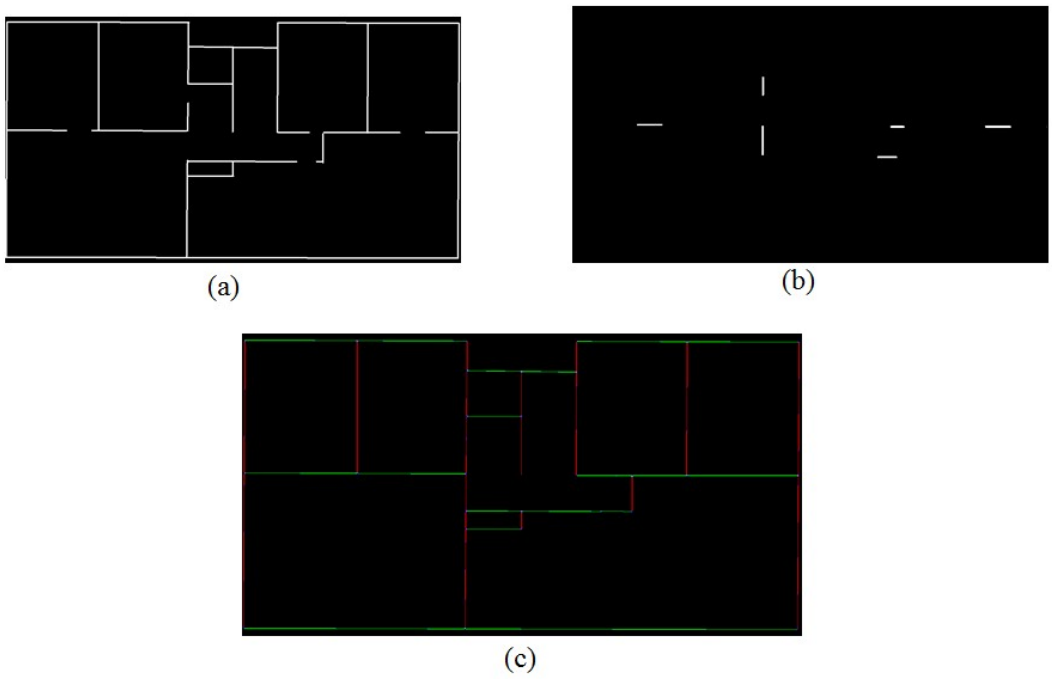

Figure 3.5: Floor map digitization results, (a) identification of walls, (b) identification of doors, and (c) overall detection with angular assignment to the walls and doors

As a summary, a simple yet effective image processing method is proposed in order to digitize the floor map blueprint into computer memory. It is crucial part in this research where the information about the map are known and identified.

3.5 Proposed Methods

Optimization of the wireless nodes placements is necessary to guarantee the signal coverage for human users as well as minimizing the positioning error for the mobile robot. Initially, the floor map which resulting from the image processing is divided into several grids where each intersection of the grids can be nominated as the placement candidate. Assuming a 30×16 meter area, then there are about 480 candidates of placement if 1 meter granularity spacing is taken into consideration. A smaller granularity however is often needed to increase the accuracy [66]. Therefore, using the usual brute search algorithm is a challenging method. Hence, a modified brute search algorithm is proposed, namely the Grid Greedy Logic Search (GGLS) algorithm with the combination of Hierarchy Tree in order to find the optimal placements.

3.5.1 GGLS Algorithm

Figure 3.6 shows the flowchart of the proposed placement method. The map is firstly initialized from the image processing, converted into Cartesian space and divided into equal grids. Then the initial placement N_0 is assigned along with the initial variables such as the threshold *th* and the coverage map logic for the initial placement C_{N0}. GGLS algorithm works by finding the next placement candidate whenever the initial placement is on the threshold value. Since the ideal signal propagation is in a circular form similar to water ripples, we can expect how far the signal could traverse. This is also because the nature of wireless signal that has the fading effects, where the further it goes, the more it fades. Thus, the concept of threshold is introduced. Threshold in this work describe the maximum distance that a WiFi signal could reasonably travel.

The IEEE 802.11 WiFi network has a range that is generally limited by transmission power, antenna type and the surrounding environments. A typical WiFi AP in an indoor environment employing 2.4GHz 802.11n/g with stock antenna might have an ideal range of about 32 meters [67]. This range however is affected and greatly reduced due to the complex propagation and fading, walls and ceiling absorption, Non-LOS obstruction, overlapping channels as well as interferences from other wireless devices. Moreover, residential electronics such as microwave ovens also operates around the same frequency as wireless access point. Thus, for this works, the coverage threshold at 15 meter is set that performs well in a dynamic, multi wall and cluttered office environment. Then, at the edge of the threshold, another WiFi AP can be placed to guarantee coverage to the next 15 meter threshold. This is a feasible technique since it yields an overlap between APs as shown in Figure 3.7 on the grayish area. The overlapping is a good area for a mobile robot since in that particular area, the strong signals from multiple AP are guaranteed and thus increases the database trustworthiness.

Afterwards, the greedy search algorithm is formulated in order to determine the number of required APs that guaranteed the total coverage in an environment. A grid is made from a digitized version of the floor area as discussed previously. In this works, a granularity of 1 meter spacing is used which is a fair trade-off between processing time and complexity level. Later, N is determined by the number of grid intersections. The pseudo-code for the GGLS algorithm can be found in *Algorithm 1*.

In this algorithm, the initial placement of the WiFi AP is set by the user. This is subjective rather than important because in some buildings, there is a need to have uninterrupted wireless connectivity in specific rooms, for example the server room in an ICT department, or inside the primarily used rooms in an office. From multi-robot point of view, the initial placement should be in the common boardroom for the team of robots, since it allows the robots to exchange coordination and information amongst themselves while carrying data collected from the surrounding environment and is useful for localization or mere data gathering purposes [68]. The coverage at any point in the spatial area *mn* from N_i is computed using

Euclidean at threshold parameter *T*. This distance threshold parameter is easily interchanged to a path loss parameter. However, since no accurate modeling is available, the distance threshold works similarly well.

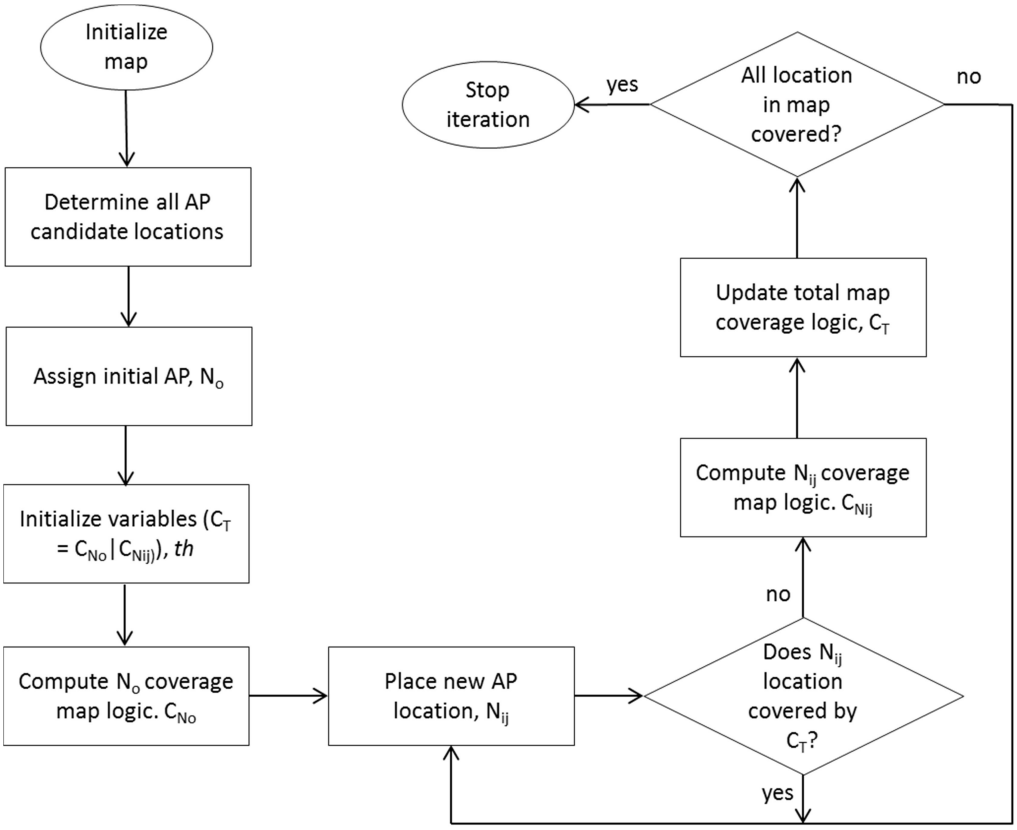

Figure 3.6: The flowchart of the proposed GGLS algorithm

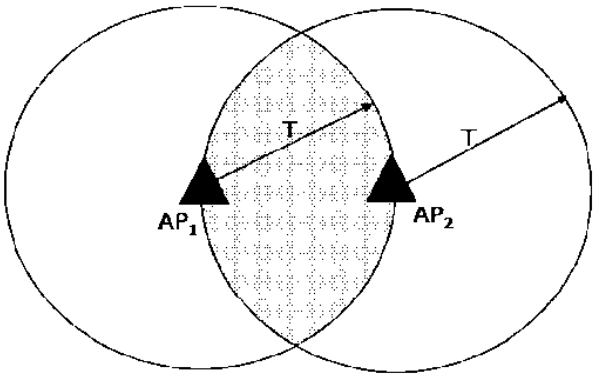

Figure 3.7: Illustration of signal overlapping of two AP's coverage by distance threshold, *T*.

Algorithm 1: Greed Greedy Logic Search (GGLS) algorithm

```
1. Initialization (create grid, define all N, place initial N0, define threshold)
2. Compute coverage for initial N0, Ctotal
3. WHILE (all area not covered)
4.      Assign new Nj
5.        CASE (new Nj in range of Ctotal)
6.             Release new Nj
7.        CASE (new Nj not in range of Ctotal)
8.             Accept location of new Nj
9.             Compute coverage for new Nj, Cnew
10.            Update Ctotal  (Ctotal = Ctotal | Cnew)
```

3.5.2 Extension to Hierarchy Tree

In Figure 3.7, there are numerous 'next' AP candidates that can be observed at the edge of the circle. Thus, assuming the initial placement as N_0, the next placement candidatures could be represented as a second level tree at $\{N_1, N_2, \ldots, N_m\}$. At the m tree branch, the next placement candidate could be represented as $\{N_{m1}, N_{m2}, \ldots, N_{mn}\}$. The tree could be later expandable to as much as required in order to guarantee total signal coverage in an environment. Figure 3.8 shows an example of a hierarchical tree at 4-levels of tree branch, where the placement of an AP is located at the configuration N_{mnp}.

Each branch will be terminated whenever stopping criteria is met, which is whenever total coverage has been located. In addition, a selection function in terms of cost function is introduced in order to find the most optimal solutions.

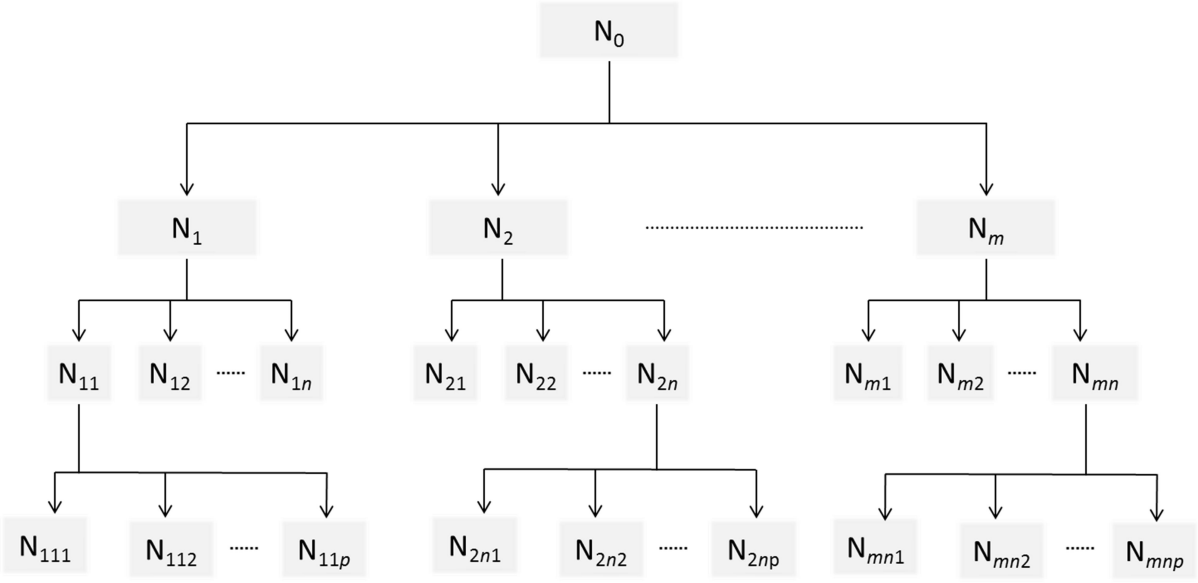

Figure 3.8: Hierarchy Tree for WiFi AP placement

3.5.3 Selection Criteria

The above tree hierarchy was indeed an efficient approach for finding all the possible locations of wireless nodes that guarantee overall environment coverage. This fact is the most vital part for mobile robot wireless indoor positioning. The next step is to find the optimal tree branch. Therefore, a selection criterion must be formulated.

The selection criteria formulation is as follows;

For k number of wireless nodes in a defined nodes N that is bonded by an environment mn, the received power could be estimated by a suitable path loss model PL. Thus at any N_{mn}, there will be k number of PL. The nature of the received signal density is inversely proportional to the distance separation by means of the inverse square power law. Hence, a diffusion approach could be taken to formulate the selection criteria.

The density of received signal power is roughly between 0dBm to -120dBm. Beyond the value of -120dBm, the WiFi signal is gone astray and non-usable for positioning works. In our measurement, the close-in reference distance, d_0 between Tx-Rx separations at less than 0.5m yield in saturated -40dBm. In formulating the selection criteria, using negative path loss value is an undesirable option. Instead, a normalized scaled was used as depicted in

$$r_{mn}(\text{scaled}) = \frac{r_{mn} - r_{\min}}{r_{\max} - r_{\min}}, \qquad \text{(Eq. 3-4)}$$

where r_{mn} represents the received power at mn location, $r_{\max}$ is saturated at d_0 and $r_{\min}$ is the least received power. The selection function is made from the mean and variance of the received signal strength from $\text{AP}_1, \text{AP}_2, \ldots, \text{AP}_k$. This is reasonable since the location that is near to the AP location has the highest RSS. From each location in the floor plan (or so called the WN candidates), the mean and variance are given in (Eq. 3-5) and (Eq. 3-6), respectively.

$$\overline{r_{mn}} = \frac{1}{N_T - 1} \sum_{m=1}^{M} \sum_{n=1}^{N} r_{mn} \qquad \text{(Eq. 3-5)}$$

$$\sigma_{r_{mn}}{}^2 = \frac{1}{N_T - 1} \sum_{i=m}^{M} \sum_{i=n}^{N} \left(r_{mn} - \overline{r_{mn}} \right)^2 \qquad \text{(Eq. 3-6)}$$

$$\arg\min_{x \in \mathbb{R}^2} J = \sum_{m=1}^{M} \sum_{n=1}^{N} \omega_1 \frac{1}{\overline{r_{mn}}} + \omega_2 \sigma_{r_{mn}}{}^2 + P \qquad \text{(Eq. 3-7)}$$

The variable N_T represents the total number of locations (from the intersection of the grid) on the floor map. The selection function, J is then given in (Eq. 3-7). The mean and variance are weighted by the variables ω_1 and ω_2 in order to emphasize the significant variables. In addition, it is also possible that with any AP placement configuration, there will be locations where there are no WiFi signals at all, or a *dead zone*. Thus, the variable P is introduced as a penalty parameter. If such a condition is met, then P will be assigned to a large value so that the cost function J will result in a large value, thus avoiding such a configuration to be selected.

Validation of the Selection Criterion Function

The above-described criteria function is evaluated and validated by using the six wireless nodes arrangement described in [59]. The six different configurations are used either four or five WiFi AP, in which four of them are in symmetrical order and the other two are not. Figure 3.2 shows all six configurations; with the triangle symbol representing the WiFi AP locations. In the report, configuration five was chosen because it had the minimum localization error. Moreover, this selection was also visually chosen since the AP placements were equally distributed in the alley.

To validate the selection function reliability, configurations similar to their research in our floor plan are chose which is rectangular in shape and a size of 30x16 meters. Table 3.1 shows the results of the cost function applied to all six configurations. We could clearly perceive that by employing the simplest free space propagation model, the same configuration (*configuration 5*) is selected which yields the smallest J with $\omega_1 = 0.5\omega_2$, thus validated our selection function.

Table 3.1: Computation results of the six principle configurations

Configuration	$\overline{r_{mn}}$	$\sigma_{r_{mn}}^{\ 2}$	J
1	0.2930	0.0512	1.7574
2	0.2895	0.0433	1.7706
3	0.2149	0.0363	2.3627
4	0.3008	0.0470	1.7091
5	**0.3050**	**0.0433**	**1.6825**
6	0.2957	0.0465	1.7374

3.6 Results and Discussions

The simulation works are conducted using the floor map blueprint second floor of the Center for Human-Robot Symbiosis Research building of the Toyohashi University of Technology campus. Since there is no WiFi AP as yet in Terapio experimental area, it was a good initiative for us to determine how many WiFi APs would need to be installed that would guarantee total coverage. Thus GGLS was applied.

3.6.1 GGLS Results

Figure 3.9 shows the preliminary placement result of the GGLS algorithm, without the use of the hierarchy tree. The 'dot' symbol represents the candidates for the AP placement locations while the 'star' symbol represents the actual AP placement location. The initial AP is placed at location (29,4) since this is the main area for mobile robot experimentation activity. This result suggests that only three WiFi AP's are required to be installed on this floor, where the other two locations were at (15,14) and (6,0). In this primary algorithm, the next placement is decided whenever the set of candidates vector N reach the point of threshold value T, therefore this is not the optimal configuration, imperatively. As such, the later works is much more desirable where the hierarchy tree approach is applied to the GGLS with the optimization function J. Subsequently, the signal coverage of the AP placement can be observed by employing an appropriate signal propagation model.

The signal propagation model chosen in this works is the ITU-R P.1238 multi wall and floor (MWF) model [69]. This model is applied to the individual AP in order to observe their coverage in the indoor environment. As depicted in the Figure 3.10, some of the areas for instance the top left and right rooms have fairly low coverage signals, roughly at about $\leq -120\text{dBm}$ .This poor signal may result from the thickness of the surrounding walls, which absorb about 14dB of transmitted signal [69]. Nevertheless, this initial GGLS algorithm has proven that the WiFi AP placement is possible. This technique is a simple but effective approach that uses logic reasoning while avoiding the complexity of mathematical computation.

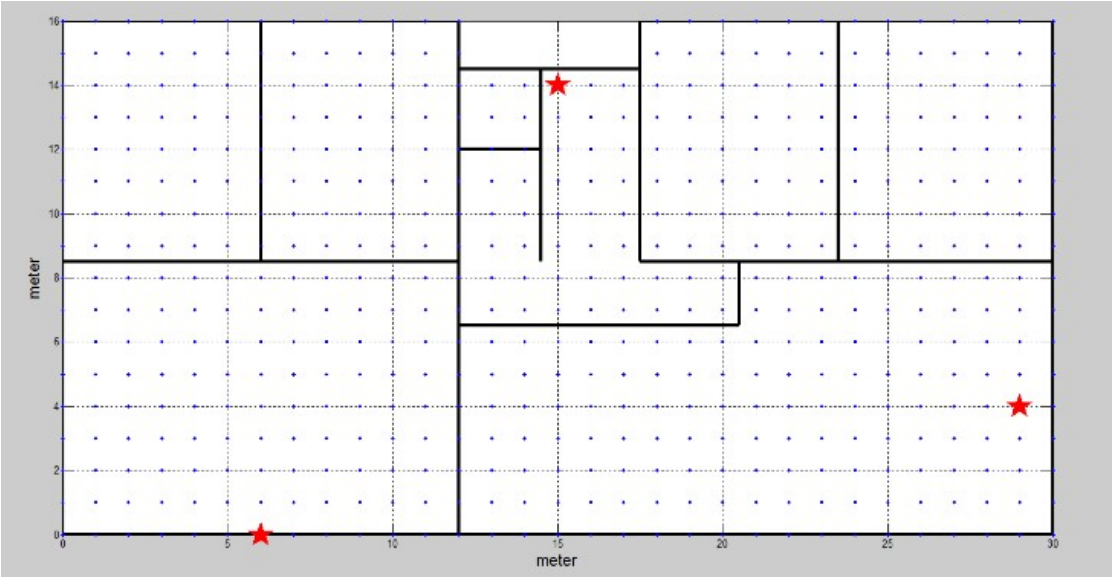

Figure 3.9: Preliminary result of the GGLS algorithm

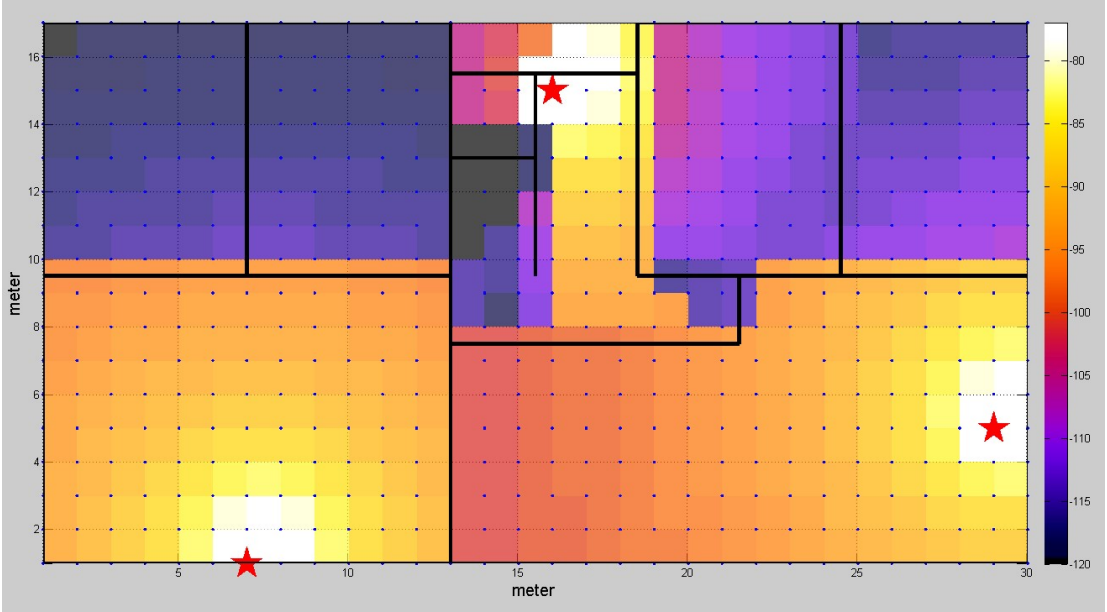

Figure 3.10: Coverage map of result using the ITU-R P.1238 MWF signal propagation model

3.6.2 Hierarchy Tree Results

Even though GGLS could place the APs generically in the specific floor, the placements however, might not be optimum since there is no cost function used to evaluate effectiveness. Moreover, if the AP candidate vector N is rearranged, the result might be changed. Rearrangement of candidate vector N is not an option when taking into consideration the size of the candidate vectors which would result in enormous time computation at $O(|N|!)$, which is the same problem as brute search algorithm. Thus, the hierarchy tree is proposed in order to solve this issue.

By applying the hierarchy tree, there are 61 possible configurations (tree branches) of AP placements that guarantee total coverage on the particular building floor. Then the selection criteria are used to evaluate which tree branch has the minimum value, which is in fact the global minima of the cost function J. This is shown explicitly in Figure 3.11. The global minima, marked as an 'o' symbol, represents the result of the selection tree branch – in this analysis tree branches number 34. Interestingly, the number of required Wi-Fi AP's in this particular selection is four, which are at (14,11), (0,2), (21, 16), and the initial AP remains at (29,4) as with the initial result of the GGLS algorithm.

The coverage at this placement by applying similar propagation models as in GGLS, i.e. ITU-R P.1238 MWF model, is shown in Figure 3.12. From the result, we could observe that the coverage is indeed well distributed across the floor and the placements shows that good, as well as guaranteed, signals could be obtained at practically all locations in the floor. This coverage shows that the maximum received signal strength is -40dBm at d_0 and the least received signal strength is $\geq -100\text{dBm}$. Figure 3.13 on the other hand, shows the signal strength distribution from all four AP observed from the floor point of view (rotating Figure 3.12 z-axis at 90°), which assures optimal signal coverage.

In order to check the signal validity for mobile robot positioning via the fingerprinting method, a sliced floor map in the direction of the x-axis is made. The slicing locations were chosen at mid-area from locations (0,9) to (30,9). The signal strength distributions from these locations are plotted in Figure 3.14. In this graph, assuming that the *poor reception* is roughly at -120dBm, we could observe that at any point there were more than one AP's yielding a signal larger than the *poor reception* signal. Thus, the placement is satisfactory for the fingerprinting database. The accuracy of the positioning system is discussed afterwards.

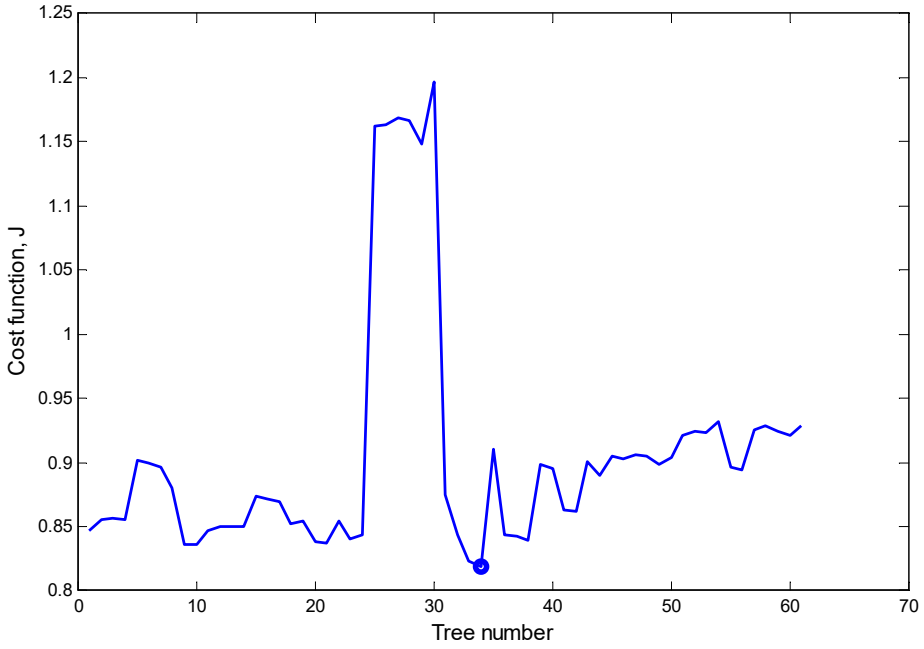

Figure 3.11: The graph of the cost function *J* for the hierarchy tree

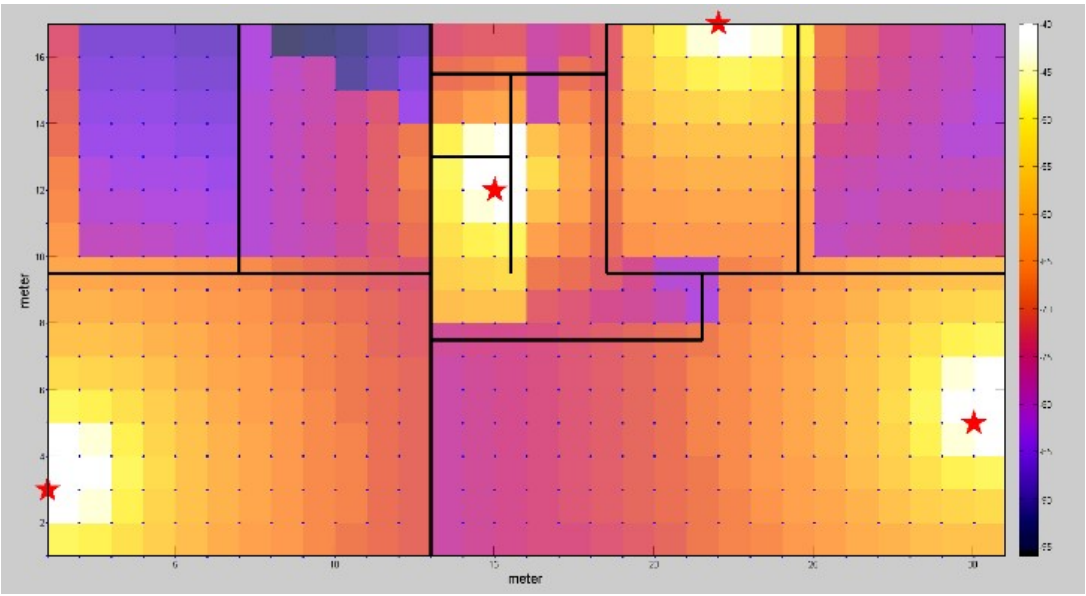

Figure 3.12: AP placement result of using Hierarchy Tree at the selected branch number 34

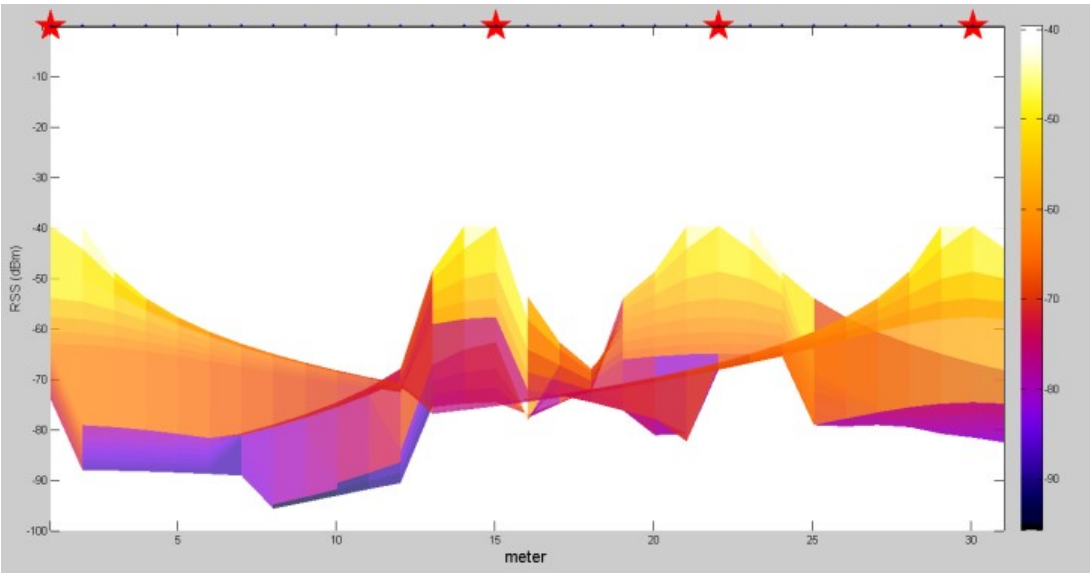

Figure 3.13: Signal strength distribution of all four AP

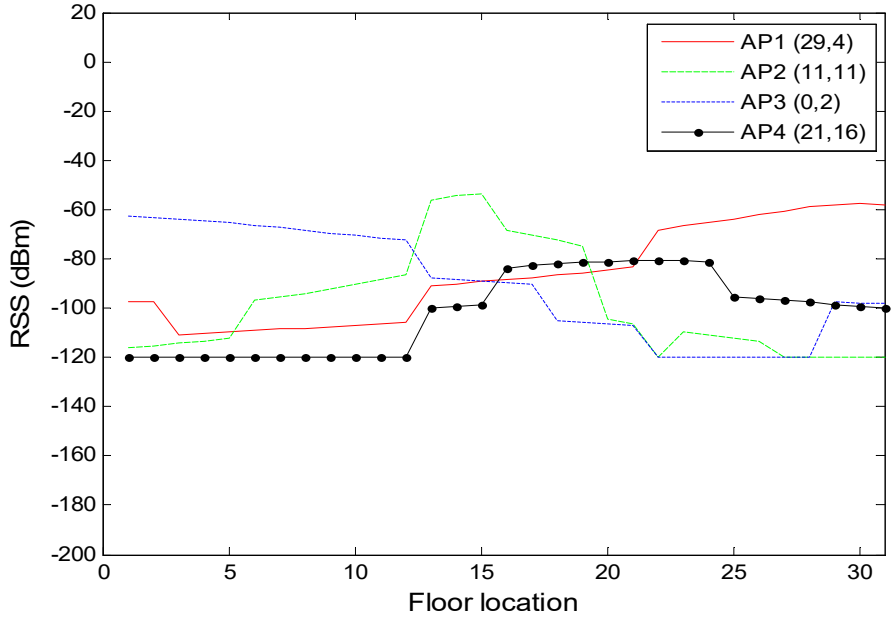

Figure 3.14: Received signal strength simulation at location (0,9) to (30,9) from all four APs.

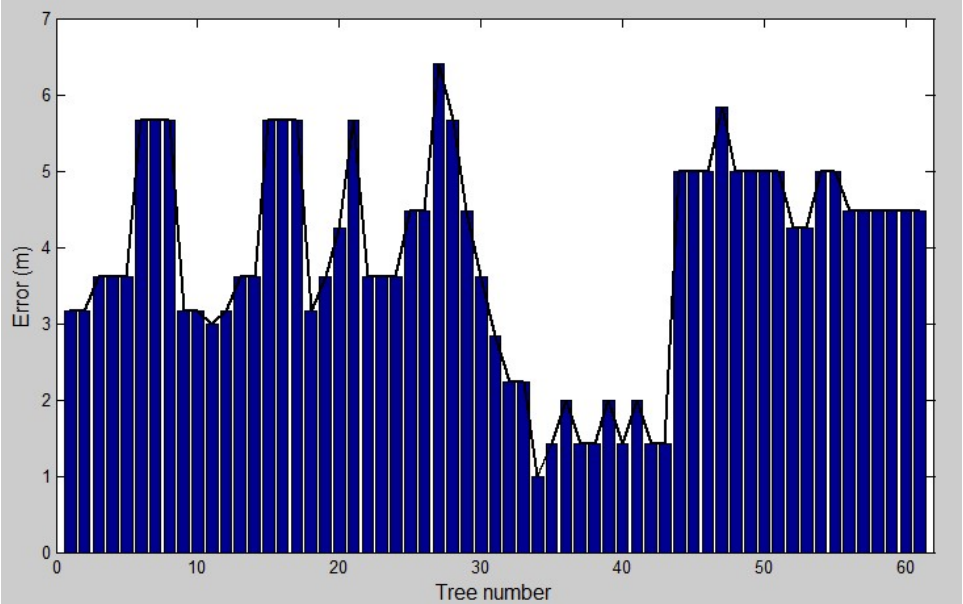

Figure 3.15: Histogram of positioning error at all branches of hierarchical tree

3.6.3 Positioning Accuracy of the Proposed Placement

Positioning accuracy is measured by averaging the errors at the test location, which contains the data associated to a particular location of interest. These data then were applied to the WKNN in order to obtain estimated position. The estimated position is later compared with the real position, computed using (Eq. 3-8)

$$Le = \sqrt{\left(x_s - x_e\right)^2 + \left(y_s - y_e\right)^2}\,, \qquad \text{(Eq. 3-8)}$$

where (x_s, y_s) is the known position and (x_e,y_e) is the estimated position.

The average positioning error relies on the true and estimated location to calculate a value that correctly expresses the accuracy of the system. The process to obtain the average positioning error is by the summation of positioning errors obtained per location and divided by the total number of locations, and expressed as $\overline{PE} = \left(\sum_{i=1}^{N} Le_i\right) \Big/ ND$. $\overline{PE}$ is the average positioning error, Le_i is the positioning error at i-th location and ND is the total number of sample data.

The positioning error at all tree branches is shown as a histogram in Figure 3.15. The error is calculated according to (Eq. 3-8) by using the WKNN positioning method, with $\mathrm{K} = 3$ neighbors. At any of the placement configurations, the fingerprint database is generated by using the signal propagation model and the parameter used for matching is the average RSS reading. Thus, the database size became $30 \times 16 \times \mathrm{R}$,

where R is the number of WiFi AP's required on the said floor. Therefore, the WKNN algorithm tries to match the sample data to the signal fingerprinting database at any of the placement configurations.

The tree branch corresponding to number 34 has a minimum positioning error at about 1 meter, while the other branches yield an error larger than 2 meters. This result concurred with the previous result from using the selection function *J*. Therefore, we could summarize that the tree branch number 34 with four AP's has the optimum locations to install the Wi-Fi AP that maximizes coverage as well as resulting in a minimum number of errors for the mobile robot indoor positioning system.

3.6.4 Optimality Analysis

A comparison was undertaken analyzing the selected placements resulting from the GGLS algorithm and the deployment patterns from the previous work. The comparison condition is made such that the initial placement of the WiFi AP's should be at similar locations since the initial placement is placed inside the experimental area. Therefore, the initial placement location has the absolute significance. Then, the symmetrical placements were deployed and optimality was observed by using the cost function *J* and also computing locations with *dead zone*. Finally, the total coverage is also simulated by using the ITU-R P.1238 MWF model assuming that the least received coverage is beyond -120dBm, which is calculated as the number of *dead zone*.

Table 3.2 shows the WiFi AP placement of the proposed configurations and the symmetrical placements suggested by the literatures, which are in forms of rectangular and triangular shapes. The initial AP placement is set at location (29,4) in all configurations so that non-bias results could be obtained. Figure 3.16 shows the actual placements of the configurations and their coverage mapping utilizing the ITU-R P.1238 MWF signal propagation model.

Table 3.2: Location propositions for comparison

Methods	**Suggested placement**
Proposed	(29,4), (14,11), (0,2), (21,16)
Rectangular	(29,4), (29,12), (1,4), (1,12)
Triangular	(29,4), (1,4), (15,15)
Triangular II	(29,4), (1,4), (15,11)

Table 3.3: Comparison between the proposed placement and the typical symmetrical placement

Configuration	Mean, $\overline{r_{mn}}$	Variance, $\sigma_{r_{mn}}^2$	*J*	No. of *dead zone*
Proposed	1.2817	0.0385	0.4286	0
Rectangular	1.2078	0.0544	12.468	23
Triangular	0.9658	0.0187	5.5364	0
Triangular II	1.0072	0.0183	8.5147	15

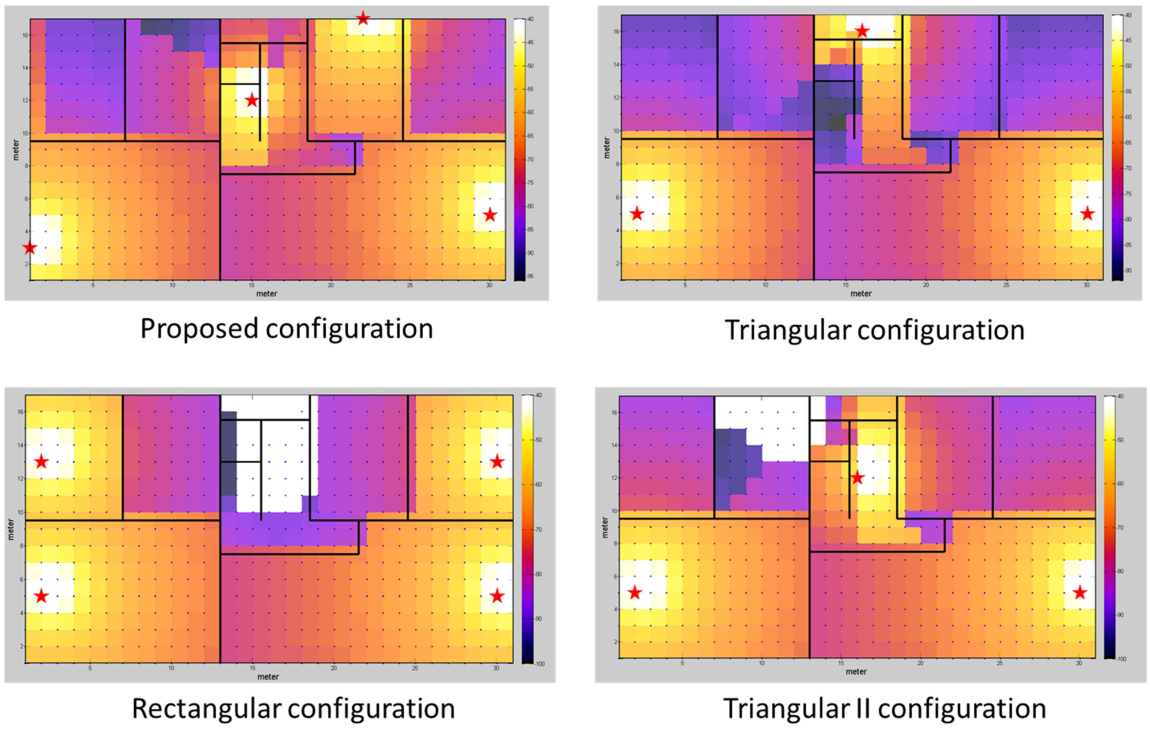

Figure 3.16: The locations of the AP placement with regards to the propositions for comparison and optimality analysis

Table 3.3 on the other hand, tabulated the result of the proposed placement and a comparison in terms of the scaled coverage mean and variance, cost function *J* as well as the number of *dead zone* by employing the ITU-R P.1238 MWF signal propagation model. The proposed method has the highest scaled mean across all configurations. The proposed method has 40% more coverage than the other configurations. Moreover, this placement does not have any *dead zone*, assuring that we could receive WiFi signals at all locations on the floor map. Configuration rectangular and triangular II have quite a large value of *dead zone* and apparently should be avoided. This might result from the initial placement, which was placed near the wall and thus the

other mirrored placement are also placed near the opposite wall. Therefore, in such a configuration, wall attenuation and absorption play important roles.

3.7 Summary

In this chapter, the concepts and the importance of WiFi Access Point (AP) optimal placement are discussed emphasizing on the need of total coverage for human use whilst being suitable for mobile robot positioning via the fingerprinting technique. The dedicated floor map is firstly digitized through image processing method known as color overlay technique. The digitized map is further used to find the optimal location to place the WiFi AP.

The computation of optimal placement of the WiFi AP is indeed a non-trivial problem. A systematic technique based on brute search method to place the WiFi AP has been proposed, namely the GGLS and hierarchy tree approach, where the initial location of the AP is determined by user requirements.

The proposed GGLS algorithm is a simple technique to obtain the placement location but optimization is not assured. Then, the hierarchy tree based on the GGLS algorithm was proposed for optimization along with an effective selection function in order to find the minimum number of required AP's that satisfies the requirement to maximize coverage as well as minimizing positioning errors. The resulting placement also suggests that WiFi AP placement does not necessarily need to be in a symmetrical pattern. In addition, this proposed system is also suitable for facilities modeling i.e. for network management and administrative entity in order to plan the locations for WiFi AP installations in a building.

Chapter 4 WiFi SIGNAL ASSESSMENT

"*Whatever the mind of man can conceive and believe, it can achieve*'

- Christopher Columbus, 1930s

4.1 Introduction

Wireless signal such as the 2.4GHz 802.11 a/b/g/n WiFi signal is a practical option for WPS system since many recent building incorporates WiFi solutions in their building. In many works on fingerprinting method, there are little to no concern about the quality and the order of measurements when collecting the data for creating the signal fingerprint database [70][71]. The measurements for positioning algorithm are normally made from the separation distance between the transmitter and receiver (Tx-Rx) basis, and sometime the receiver antennae orientations when there are no omni-directional antennae used [72].

Since the experimental works are conducted in the dedicated indoor environments where the locations of the WiFi APs are known, then there is a requisite to examine the correlation between the antenna heights parameter with the separation distance of the transmitter and receiver (Tx-Rx). The study also could help in finding the most relevant antenna heights at any placement in order to obtain the minimum positioning error. One of the most useful tools that can be used to perform this study is the statistical test tools such as ANalysis Of Variance (ANOVA) that could correlate and differentiate the means between the investigated parameters.

This chapter describes the works related to hypothesis testing with respect to the two parameters explained in the above.

4.2 Hypothesis Testing

The proposed WPS system is based on the fingerprinting technique. Such technique requires the signal fingerprint radio map or database to be made beforehand. Traditionally, the fingerprint database is made by measuring the signal strength (RSS) at predefine locations. In this example, the main parameters for the fingerprinting database is related only to the separation distance of the Tx-Rx, and the other parameter i.e. antenna heights are not of concerns. Hence, the objectives of this works are to investigate and analyzed the effects of Tx-Rx separation and the antenna heights using the DoE approach as well as evaluating the positioning error from mobile robot positioning point-of-view.

To achieve this objective, experimental hypothesis must be made. The null hypothesis H_0 is then defined as the mean of the RSS measured by a mobile robot at each antenna height level and at each separation distance between WiFi AP transmitter and receiving mobile robot (Tx-Rx separation) are all equals. Alternative hypothesis H_1 is defined as at least one pair of the parameter is not equal. The formal hypothesis testing statements are;

H_0 : the μRSS of all experiment orders are equal, and

H_1 : at least one pair of μRSS is not equal.

To test the hypothesis in the present works, a commonly used significant level of $\alpha = 0.05$ is used. In addition, the statistical software Minitab® was used to analyze the data.

4.3 Experiment Setup

The experiments are conducted at the Terapio experimental area, which is at the 2nd floor of Center for Human-Robot Symbiosis Research at Toyohashi University of Technology, Japan. Since the experiments are about the measurement and assessment of WiFi signal, then the appropriate apparatus is chosen. The WiFi transmitter used is the high power Alfa AIP-W525H dual antenna with 5dBi gains each. This WiFi AP transmits 2.4GHz wireless signal with the channel set to channel 1. The wireless receiver used in this experiment is the common receiver adaptor model Broadcom BCM43142 Wireless Network Adaptor embedded in mobile computer. The signals were recorded using the Homedale® [73] open source code for wireless surveillance running under the Windows 8.1 operating system. The sampling time at each location for measurement is roughly about 3 minutes in the interval of 2 seconds in order to obtain the generic behavior if the wireless signals.

The properties of the network are tabulated in Table 4.1, where the Media Access Control (MAC) address is the default address from the Alfa Inc., and the Service Set IDentifier (SSID) is an open connection as Terapio_AP1. The frequency for this setting is the nominal frequency of 2.4GHz and set to channel 1 which span across 20MHz broadcasting between 2.400GHz to 2.412GHz. Since the required data is the Received Signal Strength (RSS) from the WiFi AP, then the internet connection is not needed and the network remained disconnected with it. In addition, the condition between transmitter and receiver was clear and unobstructed Line-Of-Sight (LOS). However, the surrounding environment was fully uncontrolled due to the multipath fading effects, people walking in and out of experimental room, nearby WiFi and Bluetooth® interferences and so on.

Table 4.1: The Setup of the network for the DoE experiment

No.	Properties	Details
1	MAC address	00:C0:CA:83:66:A8
2	SSID	Terapio_AP1
3	Security	none
4	Channel	1
5	Internet connection	disable

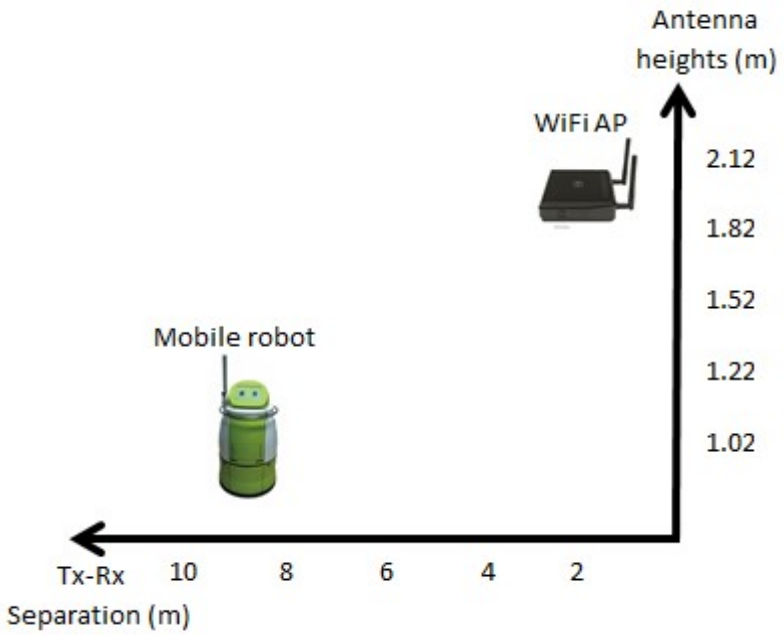

Figure 4.1: Parameter variation in the experiment

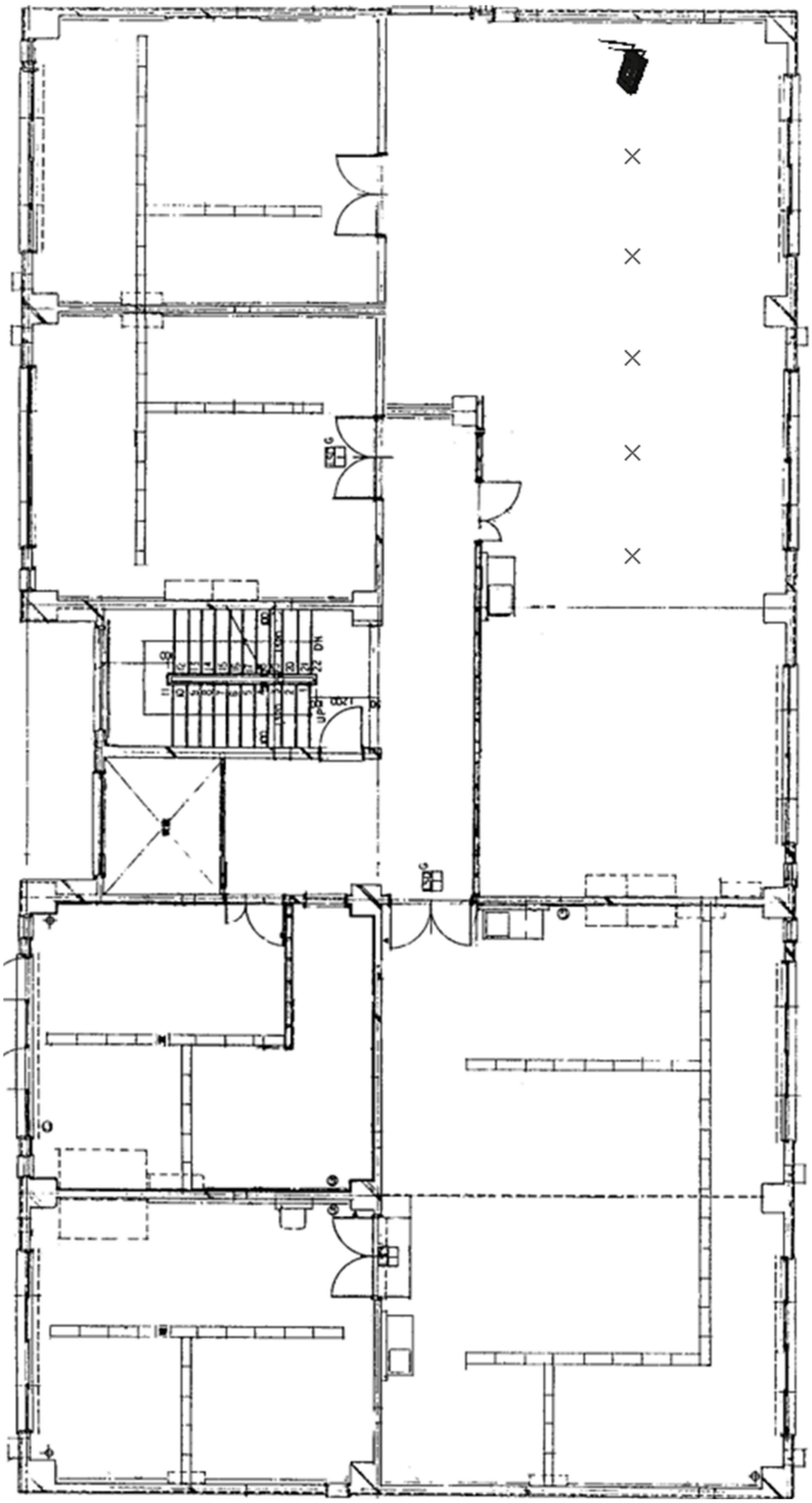

Figure 4.2: The experimental area showing the location of the WiFi AP and the five measurement locations at horizontal direction

There are two parameters to be investigated in this experiment, namely (1) the antenna heights, and (2) separation distance between transmitter and receiver (Tx-Rx). In order to obtain unbiased result, these two parameters are varied by five levels as indicated in Figure 4.1. The antenna height is measured from the floor level in the experimental area of about 8×10 meter. The ceiling height is about 2.3 meter and the minimum antenna height is at least equal to the receiver's antenna. The mobile computer i.e. the receiver adaptor is placed about top of the mobile robot at about 1 meter height, similarly measured from the floor level. Figure 4.2 shows the experimental area in the said building (cleaned) with the placement of the WiFi AP as well as the five measurement locations. In this case, the directions of the measurements with respect to the WiFi AP are horizontally at 0°. In the experiment for positioning assessment, the directions of the measurements with respect to WiFi AP are arbitrary in order to create the signal fingerprint database for positioning algorithm, described in later Section 4.6.

4.4 Design of Experiment (DoE) Technique

Design of Experiment (DoE) is a formal mathematical method for systematically planning and conducting scientific studies that change experimental variables together in order to determine their effect of a given response [74]. DoE is an efficient technique that standardize the approach of changing "one variable at a time" in order to observe the variable's impact on a given response. Generally there are four steps in planning for DoE, which are

(1) The design of the experiment, such as the investigated parameters,
(2) The collection of the data i.e. the WiFi RSS
(3) The statistical analysis of the data, and
(4) The conclusions reached and recommendations made as a result of the experiment.

The similar steps are taken in this works. In the data collection step, as oppose to conventional approach were the signal is recorded at predefine locations according to the order, randomized measurement with respect to the two parameters were initiated.

4.4.1 Measurement Order

Since the WiFi RSS data suffers fluctuations badly, a non-bias and systematic measurement must be sought. Thus, Minitab® was used in order to generate an unbiased observation order. Minitab® is powerful statistical software that provides comprehensive set of statistical tools such as descriptive statistics, probability distributions, statistical inference, confidence intervals, t-tests, etc. A full factorial design of experiment was conducted. Randomized measurement order was generated by the software. Randomization

is a technique used to balance the effect of extraneous or uncontrollable conditions that can impact the results of an experiment [74], thus reducing the chances that differences between both parameters biased strongly. Randomization techniques also lead to the vital estimation in the inherent variation so that valid statistical inferences could be made.

In this works, the experiments were replicated one time in order to obtain reliable data while reducing the probability of outlier data occurrence. To the extent that we know, as of this dissertation publication date, this order is the first being studied for assessment of WiFi RSS quality.

4.4.2 Measurement Methods

Experimental design is a critically important tool in the scientific and engineering world for improving the product realization process. Critical components of these activities are in new manufacturing process design and development, and process management. Designed experiments also found extensive application in marketing, market research, transactional and operations, and general business operations [74]. Based on these criteria, we found that Design of Experiments (DoE) suit well in order to find the most significant parameter in WiFi RSS assessment.

By using the Minitab® software, the experiment table is automatically generated for full factorial design with randomization. Antenna heights and Tx-Rx separation are the investigated factors of the DoE in order to evaluate their effects on the WiFi RSS data. The five antenna height treatment levels (1.02, 1.22, 1.52, 1.82 and 2.12 m.) and the five Tx-Rx separation treatments (2, 4, 6, 8 and 10 m.) are chosen for the DoE. Table 4.2 shows the randomized measurement order in this work. The first measurement was conducted on Jul 29th, 2015 morning. Later replicate test was conducted on Aug 4th, 2015 afternoon. Accordingly a total of 50 run were made. Theoretically, with about 100 data per run, we are having generously 5000 WiFi RSS data to be evaluated, which is sufficient for the statistical analysis.

To analyze the effects of the treatment variables, the WiFi RSS data is very important for evaluation. A multivariate analysis of variance (ANOVA) and the complementary statistical tests are used to evaluate which treatments significantly affect the dependent variables [11]. The DoE presented provides statistical correlations between each factors (i.e. treatment variables) and observation response (WiFi RSS). Treatments that had statistically significant correlations were identified using significance value of $\alpha = 0.05$.

Table 4.2: The randomized measurement order run in two separated day, with μRSS represents the average of the WiFi signal strength data.

Run Order	Antenna height (m)	Tx-Rx separation (m)	Observation response, μRSS (dBm)	Run Order	Antenna height (m)	Tx-Rx separation (m)	Observation response, μRSS (dBm)
1	1.82	6	-39.89	26	1.01	6	-39.39
2	1.52	4	-40.78	27	1.22	8	-42.09
3	1.22	4	-40.66	28	1.82	2	-32.44
4	1.82	4	-46.39	29	2.12	10	-44.24
5	2.12	6	-41.99	30	1.22	4	-33.22
6	1.82	8	-47.97	31	2.12	2	-40.84
7	1.52	10	-41.42	32	1.82	4	-41.13
8	2.12	4	-36.74	33	2.12	6	-39.49
9	1.22	6	-41.87	34	1.52	2	-37.52
10	1.02	2	-38.55	35	1.01	4	-40.26
11	2.12	10	-46.00	36	2.12	4	-37.38
12	1.02	10	-38.06	37	2.12	8	-47.44
13	1.52	6	-45.70	38	1.82	10	-46.45
14	1.22	8	-40.62	39	1.52	4	-44.67
15	1.82	10	-47.79	40	1.52	8	-41.61
16	1.02	8	-45.01	41	1.01	10	-46.53
17	1.22	2	-40.93	42	1.01	2	-38.71
18	1.22	10	-44.44	43	1.52	6	-41.85
19	1.52	8	-45.28	44	1.22	10	-48.65
20	1.82	2	-40.08	45	1.01	8	-44.75
21	2.12	8	-41.47	46	1.82	8	-43.53
22	1.02	4	-37.91	47	1.52	10	-39.36
23	1.52	2	-33.27	48	1.22	6	-41.24
24	2.12	2	-36.92	49	1.22	2	-31.71
25	1.02	6	-40.33	50	1.82	6	-46.24

Table 4.3: Analysis of Variance (ANOVA) Table (Two-factor factorial) of the RSS data

Source of Variation	Sum of Squares	Degree of Freedom	Mean Square Squares	F0	*P*-value
Antenna Height	44.544	4	11.136	1.03	0.411
Tx-Rx Separation	354.507	4	88.627	8.22	0.000
Interaction	165.309	16	10.332	0.96	0.525
Error	258.829	24	10.785		
Total	825.043	49			

4.5 DoE Analysis

In this section, the result of hypothesis testing can be divided into two parts, i.e. the Analysis of Variance (ANOVA) and the two parameters observation. The two-factor factorial analysis in the ANOVA is conducted using the Minitab® software.

4.5.1 Analysis of Variance (ANOVA)

Table 4.3 presents the result of the factorial design analysis based on the WiFi RSS data tabulated earlier. The antenna height parameter with five treatment levels has the *P*-value equal to 0.411. Since it is larger than $\alpha = 0.05$, then we can conclude that it has no significant effects to the WiFi RSS. This matter indicates that we could generally place the WiFi AP at any heights of the experimental room, or more specifically between the treatment levels i.e. from 1.02 meter to 2.12 meter. On the other hand, the Tx-Rx separation with five treatment levels have *P*-value equal to zero, which is very much smaller than $\alpha = 0.05$, thus explaining that it has a significant effect to the WiFi signal strength quality. Interaction between antenna height and Tx-Rx separation are not significant effect to WiFi RSS too since its *P*-value is equal to 0.525. Thus we could focus only to the separation distance when creating the fingerprinting database.

4.5.2 Parameter Observation

Figure 4.3 (left) plots the relation between antenna heights and the WiFi RSS. The explicit difference RSS value does not correlate with each of the antenna height in the experiment. The box trend is likely to be similar although the heights are varied further up to 2.5 meter which is the ceiling heights. These trends are undoubtedly concurred with the P-value results previously. Figure 4.3 (right) on the contrary shows the box plot of the relation between Tx-Rx separation and the WiFi RSS. Over distances, the WiFi RSS decrease logarithmically concurs with the inverse power law functions, which has been further extended into Friis equation that describe basic function of signal propagation path loss with the distance in the free space. From the boxplots, we could see that the outlier data were not present, meaning that the fluctuated signal could be observed as the correct function of distribution except in the 1.22 meter antenna height. Therefore, we could conclude that, the randomize measurement order is good technique to collect the data.

Figure 4.4 investigated the independence of the residuals on the WiFi RSS data. Ideally, the residual must be normally distributed random variation from the experiment process. The data must not be affected by any bias. On the normal probability plot, the general impression is that the residuals are approximately normally distributed. The similar pattern is shown in the histogram plot, where we can see that the residuals appear on both side of zero and the residual mean peaked at zero. The versus fits subplot shows the relation

between the residuals and the fitted values of the experiments. There are no apparent unusual structures since the residuals bounce randomly around the zero lines that suggesting the linear relationship is reasonable. This is in fact a classical example of well-behaved residuals versus fitted plots. The plots of residuals are in the sequence of time (observation order). This order depicted in the versus order is beneficial in detecting the correlation between the residuals and observation order with the problem of WiFi signal fluctuations. Hence there is no reason to suspect any violation of independence or constant variance assumptions. The independence assumption was investigated, and the results are suggested as normal. Therefore, ANOVA has confirmed the WiFi RSS measurement results.

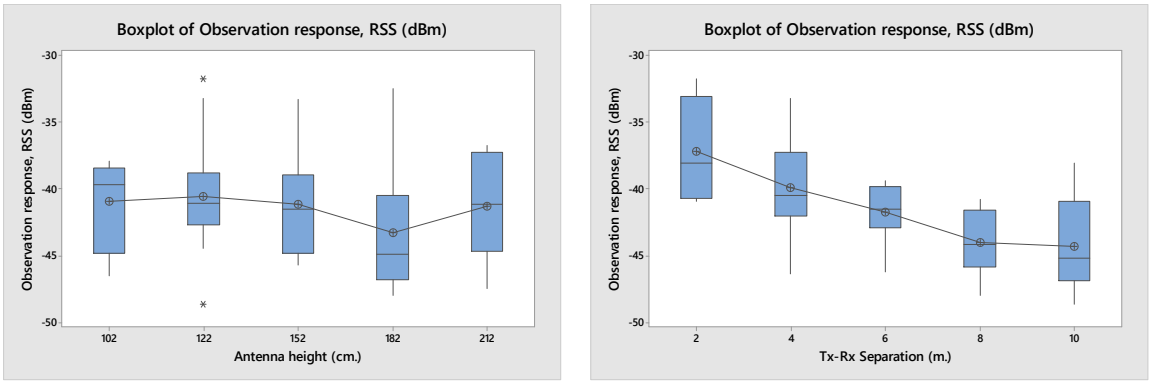

Figure 4.3: (Left) Boxplot of RSS vs antenna heights, (right) boxplot of RSS vs Tx-Rx separation

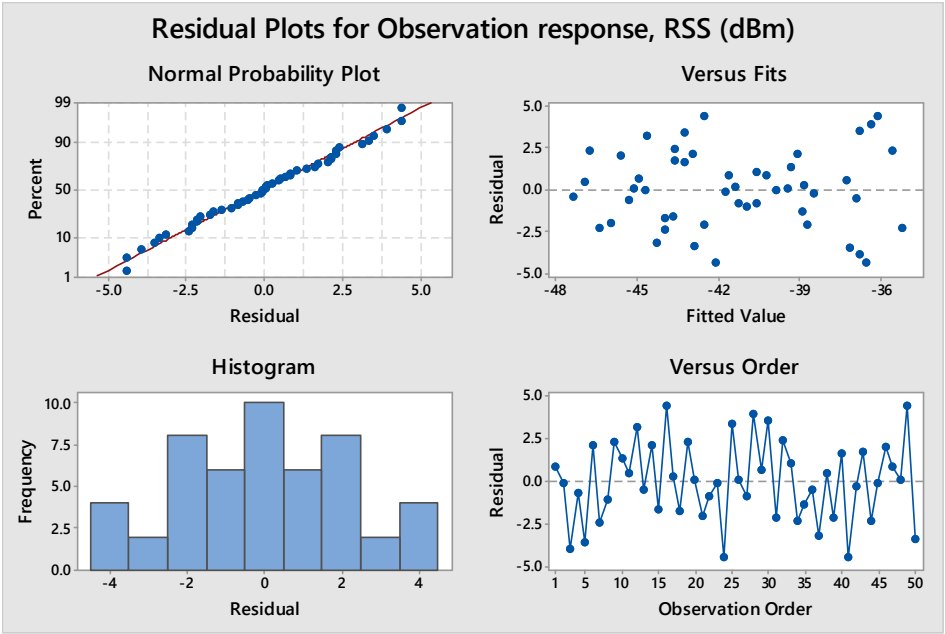

Figure 4.4: Residual plot of the DoE

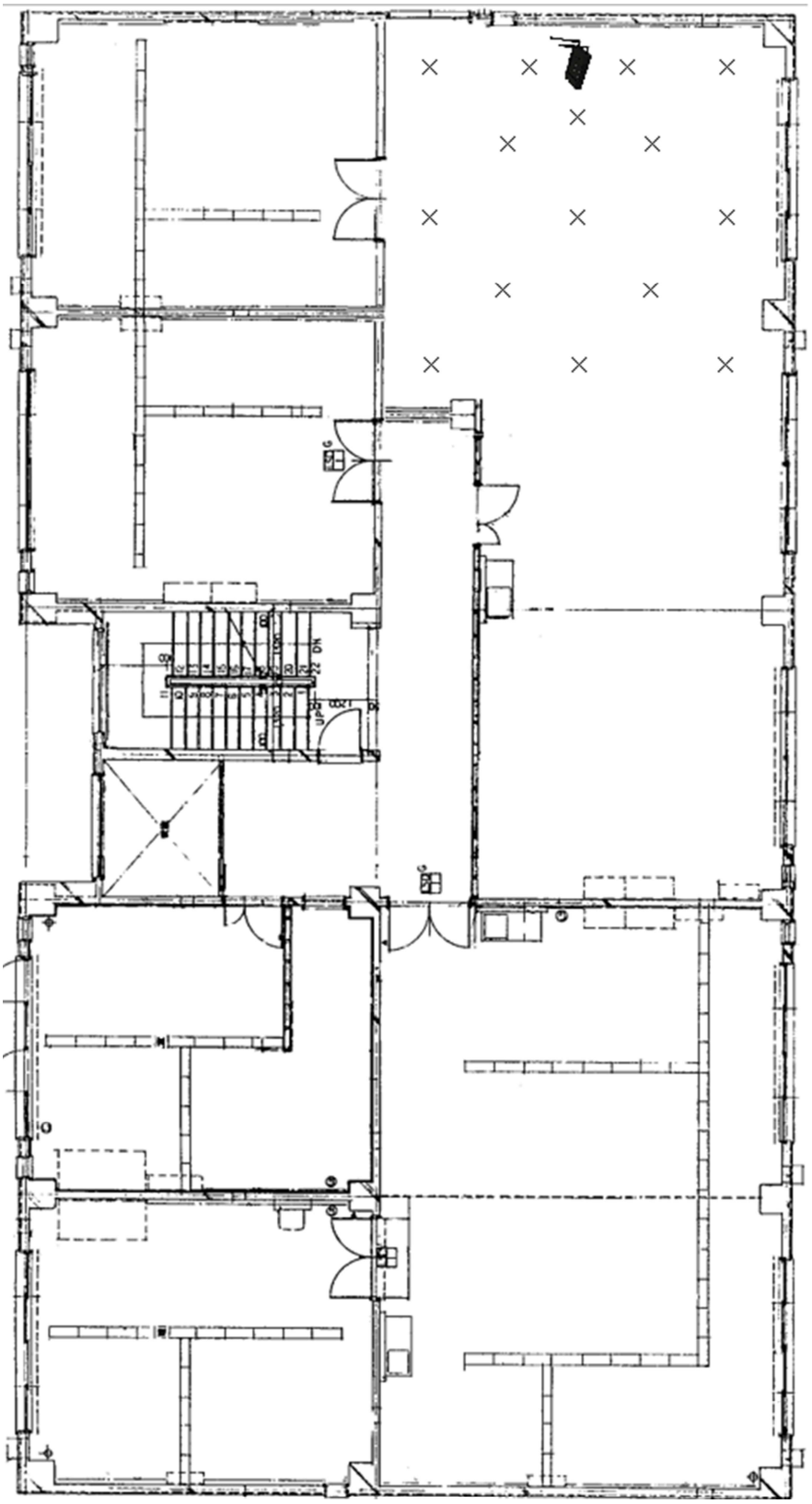

Figure 4.5: The experimental area showing the location of the WiFi AP and the location of data collection at arbitrary direction

4.6 Positioning Assessment

The statistical results are further validated by actual experiments on the mobile robot. The WiFi RSS data in the surrounding area are re-collected in order to create the fingerprinting database of the spatial area, as well as varying the antenna heights to the five levels as before. The location of the data collection is depicted in Figure 4.5.

The fingerprinting database is made from the mean value of RSS at each location. Thus we have five different database vectors corresponding to five antenna heights, for which each database consists of $\left[Loc_j \quad \mu RSS_j \right]$, where variable Loc_j is a matrix of the j-th location corresponding to x and y coordinates respectively. Therefore, when an unknown RSS is present, the matching algorithm will try to match it to the μRSS vector by means of minimal distance metric, for instant Euclidean metric, and the estimated position is returned at the appropriate Loc. In this assessment, the matching algorithm known as Weighted K Nearest Neighbor (WKNN) [75] is adapted.

In the ANOVA analysis, we previously assumed that the WiFi RSS data is normally distributed. Figure 4.6 shows the distribution of RSS data at all fingerprint locations, where we could observe that the data is somewhat fitted to the Gaussian model given in (Eq. 4-1), hence corroborated the assumption beforehand.

$$f(x) = 19.65e^{-\left(\frac{(x+64.9)}{8.14}\right)^2} \qquad \text{(Eq. 4-1)}$$

The WKNN matching algorithm has only one tuning parameter which is the number of nearest neighbor, K. Table 4.4 tabulated the results of average positioning error with regards to the tuning variable K as well as the antenna heights level. No means actually exists for selecting the best value of K other than by observing the one that minimizes the positioning error; in this case at standard deviation of the positioning error $\sigma = 0.34$ meter, the optimal choice was $\mathrm{K} = 3$. As one can see, the variation of errors is rather small and insignificant throughout the average positioning errors with respect to K values. Thus, we could conclude that the ANOVA results presented earlier is validated by the actual experiments where the antenna height is not a significant parameter for mobile robot wireless positioning.

Figure 4.7 shows the cumulative positioning error at a stationary location for a period of 30 seconds using WKNN positioning algorithm at $\mathrm{K} = 3$. The errors are varied due to the WiFi data fluctuations over sampling period. Most of the positioning errors with respect to antenna heights settled roughly at 2.33 meters. At height level H5 (2.12 meter), the positioning algorithm works the best with the minimum probability error at less than 1 meter with 0.65 probability compared to the other four height levels. That being said, we could perceive that the positioning errors might be reduced at this particular height. This is due to the fact that this

is the highest level of antenna height, and therefore the angle of multipath signal is even throughout the experimental area. Hence, the better cumulative errors.

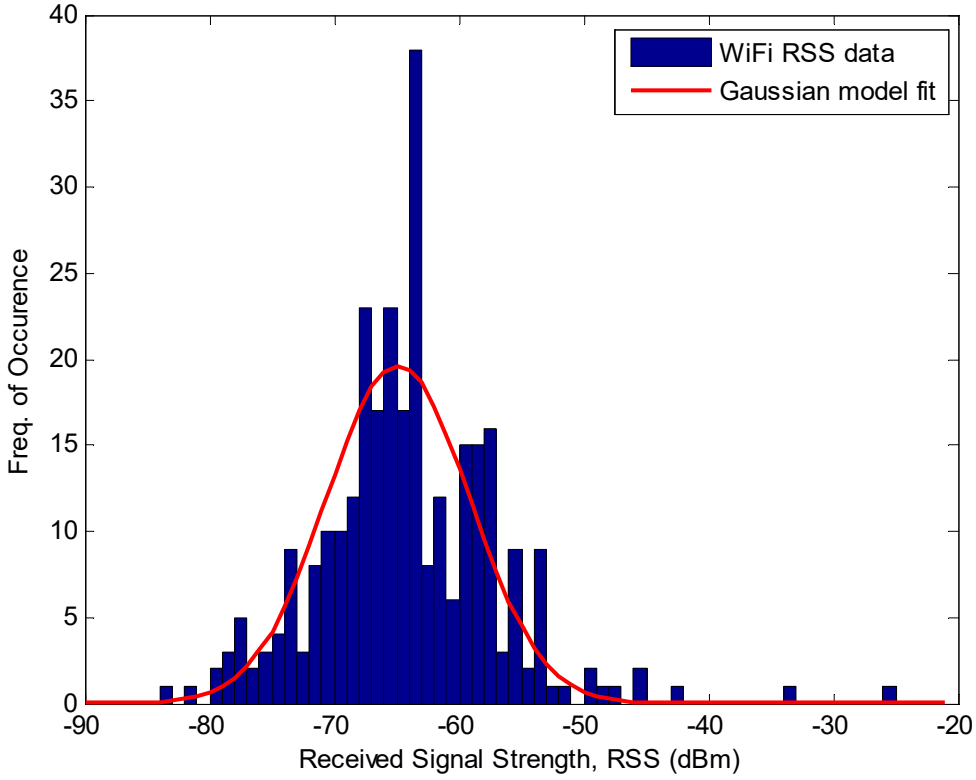

Figure 4.6: Distribution of WiFi RSS data of the fingerprinting database

Table 4.4: The effect of K parameter with respect to the different antenna height levels.

K	Average positioning error (meter)					SD (σ)
	H1 (1.02m)	H2 (1.22m)	H3 (1.52m)	H4 (1.82m)	H5 (2.12m)	
1	3.41	3.07	3.44	2.83	2.21	0.51
2	2.29	2.13	2.50	3.34	2.88	0.49
3	2.27	2.21	2.43	3.01	2.21	0.34
4	2.42	2.37	2.64	3.11	2.13	0.36

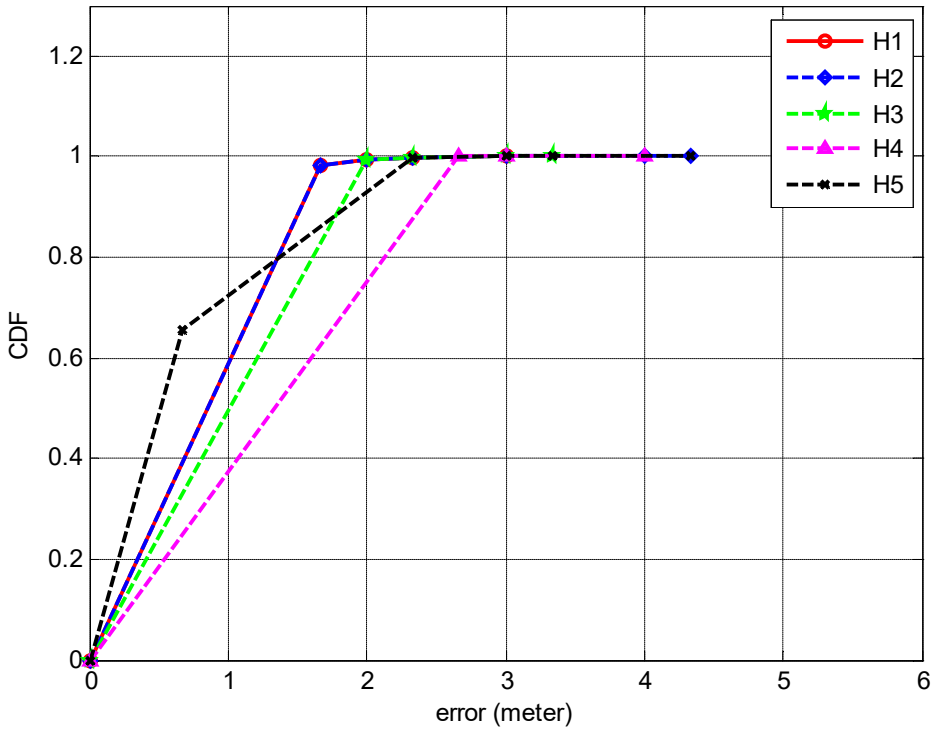

Figure 4.7: Cumulative Distribution Function (CDF) of the positioning error for the five different antenna heights level

4.7 Conclusion and Summary

The wireless positioning system for a mobile robot application is an interesting choice due to its cost effectiveness. In this works, we proof that the transmitter heights are not significant for mobile robot fingerprinting database by both statistical analysis and actual positioning experiments. Hence, it is much more importance to concentrate on the distance between the transmitter and the receiver. That being said, we could place the WiFi AP literally at any heights with the use of omnidirectional antenna for both transmitter and receiver, presumably from 1.02 meter to the ceiling height at 2.50 meter as in this experimental condition.

The proposed measurement strategy i.e. the randomized measurement order by means of Design of Experiment (DoE) is a relevant and good technique in order to avoid outlier measurement data. Moreover, randomized measurement order could be used to get a decent, outlier-free database. In addition, such strategy is the first time being employed in this field.

The experimental data were analyzed using statistical analysis i.e. the ANOVA. The ANOVA for antenna heights is higher than significant level, α while the ANOVA for Tx-Rx separation is lower than significant level, α. The interaction between antenna heights parameter and Tx-Rx separation distance is also not significant since it has larger value than is significant level, α. Hence the antenna heights and its interaction possesses no affect towards the positioning system of a mobile robot in an indoor environments as specified in the research conditions.

The ANOVA results were further validated using the actual positioning technique where WKNN algorithm is used to match the location data of those in the fingerprinting database. The results showed and proved that the transmitting antenna heights have no significant effects to the mobile robot positioning error whereas the maximum height in the experiment yields in the minimum cumulative positioning errors. However, the generality is not guaranteed since this finding is limited to the research condition as specified in the earlier sections.

Chapter 5 WPS USING FINGERPRINTING TECHNIQUE

"*The starting point of all achievement is desire*"

- Napoleon Hill, 1930s

5.1 Introduction

Generally, the Wireless Positioning System (WPS) can be realized using two different techniques. The first technique, known as trilateration or triangulation requires the knowledge of the transmitting sources and the inferences about the signal such as the angular, or the distance. Then the positioning system is computed using geometrical solution. However, since no accurate modeling of the signal is available, attainment of the correct distance values often lead to high error and offers bad reliability. Moreover, expensive modification of the transmitting sources is needed in the case of triangulation technique.

The fingerprinting technique on the other hand works by matching the unknown signal to the signal 'fingerprint' (radio map) that is recorded beforehand. Since this technique revolves in the area of recording floor map, then the result is usually better than the trilateration/triangulation technique. However, fingerprinting technique has one obvious problem, which is the signal fingerprint recorded beforehand requires tremendous amount of effort and workload as well as time consuming. Hence, a solution must be sought to tailor this problem.

This chapter presents the works taken related to solving the problem in fingerprinting technique.

5.2 Fingerprinting Methodology

The wireless signal fingerprint may be derived from the similar words as the human finger prints. Human fingerprint is unique, every person have different fingerprints. Such uniqueness is an important measure for security purpose for instance the recovery of fingerprints from a crime scene in the forensic science studies and the biometric fingerprint registration in automated fingerprint authentication system. Biometric fingerprint authentication system has become standard in today's technology, for instance their integration into cheap and affordable smartphones.

Such characteristic can be also applied to the wireless signal granted that at each designated location, the wireless radio signal has a unique signal 'fingerprint'. That being said, if a positioning system has a vector of signal fingerprint database at the designated location, then a matching with unknown signal strength can be made during online measurement so that the estimated location is returned from the designated location. This fingerprinting positioning technique is depicted in Figure 5.1. In the training phase, a laborious effort is needed to create the signal fingerprint database. At n $\{n \in \mathbb{R}, n = 1,2,\ldots n\}$ pre-defined training locations, where training locations are the spatial Cartesian coordinate in the form of (x,y), the average of the signal strength received from p WiFi Access Points (AP) are recorded and stored.

In the positioning phase, when the mobile robot is at unknown location, the measured WiFi signal receivable from the p AP can be match to those in the database. The RSS matching can be in term of shortest distance denotes by any distance metric. Then the estimated location is returned at the particular distance.

In general, the positioning accuracy depends on many factors such as the reliability of the online signal and more importantly the size of the database. With a larger database, one could foresee that the positioning accuracy will increase since larger database means higher number of designated reference locations. One problem is that the larger database also means that the effort needed to collect the signal fingerprint is inevitably increased. Hence, the challenges.

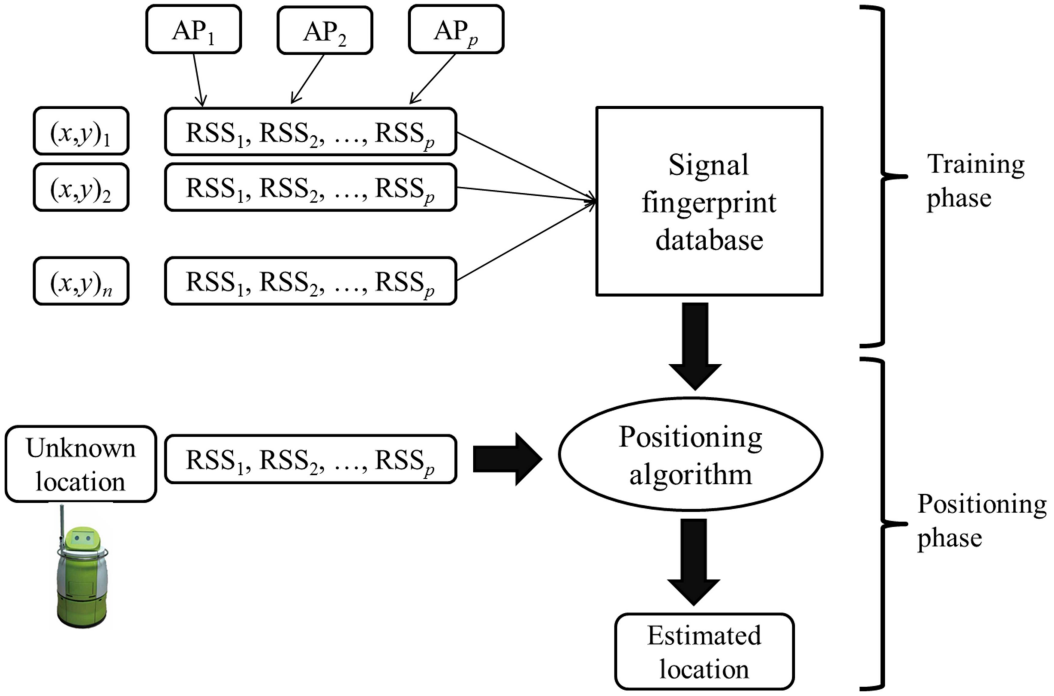

Figure 5.1: Mobile robot positioning model using the fingerprinting technique

5.2.1 Floor Map Granularity

The floor map granularity can be defined as a scalar that equally gridded the floor map into a particular spacing. For instance, consider a floor map of $M \times N$ size, then a 1 meter spacing could yield in MN number of database in that particular floor. This level of granularity requires the user to make the WiFi RSS observation for MN times. Thus, if the higher granularity level is required, the more efforts are needed to make the observations.

The higher level of granularity is however much desirable to yield satisfactory positioning accuracy [66]. Hence, it is suggested to have higher level of floor map granularity i.e. smaller spacing between the locations in the database. Table 5.1 tabulated the size of database location in a 30×16 meter area. It can be seen that the higher level of granularity will yield in higher database size, thus the efforts needed to collect the RSS at these locations will increase as well.

Table 5.1: The size of database according to the granularity level in the 30×16 meter area space.

Granularity level (meter spacing)	Size of the database
4	120
2	240
1	480
0.5	960
0.25	1,920

5.2.2 WiFi Signal Fingerprint Database

The signal fingerprint (radio map) database is the vital part in this works. A common radio map database contains information such as the spatial coordinate of a particular location and their corresponding RSS. The signal received from the *p* WiFi AP is typically identified using their Service Set Identifier (SSID) or Basic Service Set Identifier (BSSID).

To avoid large signal interferences, it is ideal to assign non-overlapping channel to the WiFi access point. In this research works, three WiFi APs are chosen to be used for the positioning system. Thus, the ideal non-overlapping channels such as the channel band 1, 6 and 11 can be used. These non-overlapping channel selections are shown in Figure 5.2. The use of three WiFi access point with the non-overlapping channels assignment theoretically is able to reduce the 2.4GHz spectrum interferences as much as possible.

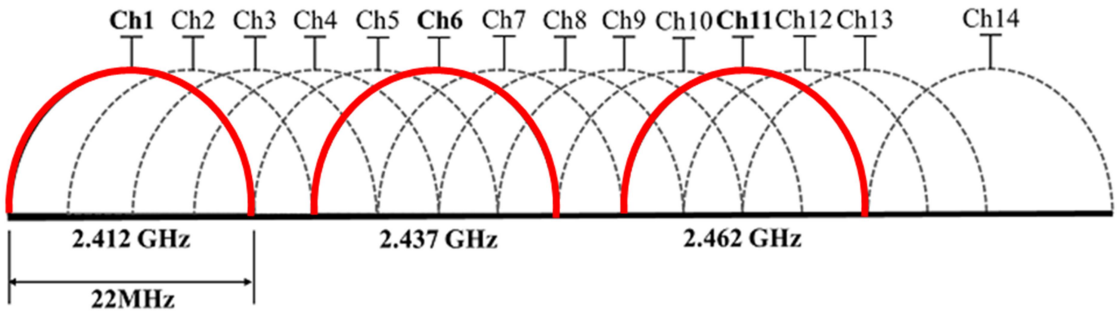

Figure 5.2: The WiFi 802.11 channels in 2.4GHz spectrum

At any locations, a series of WiFi RSS data can be observed and recorded. Due to the wireless signal fluctuations nature, it is often suggested to use the average of the signal strength for the database. It is in fact practical to store the database *v* in vector tuple form given in

$$v = \left[\bar{z}_i^{\,p} \; L_i \right]^T \qquad \text{(Eq. 5-1)}$$

, where $\bar{z}_i^{\,k}$ is the vector of the average of WiFi received signal strength at *i*-th location of AP *p*. These *i* location can be described as L_i in Cartesian space comprising of location coordinate *x* and *y*, respectively.

5.2.3 WKNN Positioning Algorithm

The Weighted K Nearest Neighbor (WKNN) algorithm is often regarded as the state-of-the-art in the deterministic wireless positioning system [61][76][77]. The basis of WKNN algorithm is the nearest neighbor (NN) algorithm, where the rule identifies the category of an unknown data point on the basis of its nearest neighbor whose class is already known (fingerprint database) [78]. However, the most nearest neighbor does not always guarantee the best result since the quantity of measurement might be different in the training data. Instead, the surrounding neighbors in the sense of K neighbors are taken into consideration as illustrated in Figure 5.3.

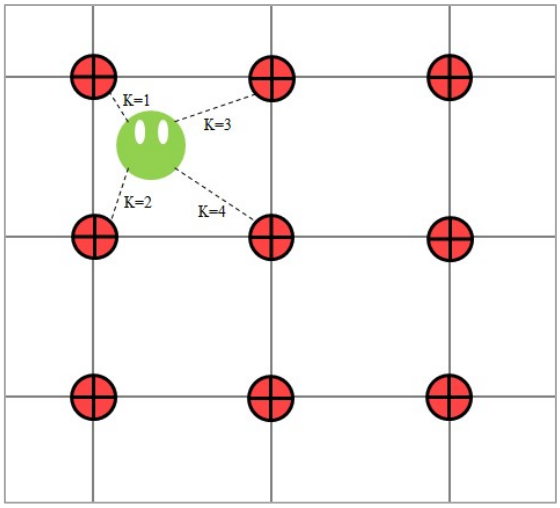

Figure 5.3: An illustration of K-NN algorithm

Given a complete signal fingerprint database at an area, WKNN method estimates the location by searching the best matching fingerprints in the database. It is natural to use distance measured between the signal received from an unknown location to the database, such as finding the nearest neighbor (NN) using the distance norm ℓ as stated in

$$d_j = \frac{1}{N_p}\left(\sum_{i=1}^{M}\left|z_u{}^p - z_i{}^p\right|^{\ell}\right)^{\frac{1}{\ell}}, \qquad \text{(Eq. 5-2)}$$

where N_p is the total number of WiFi AP, $z_u{}^p$ is the unknown WiFi RSS data, and $z_i{}^p$ is the observed and interpolated database $\{i = 1, 2, \ldots, MN\}$ from p WiFi AP, MN is total number of database defined by the level of granularity. However, as explain before this idea is rather prone to noisy samples which show unpredicted errors. Therefore, instead of taking the nearest neighbor, surrounding neighbors around K can be used. To further increase the effectiveness of the matching algorithm, a weightage λ can be included as a function of inverse distance to emphasize the significant of 'close' neighbors while neglecting those 'far' neighbors.

By matching the unknown of location of known WiFi RSS to the database, the estimated location can be computed as

$$\left(\hat{X}, \hat{Y}\right) = \sum_{j=1}^{K}\left[\lambda_j \times (X_j, Y_j)\right], \qquad \text{(Eq. 5-3)}$$

where $(\hat{X}, \hat{Y})$ is the estimated location and λ_j is the weight of the corresponding data, which can be computed as

$$\lambda_j = \frac{1/d_j}{\sum_{j=1}^{K} 1/d_j}. \qquad \text{(Eq. 5-4)}$$

5.3 The Need of Database Interpolation

In previous sections, it has been justified that a larger size of database is required in order to obtain a better positioning accuracy. However, a tremendous amount of workforce and time are needed since recording the signal fingerprint is a laborious works. This issue has become a problem when enormous efforts are required to collect the RSS. Thus, in order to reduce the workloads, signal interpolation is proposed where the measurements are made at small number of locations, and interpolated at the other locations. The WiFi RSS could be reasonably interpolated since the value at observed locations provides not only its own value, but also its surrounding values with respect to the transmitting sources.

Interpolation of the wireless signal has been proposed by several related literatures. The more conventional interpolation method is known as the inverse distance weighting (IDW). The IDW method can be considered as conventional multivariate interpolation algorithm since many literatures compared their technique to the IDW, which is hassle-less to implement. Lee and Han [79] proposed a unique interpolation method called Voronoi tessellation method where the core idea is to use a signal propagation model such as Log-Distance Path Loss (LDPL) model. This method neatly estimates the parameters of the signal propagation model, which conversely prone to signal fluctuation problems. Other method such as linear interpolation [80] and Radial Basis Function (RBF) [81] are also proposed to find the missing fingerprint data. An interpolation of missing data near to wall which abruptly absorbs wireless signal is studied in [82] where adaptive smoothing algorithm is proposed to solve the absorption problems. A color based interpolation has been proposed in [83] where colors are assigned accordingly to the signal strength and later interpolated on the verge of mixed colors corresponding to the pixel values.

Recently, a geostatistical based interpolation i.e. Kriging algorithm has emerged and being popular for WiFi missing data interpolation [66][84][85]. Kriging is a well-known interpolation method particularly in the environmental and geospatial science, where the application is on regular basis with several programming toolbox. Kriging algorithm has found a way into wireless signal interpolation in recent years, and claimed reputable outcomes over many other mathematical interpolation methods. However, due to the diverse techniques in Kriging algorithm such as Simple Kriging, Ordinary Kriging, Co-kriging to name a few [86], one may find no Kriging is superior to other Kriging. Moreover, data sparsity may affect the Kriging variogram dramatically [85] prior to separation distance between the transmitter and receiver.

5.4 WiFi RSS Interpolation Methods

The interpolation methods introduced in previous sections are nonetheless focus on the creating a larger signal fingerprint database in order to obtain better positioning results. In this dissertation, a variation of IDW method is proposed for interpolation and later improvised using a novel method known as the Signal-Propagated Modified Shepard Method (SP-MSM) and the comparison is made with the conventional IDW method as well as the recently popular stochastic Ordinary Kriging algorithm.

5.4.1 Inverse Distance Weighting (IDW)

The inverse distance weight (IDW) interpolation is a famous method employed in many interpolation literatures tracking back from its history in 1968 [87]. IDW is often regarded as the conventional interpolation method and served as a baseline for interpolation comparison. In the sense of generating the WiFi RSS fingerprinting, the relation between the measured/observed locations to the interpolated location is on the distance basis.

If $z(x_i)$ represent the measured WiFi RSS at location pair x_i $i = 1, 2, ...N$, then the global interpolation function at known location x_k is given as

$$\hat{z}(x_k) = \sum_{i=1}^{N} W_i z(x_i), \qquad \text{(Eq. 5-5)}$$

where the interpolation weight W_i is given as

$$W_i = \frac{1/d_i^{\,p}}{\sum_{i=1}^{N} 1/d_i^{\,p}} \qquad \text{(Eq. 5-6)}$$

One can see that the distance between the interpolation and measured location is inversely related, thus inverse distance notation. Parameter p denotes the power parameter that effect on the neighboring location i.e. larger p has greater influence to values closest to the interpolated location.

5.4.2 Kriging Algorithm

The Kriging algorithm originated from Danie G. Krige, who is the pioneering plotter of distance-weighted average gold grades at the Witwatersrand reef complex in South Africa. Krige sought to estimate the most likely distribution of gold based on samples from a few boreholes. The methods were then improved over times. Unlike IDW where the interpolation is solely on distance basis, the Kriging method works by modeling the spatial correlation between measurement values to construct variogram. Then, the values at unknown locations can be interpolated based on the fitted model function from the variogram yielding the Kriging weight. Figure 5.4 shows the flowchart of the Kriging algorithm employed in many research works.

Variogram can be defined as the variance of the difference between field values at two locations x and y across realizations of the field. It is the fundamental prerequisite for Kriging interpolation method. Assuming the spatial random variable have a correlation between relative locations, the theoretical semivariance γ is given by

$$\gamma(h) = \frac{1}{2} Var\left[z(u_i) - z(u_j) \right] \quad \text{(Eq. 5-7)}$$

, where h is the distance between points u_i and u_j, Var is the variance and $z(u)$ is the WiFi RSS data at location u. Then the experimental semivariance $\hat{\gamma}$ is mathematically estimated from the actual WiFi RSS measurement data as in

$$\hat{\gamma}(h) = \frac{1}{2N(h)} \sum_{N(h)} \left[z(u_i) - z(u_j) \right]^2 \quad \text{(Eq. 5-8)}$$

,where $N(h)$ is the number of pairs of sample locations separated by h. Hence at present, both theoretical and experimental variogram are available, and variogram can be drawn on a plot of γ against h, shown in Figure 5.5.

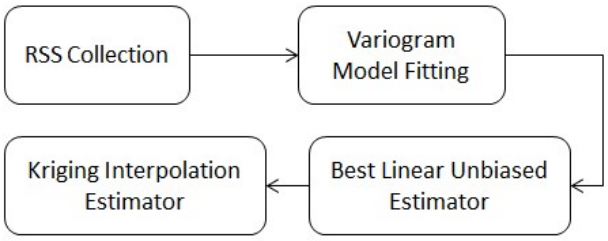

Figure 5.4: General flowchart of the Kriging algorithm [84]

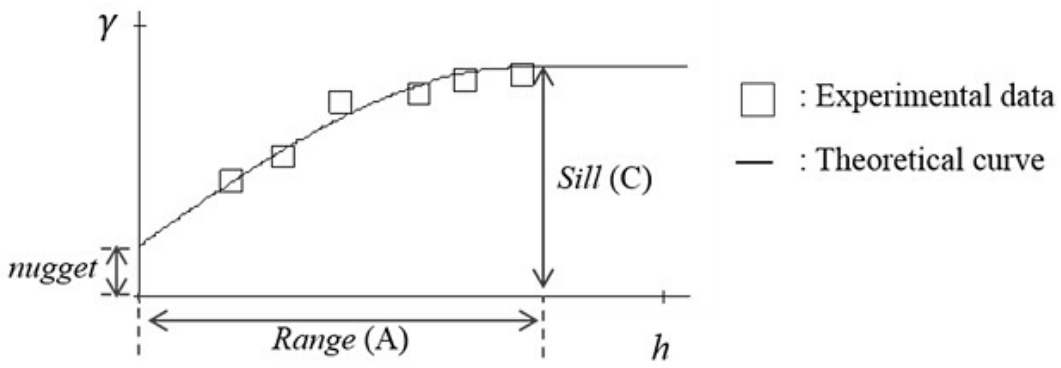

Figure 5.5: A typical variogram showing the experimental data and theoretical curve [84]

This variogram however contains value at limited number of separation distance *h*. In order to interpolate the WiFi RSS at an unknown location, the access to *h* between scattered locations in the variogram is needed. Therefore, a mathematical model will be fitted to the variogram, where the parameter 'A' and 'C' resulting from the variogram are used. Range 'A' is the influence of range in the experiment, and sill 'C' is the critical variance in the influence range [84][85]. The fitted models are usually chosen namely *Exponential* model, *Spherical* model, and *Gaussian* model [88].

Once the variogram has been fitted using these models, the next step is to formulate the function of an unbiased estimation with minimum error variance at the unknown locations. The Kriging estimators satisfy the Best Linear Unbiased Estimate (BLUE). Then, similarly to the IDW interpolation method, the Kriging algorithm estimates the RSS value, $\hat{z}$ at an unknown location u_0 as a weighted sum of *n* known neighbor RSS data $u_i \; i = 1,2,\ldots,n$ as in (Eq. 5-9).

$$\hat{z}(u_0) = \sum_{i=1}^{n} \lambda_i z(u_i) \qquad \text{(Eq. 5-9)}$$

where λ_i are the Kriging weight given by

$$\begin{bmatrix} \lambda_1 \\ \vdots \\ \lambda_n \\ L \end{bmatrix} = \begin{bmatrix} \gamma_{1,1} & \cdots & \gamma_{1,n} & 1 \\ \vdots & \ddots & \vdots & \vdots \\ \gamma_{n,1} & \cdots & \gamma_{n,n} & 1 \\ 1 & \cdots & 1 & 0 \end{bmatrix}^{-1} \begin{bmatrix} \gamma_{1,u} \\ \vdots \\ \gamma_{n,u} \\ 1 \end{bmatrix} \qquad \text{(Eq. 5-10)}$$

where L is the Lagrange multiplier, $\gamma_{i,j}$ is the variogram value between the i-th and j-th neighbor, $\gamma_{i,u}$ is the variogram value between the i-th neighbor and at the interpolation location. A proper derivation of Kriging weights is neatly explained in [85].

Then, the (Eq. 5-9) satisfies the BLUE in

$$\mathbb{E}\left[\hat{z}(u_0) - z(u_0)\right]^2 = 0 \qquad \text{(Eq. 5-11)}$$

and has the minimum variance as in

$$\min\left\{Var\left[\hat{z}(u_0) - z(u_0)\right]\right\} \qquad \text{(Eq. 5-12)}$$

Despite the heavy computation needed for Kriging algorithm, it has been demonstrated that this algorithm works well especially in the case or regular-shaped data sparsity [66][84]. It is however, may be jeopardized in the event of irregular-shape data sparsity as such required by WiFi fingerprinting database since the variogram model fitting may be affected [85]. A full derivation of Kriging weight is presented in the Appendix section of this thesis.

5.4.3 Modified Shepard's Method (MSM)

The IDW interpolation method has several disadvantages despite its simplicity which is considering weights even for the far reference nodes making it global interpolant. This may result in problems in the presence of distant outliers. The Modified Shepard's Method (MSM) [89] solved this matter by assigning radius of influence over the neighbors, R_w making it local interpolant. Moreover, the interpolation is no longer dependent of neighbor's RSS, but it introduces the nodal function Q that yield from multiple regression function between the observation locations. These two factors i.e. the radii of influence and the used of nodal function are the main difference between MSM method and other methods such as the IDW and Kriging algorithm.

In general, the interpolation methods including the MSM method requires the reference data which is the WiFi RSS collection at designated locations, locally known as Reference Locations (RL). However, MSM interpolation function requires the nodal function in the RL instead of the RSS. The nodal function is calculated at each of the RL on the relationship between the neighbors delimited by the radii of influence in the reference locations. After the nodal function has been obtained, then the interpolation can be made to the targeted interpolation locations, also delimited by the radii of influence in the interpolant.

The formulation of the MSM for WiFi RSS interpolation is as follows;

If $f = f(x,y)$ denotes the underlaying real functions with known RSS values z_i^k at known location $(x_i, y_i), i = 1,2,3,\ldots N$, then the general MSM interpolant is given by

$$\hat{z}(x,y) = \frac{\sum_{i=1}^{N} W_i(x,y) Q_i(x,y)}{\sum_{i=1}^{N} W_i(x,y)}, \qquad \text{(Eq. 5-13)}$$

where $\hat{z}(x,y)$ is the interpolated RSS at known location (x,y), W_i and Q_i are respectively the MSM weight and nodal function of the RL $(x_i, y_i), i = 1,2,3,\ldots N$. Contrary to IDW which well-known as global interpolant, MSM is reputed as local interpolant since the computation is within the radii of influences. The two radii of influences R_q and R_w are defined as the radius of influence in the reference location and the radius of influence in the interpolant, respectively given as

$$R_q = \frac{D}{2}\sqrt{\frac{N_q}{N}}, \quad R_w = \frac{D}{2}\sqrt{\frac{N_w}{N}} \qquad \text{(Eq. 5-14)}$$

, where D is the maximum distance between observation locations and N is the total number observation locations. The scalar value N_q and N_w are the tunable parameters that could be interpreted as number of required reference data to lie within the radii of influences. If these parameters have small values, then the local shape is maintained and if it bigger enough to be equal to N, then it will become global interpolant. However, for a dense environment or sparsely populated dataset, or when the dataset is relatively small, the use of the relationship $N_q / N_w \sim 2$ is useful [90]. In addition, proper selection of these parameters can be made to reflect the nature of the wireless propagation channel [91]. Figure 5.6 illustrated the radius of influence in the RL where in this example, only three RL are taken into consideration for computation of the nodal function resulting in three linear equations.

Having defining the radii of influences, we will proceed to compute the weight in the reference location (RL). This weight calculation is solely based on the data that are sampled inside the radius of influence. The weight similar to the IDW is inversely related to the distance function ρ_i given as

$$\frac{1}{\rho_i} = \frac{\left(R_q - d_i\right)_+}{R_q d_i} \qquad \text{(Eq. 5-15)}$$

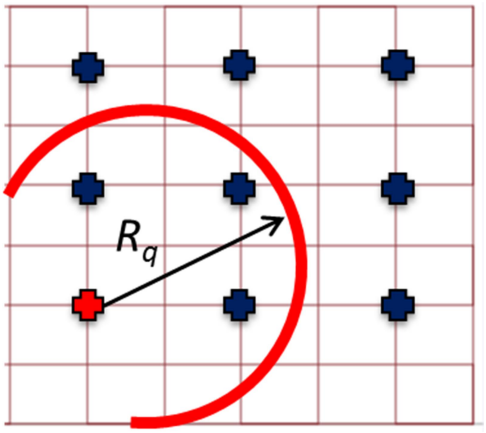

Figure 5.6: Illustrations of the radius of influence in the RL

with d_i being the Euclidean distance between the calculated RL to the i-th neighbors. The subscript + in the (Eq. 5-15) denotes only the positive part of the quantity concerned i.e.

$$(R_q - d_i)_+ = \begin{cases} R_q - d_i & \text{if } (R_q - d_i) \geq 0 \\ 0 & \text{otherwise} \end{cases} \qquad \text{(Eq. 5-16)}$$

Hence the weight W_i is zero at distance greater than R_q, or specifically at the boundary of the circle surrounding (x,y). Afterwards, the nodal function at RL which is delimited by the radius R_q can be computed. For each nodal points $(x_k, y_k); k = 1, 2, \ldots, N$, nodal function Q_k is defined by

$$\begin{aligned} Q_k(x,y) &= c_{k1}(x - x_k)^2 + c_{k2}(x - x_k)(\mathrm{y} - \mathrm{y}_k) \\ &+ c_{k3}(\mathrm{y} - y_k)^2 + c_{k4}(x - x_k) + c_{k5}(\mathrm{y} - y_k) + z_k. \end{aligned} \qquad \text{(Eq. 5-17)}$$

The multiple regression function is solved using Gaussian elimination method in order to obtained the coefficients $c_{kj}; j = 1, 2, .., 5$ that minimizes

$$\begin{aligned} &\min_{c_{kj}, j=1,2,\ldots 5} \sum_{\substack{i=1 \\ i \neq k}}^{N} \frac{1}{\rho_i^2(x_k, y_k)} \Big[c_{k1}(x - x_k)^2 + c_{k2}(x - x_k)(\mathrm{y} - \mathrm{y}_k) \\ &+ c_{k3}(\mathrm{y} - y_k)^2 + c_{k4}(x - x_k) + c_{k5}(\mathrm{y} - y_k) + z_k - z_i \Big]^2. \end{aligned} \qquad \text{(Eq. 5-18)}$$

As a summary at presents, we have obtained several information such as the RL location and its' associated RSS, and also the nodal function at the RL. Therefore, the next step is to construct the fingerprinting database in sense of interpolation by using abovementioned information.

In order to interpolate the unknown RSS at a location $\hat{z}(x,y)$, (Eq. 5-13) and the nodal function in (Eq. 5-17) are used. The interpolant weight W_k that relates to the distance function d_k can be computed similar to (Eq. 5-15) where the observation locations are within by the radius of influence R_w. This weight can be written as

$$\frac{1}{d_k(x,y)} = \frac{(R_w - d_k)_+}{R_w d_k}, \qquad \text{(Eq. 5-19)}$$

where $d_k(x,y) = \sqrt{(x-x_k)^2 + (y-y_k)^2}$. Similarly as described in (Eq. 5-16), only the positive part of the weights which is denoted by the subscript $+$ is taken into consideration prior to the choice of N_w.

5.5 Interpolation Database Assessments

5.5.1 Experimental Set-up

In order to access the effectiveness of the proposed interpolation method, experiments have been conducted. The experiments are conducted at the second floor of Center for Human-Robot Symbiosis Research, Toyohashi University of Technology. Figure 5.8 shows the locations of observation and the point of sampling. The sampling location is totally random but in a classical regular-spaced fashion as a countermeasure of the signal multipath issues. Three WiFi APs are used, where AP 1 and 2 have a clear line-of-sight (LOS) while AP 3 is obstructed by a horizontal wall as well as randomly close and open door. The observation locations on the other hand are sampled at locations marked with '×' symbol, the test location marked with 'o' symbol and the red box represents the interpolation area. This is indeed a dense area since this is the experimental area for Terapio mobility. However, the interpolation technique can be easily extended into larger area provided that enough observation samples are available.

The experimental is set-up similarly as previously in Chapter 4. The WiFi AP used is the high power Alfa AIP-W525H dual antenna with 5dBi gains each. The receiver used is embedded in the mobile robot which is the omnidirectional ALFA AWUS036NHR V2. For the WiFi APs, the set-ups is built such as none network security, default MAC from Alfa Inc. was used, and network channel set to channel 1, 6 and 11

respectively. The nominal frequency for this AP is 2.4GHz. Access to worldwide internet is disabled since such connection is not required. Again Homedale® [73] wireless surveillance open source code is used to record the wireless strength data in the interval of 2 seconds running in Windows 10 operating system. The use of 2 seconds interval is adequate to obtain reliable RSS data for the experiments.

5.5.2 Positioning at Mid-Space and Near-Wall Location

In order to conduct a thorough analysis to the interpolation methods, two stationary test locations are chosen for evaluations which are at the mid-space and near-wall locations. Figure 5.7 depicted the actual RSS signal recorded at these two locations where fluctuative natures of the WiFi signal are clearly shown. The granularity level of the floor plan is set to five different levels as shown in Table 5.2.

Table 5.2: Granularity level applied in the experiments

Granularity level (meter spacing)	Total number of interpolation location
4	7
2	16
1	54
0.5	188
0.25	694

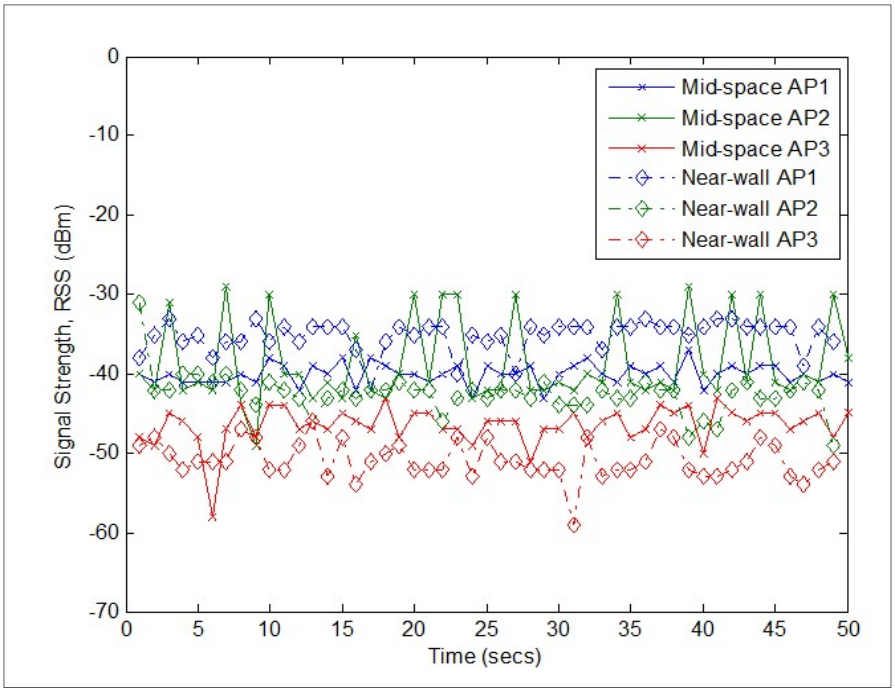

Figure 5.7: The WiFi test signal corresponding to the two test locations

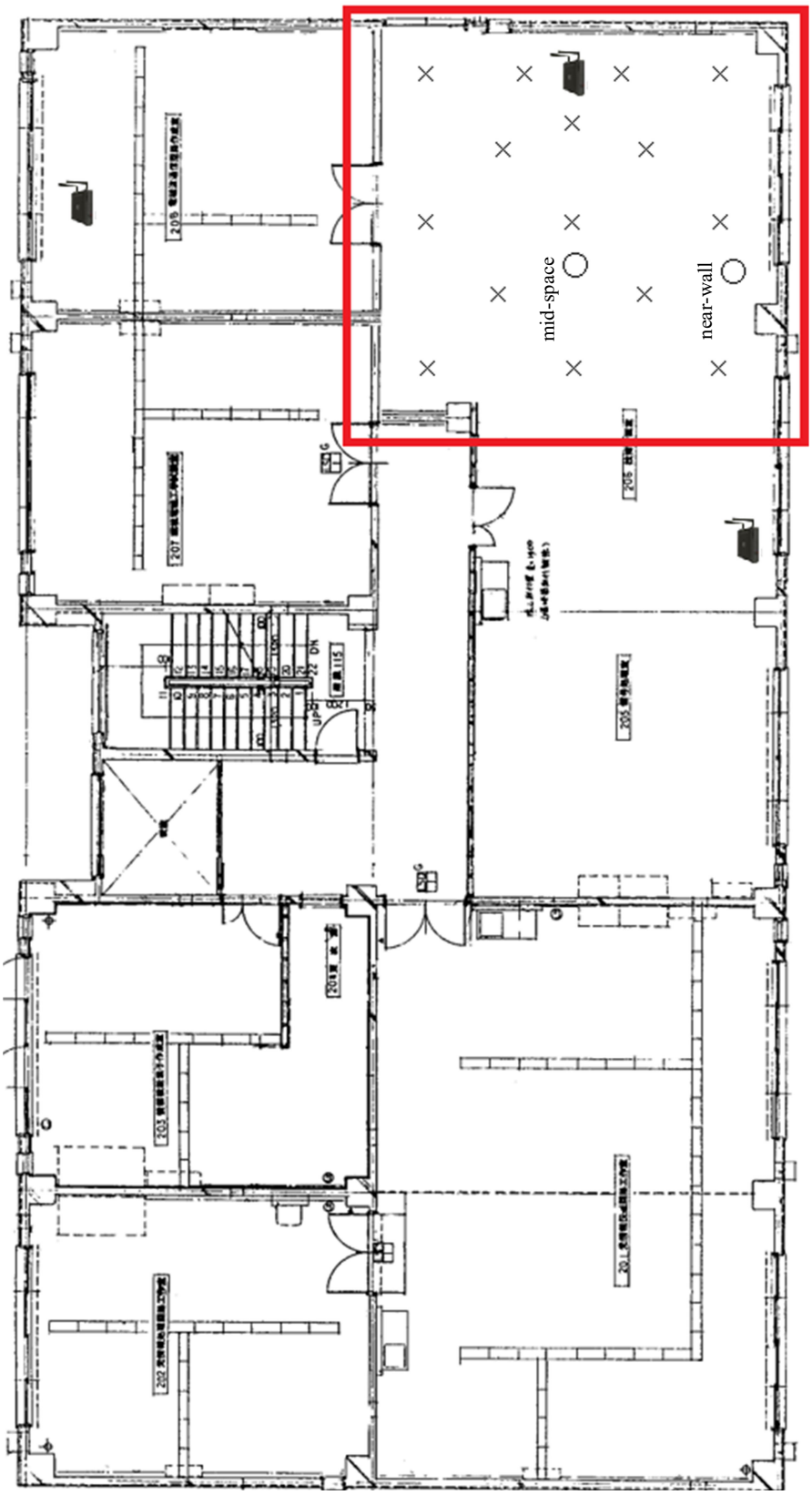

Figure 5.8: Experimental area where interpolations are taking place

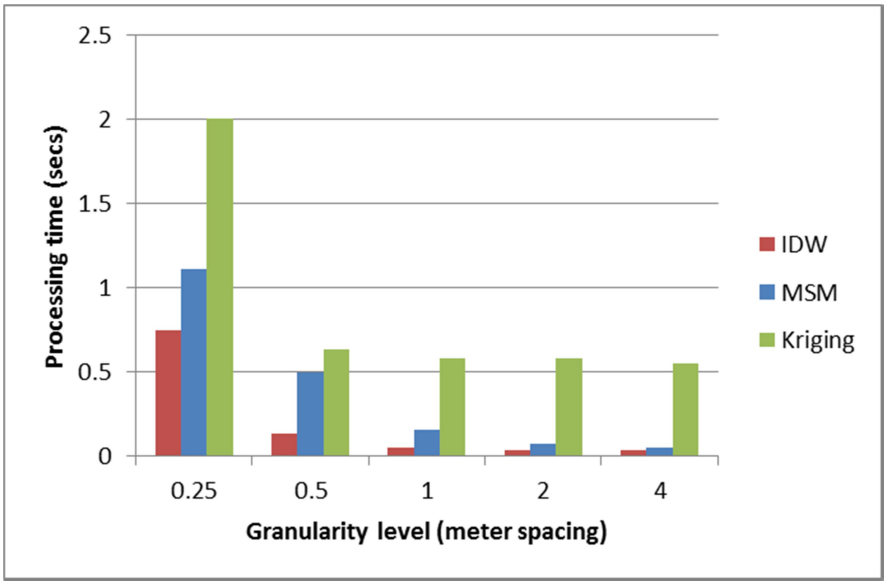

Figure 5.9: Interpolation processing time with respect to the floor plan granularity levels

Table 5.3: Stationary positioning error at mid-space and near-wall test locations

Interpolation methods	**Positioning error (meter)**	
	Mid-space	Near-wall
IDW	4.21	4.35
MSM	2.80	2.67
Kriging	3.41	4.16

Figure 5.9 compares the processing time between the interpolation methods for the WiFi RSS missing data which are the inverse distance weighting (IDW) method, the proposed Modified Shepard Method (MSM), and the Kriging interpolation method. For the Kriging algorithm, the Ordinary Kriging as discussed in [92] is used. As one may expected, with the higher level of granularity (smaller spacing between the interpolation locations), the processing time is also increase gradually despite the methods used. IDW has the lowest processing time due to its simplicity while MSM processing time is increases due to the nodal function computation. Kriging algorithm on the other hand requires pre-computation of the lag for variograms, contributing the high processing time. Henceforward, the discussions of the results are focus at 1 meter spacing of granularity level to ease the understanding.

Table 5.3 tabulated the average of static positioning error of the three interpolation methods focused at two essential test locations which are at mid-space and near-wall of the interpolation area with use of WKNN positioning algorithm at $K = 3$. The IDW method scored the highest error compared to the other two at both test locations at more than 4 meter. This is because the interpolated RSS are computed using all observation values albeit it has weightage function to discriminate further observations. The Ordinary Kriging algorithm surprisingly scored an averaged result despite its popularity as interpolation method. Kriging method also performed poorly at the near-wall test location as a result of imperfect variogram spherical model fitting. However, the Kriging method can be improved by several techniques which are by using other method of Kriging such as Universal Kriging, or by fitting the variogram using other fitting model such as exponential or more aggressively Gaussian model in the cost of higher processing time. The propose method for WiFi RSS using Modified Shepard's Method scored the lowest positioning error in our experiments, at both of test locations. This might be yielding to the radii of influence parameters that actually clustered surrounding neighbors for computation of nodal function, Q that represent the RSS regression relation between observation and interpolation locations. It is also worth to mention that MSM is mathematically easier to compute compared to the Kriging algorithm.

Figure 5.10 on the left hand side show the individual positioning result at mid-space and near-wall test location over the sampling period respectively. It can be observed, that at both locations, the MSM method works better the other two methods. In the mid-space test locations, the positioning error with respect to sampling period shows that there are several times that IDM or Kriging works better than MSM. This is caused by the signal spikes due to dynamic and changing environment such as people walking around and opening/closing the doors. However, in the near-wall test location, MSM method utterly outperforms the other two methods. It is indeed particularly useful to observe the positioning errors as a cumulative error distribution function (CDF). The error distribution function is the probability that a normal function variate in the range of [0,1], or can be explain as the probability at which specific error occurred, given by

$$CDF(d) = \frac{2}{\sqrt{\pi}} \int_0^d error^{-t^2} dt. \qquad \text{(Eq. 5-20)}$$

That being said, the probability of positioning error at some definite distance of error can be perceived depicted by Figure 5.10 on the right hand side. At the mid-space test location, the CDF for all three methods are likely to similar although MSM method is slightly better than the other two. At the near-wall test location, the proposed MSM method again outperform the other having a normal probability curve which is much better compared to the other two methods. The probability of error to occur is at 2.6 meter, 3.3 meter and 3.3 meter for MSM, IDW and Kriging respectively. Therefore it can be conclude MSM is a better method for WiFi RSS interpolation.

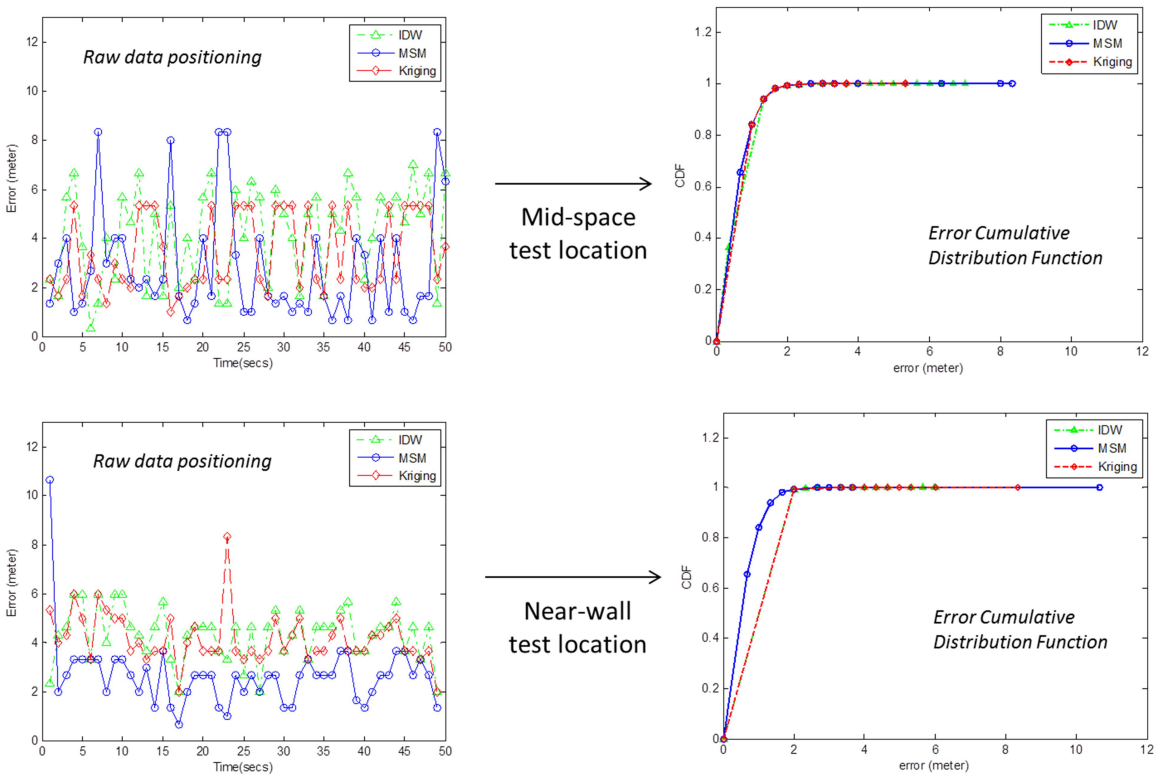

Figure 5.10: The positioning error of the two test locations and their corresponding error cumulative distribution function

Figure 5.11 presents the average positioning error with respect to the granularity levels at mid-space and near-wall test locations, respectively. At a high granularity level, for instance 4 meter spacing, the number of interpolation locations is considerably small. Looking at this fact, the proposed MSM method could perform badly due to the existent of the radii of influence that might have insufficient observation samples in order to calculate the nodal functions. This phenomenon is not much problems for mid-space test locations since it has a sound number of observation locations surrounding it. At the near-wall test location however, MSM perform very well at low spacing level i.e. below than 2 meter but perform badly at higher spacing such as at 4 meter, and likely beyond that. This might be the shortcomings of MSM's radii of influence that failed to taking into account the valuable amount of observation samples. Nevertheless, we presume that 4 meter spacing is too big for mobile robot application and 1 meter spacing is actually a practical spacing since the base of mobile robot Terapio is roughly 0.5 meter in size.

Finally, Table 5.4 summarizes the effectiveness of the interpolation methods in this works. IDW method despite its simplicity and low processing time has worst effectiveness compared to the other two. The Kriging algorithm has fair effectiveness but requires high processing time as well as complex mathematical

formulation. The proposed MSM method however, has a good effectiveness with medium algorithm complexity and processing time thus showed the merit of the proposed interpolation algorithm in order to automatically construct the fingerprinting database for the wireless positioning system.

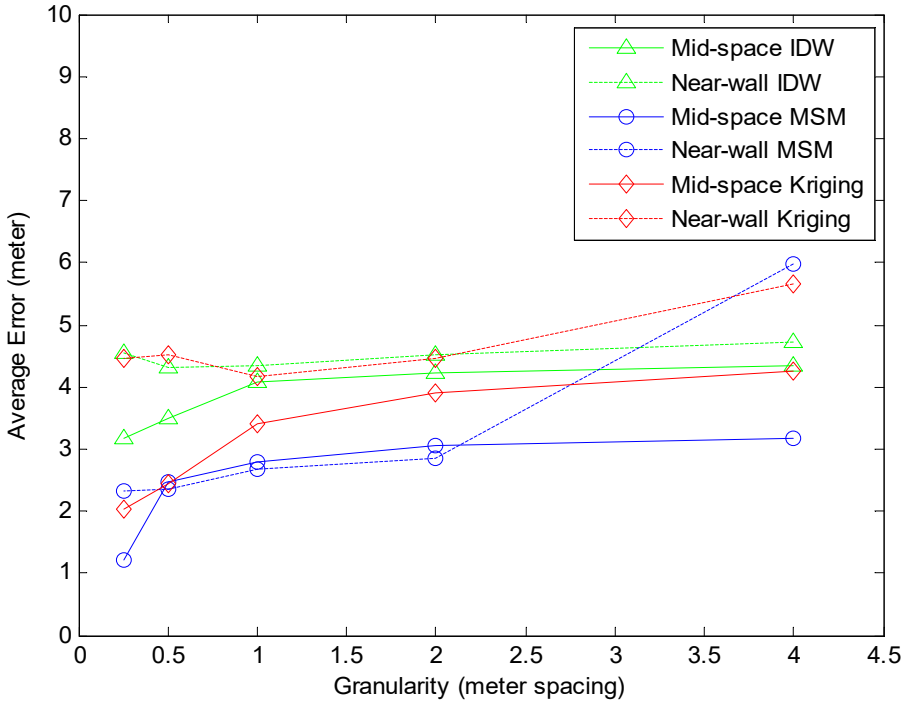

Figure 5.11: Average positioning error with respect to the floor plan granularity levels

Table 5.4: Comparison of the applied interpolation methods

Interpolation Method	**Complexity**	**Processing time**	**Effectiveness**
IDW	Simple	Low	Bad
MSM	Medium	Medium	Good
Kriging	Hard	High	Fair

5.6 Novel Method: Signal Propagated Modified Shepard's Method (SP-MSM)

In the previous sections, a details explanation of fingerprinting database creation and their effectiveness towards stationary positioning at mid-space and near-wall test locations are presented. In addition, the technical background of wireless fingerprinting techniques such as the granularity of floor levels, the WKNN positioning algorithm and the three interpolation methods (IDW, Kriging, and MSM) has been also discussed. These three interpolation methods as well as the mathematically interpolation methods such as the linear, spline and polynomials interpolation, similarly with more sophisticated methods such as the RBF and NN methods, were mainly based on spatial or mathematical data. That being said, these data are the independent data where the source(s) of data are relatively unknown for instance the rain quantity or the quality of the earth soils.

On the contrary, the source of wireless signals i.e. the location of WiFi transmitters are always known or can be identified or computed using signal propagation path loss models [93]. Therefore, the interpolation method should be able to improve heuristically. In view of that, a novel method that combined the signal propagation model parameters with an improved version of IDW interpolation method, known as the Modified Shepard's Method (MSM) [89] is proposed. As a result, this new wireless signal interpolation method is called Signal-Propagated Modified Shepard's Method (SP-MSM). In addition, the wireless signal at all possible locations of the fingerprinting database in the mobile robot experimental area are collected and stored despite the heavy works. These wireless signal collected at all possible locations can be the ground truth of the reference locations where some of them can be removed and interpolated for database evaluation.

This section will explain the proposed method in details.

5.6.1 Mathematical derivation

The Modified Shepard's Method (MSM) for database construction and its mathematical derivation has been described previously in Section 5.4.3. The core advantage of MSM over other method is that it is a local interpolant, i.e. it does not consider distant neighbors by assigning a radius of influence from the interpolant. Moreover, the interpolation is no longer computed using neighbor's RSS data, instead MSM presents the nodal function Q that yields from multiple linear regression (MLR) function from the surrounding neighbors within the radius of influence. The MSM method is beforehand improved by including the parameter of WiFi signal propagation path loss model for instance the Log-Distance Path Loss (LDPL) which is estimated using Nelder-Mead simplex algorithm [79][94].

Taking the Log-Distance Path Loss (LDPL) signal propagation model for example,

$$P(d) = P(d_0) - 10n\log_{10}(d/d_0) \quad \text{(Eq. 5-21)}$$

,where $P(d)$, n, d_0, and $P(d_0)$ represents the RSS at distance d from the transmitting source, path loss exponent, close-in distance at typically 1 meter from the transmitting source and the close-in RSS at d_0, respectively. A details explanation of the path loss exponent and their suggested values has been tabulated earlier in Table 2.2. However, n cannot be simply chosen due to the complex signal propagation mechanism that leads to the need to estimate it, and similarly for $P(d_0)$. Inspired by [79], the Euclidean based estimation function for WiFi RSS at location $z_p(x,y)$ for d is defined as

$$z_p(x,y) = \hat{c}_k - 10\hat{n}_k \log_{10}\left(\sqrt{\left(x_p - x\right)^2 + \left(y_p - y\right)^2}\right) \quad \text{(Eq. 5-22)}$$

,where (x_p, y_p) is the location of the WiFi AP p, (x,y) are the location of the RL, $\hat{c}_k$ and $\hat{n}_k$ represents the estimated close-in RSS value and path loss exponent for AP p, respectively. To estimate these two parameters, the priori observation RSS values RL are used. Let N be the number of observations, $s_{k,i}$ be the observed RSS values at location i from AP k, and (x_i,y_i) is the location of the observations. The two unknown parameter $\hat{c}_k$ and $\hat{n}_k$ are estimated using Nelder-Mead simplex algorithm, in which the sum of weighted residual squares are minimized as in

$$(\hat{n}_k, \hat{c}_k) = \underset{n_k, c_k}{\arg\min} \sum_{i=1}^{N} \frac{\omega_i}{\sum_{j=1}^{N} \omega_j} \gamma_i^2 \quad \text{(Eq. 5-23)}$$

where

$$\gamma_i = s_{k,i} - c_k + 10n\log_{10}\left(\sqrt{\left(x_k - x_i\right)^2 + \left(y_k - y_i\right)^2}\right) \quad \text{(Eq. 5-24)}$$

and

$$w_i = \frac{1}{\left|s_{k,i}\right|^p}. \quad \text{(Eq. 5-25)}$$

The variable γ_i can be defined as the difference between $s_{k,i}$ and $z_k(x,y)$ which is a residual between the observed RSS value at a location and its theoretical value given by the signal propagation path loss model. Each residual is later weighted by w_i where a proper value for the power parameter p is crucial to ensure the expected parameters. One can foresee that this method is an iterative calculation, thus the range of

parameters are required. In this works, the range of $\hat{c}_k$ is set to minimum value of -120 dBm to the maximum of -40 dBm in the increment of 1 dB per iteration, while for $\hat{n}_k$ it is set in the range of 1 to 6 with an increment of 0.1 suitable to the values of n suggested in [46].

At present, both RL RSS data and the additional information of the estimated WiFi AP data i.e. $P(d_0)$ has been obtained, the fingerprinting database can now be constructed using the Modified Shepard's Method by treating the WiFi AP as the RL utilizing the mathematical equations described in Section 5.4.3 . That being said, the WiFi AP $P(d_0)$ can be treated similarly as other RL where it can be considered inside the radii of influence and the nodal function at the WiFi AP location can be also computed.

5.6.2 SP-MSM Methodology

Figure 5.12 shows the flow chart of the methodology taken in this work. Firstly the RSS data are collected in the reference location over some period of time. For a fair comparison, we collect the data at all possible locations in this works albeit the laborious works. Then, some of the data are removed according to random Bernoulli selection process by introducing the selection probability $p(s)$. *Algorithm 2* explains the pseudo code of the selection process where the parameter $p(s)$ is the selection probability from the total measurement locations. In the sections, the Low Pass Filter (LPF) is applied to the fingerprint database as well as online signal in the effort of obtaining a better result. The details of the LPF can be found later in Section 6.2.2.

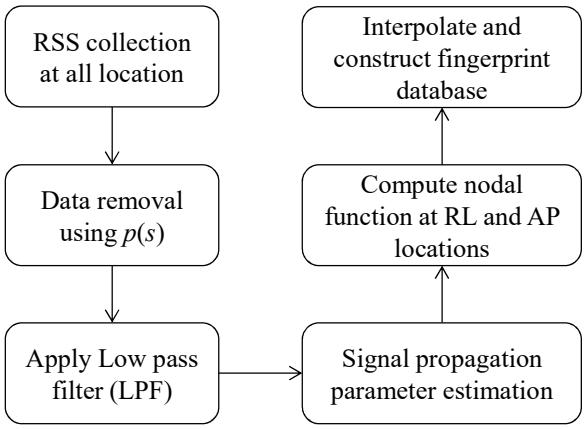

Figure 5.12: The flow chart of the proposed SP-MSM interpolation method

Algorithm 2: Random Bernoulli Selection process for data removal

```
1. Define selection probability, p(s)
2. For each sample location, L_i
3. p(L_i) = rand(1)
4.        If   p(L_i) < p(s)
5.                Select location
6.        Else
7.                 Remove location
8.        End
```

The selected data are used for Reference Locations (RL), while the data that has been removed will be the ground truth for the interpolated data. Afterwards the RSS data are pre-processed using the low pass filter discussed in previous section. Knowing the location of the WiFi AP transmitter, we then estimate the parameter of the wireless signal propagation combining the signal model such as Log-Distance Path Loss (LDPL) model and the known RSS in the RL. Once the parameters such as the close-in RSS and path loss exponent are known, the prediction of RSS value at other locations can be made in the sense of LDPL. Subsequently, using the filtered measurement data and the prediction data by LDPL, the nodal function of the proposed method i.e. Modified Shepard's Method (MSM) is calculated. Finally, the interpolation of full database can be automatically constructed and the database can be later tested using the state-of-the-art WKNN positioning algorithm.

Similarly with the previous experiments, the SP-MSM experiments are also conducted at the Toyohashi University of Technology specifically at the second floor of Center for Human-Robot Symbiosis Research. Figure 5.13 shows the location of the WiFi AP at their optimized location according to the GGLS and Tree Hierarchy algorithm described previously in Chapter 3 in order to ensure the entire wireless coverage within the experimental area. The experimental area is about 11×8.4 meter area highlighted in the black box. The building's surrounding walls are about 20 cm thick dry concrete and the doors are made from steel. A total of 64 sampling locations marked with '$\times$' are available in the mobile robot mobility area at one meter sparsity level, considering also space obstruction such as furniture and other placements as well as accommodated space for other works. Each of these 64 sampling locations is assigned to a unique location identification number (Location ID #) for later positioning assessments. The one meter sparsity level is considered suitable since our mobile robot has a base diameter of 0.5 meter that fit well between two reference locations.

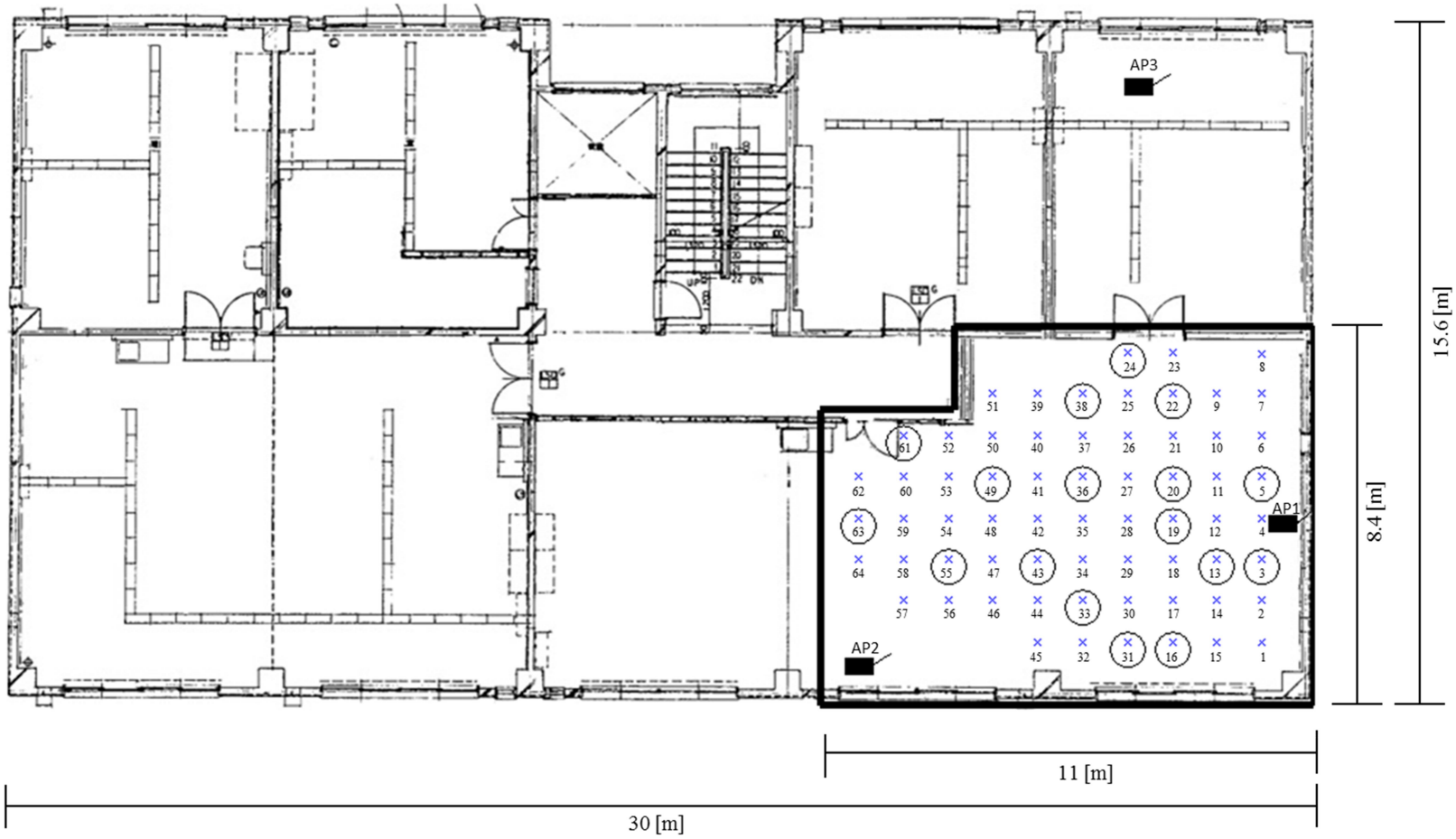

Figure 5.13: Experimental area showing the three WiFi Access Point and measurement locations with labeled IDs. Circled locations indicated the randomly selected locations as reference location prior to the choice of $p(s)$=0.25.

5.7 Positioning Accuracies

In order increase the accuracies of the proposed WPS utilizing the fingerprinting database made from SP-MSM interpolation method, the Low Pass Filter (LPF) has been applied. Instead of using the signal average for the database, the weighted histogram average is used. At each database locations, the weighted histogram average is given as

$$\overline{y} = \frac{\sum_{n=1}^{N} h_n y_n}{\sum_{n=1}^{N} h_n} \qquad \text{(Eq. 5-26)}$$

,where h_n is the frequency of occurrence at bin n, y_n is the value of filtered RSS by LPF at bin n and N is the total number of histogram ranges.

Table 5.5 delineated the effect of cut-off frequency over the signals and the comparison with the average of the raw RSS signal. As the cut-off frequency is increased, the filtered signal is more likely have the similar behavior of the raw data, and smoothen better when the cut-off frequency is smaller. A difference of 3 [dBm] is a matter of fact has a significant impact to the positioning results. Therefore in this works, we chose $f_c = 0.02\,[\text{Hz}]$ which is an equal trade-off between the difference with raw data average as well as the signal smoothens. Figure 5.14 shows a sample of WiFi signal over sampling period at location ID #1 which is adjacent to AP1, fair to AP2 and AP3 locations with the use of $f_c = 0.02\,[\text{Hz}]$. It can be observed that the fluctuative behavior of these signal as the aftermath of the spikes (outlier) have been successfully suppressed by the filter. Moreover, the difference in dB has been also been kept to lesser than 3 [dB] which is an acceptable level.

Table 5.5: The effect of cuf-off frequency of LPF

Cut-off freq. [Hz]	Weighted histogram average [-dBm]	Difference with signal average [dB]
0.01	65.13	3.06
0.02	66.28	1.91
0.05	67.25	0.95
0.1	67.81	0.40
0.2	68.02	0.17

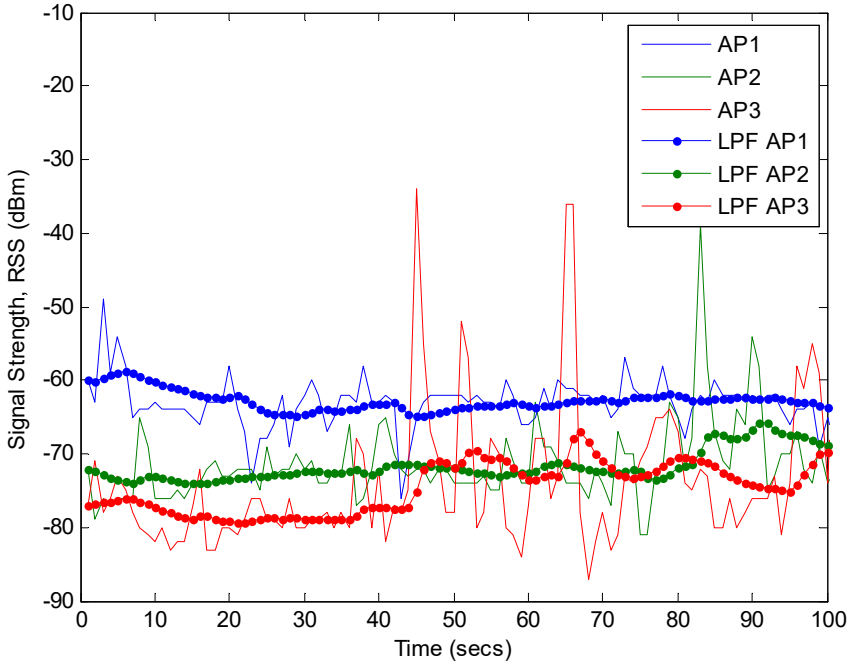

Figure 5.14: Three WiFi RSS raw signal and their corresponding filtered signal using the LPF

5.7.1 Database Evaluation

The selection probability, $p(s)$ introduced earlier from random Bernoulli selection process is an important parameter in this works. The number of selected location as reference locations (RL) for the interpolation is proportion with $p(s)$. Figure 5.15 shows the relation between the selection probability and the number of selected locations where the number of selected data increases with the increment of $p(s)$. The selection probability also results in highly irregular data pattern with random spacing between them. In addition, each location requires an average of five minutes of preparation, data recording and compilation. Hence, in order to automate the signal fingerprinting database, an equal trade-off between the number of RL and sampling time must be considered. In this works, we chose $p(s) = 0.25,$ that yield 17 reference locations. This amount of reference locations in the interpolation point-of-view should be reasonable especially in the case of irregularly space pattern.

The locations of these 17 locations are marked as 'o' in the earlier mentioned Figure 5.13. It can be seen that, the distribution of these reference locations are random and in the form of irregularly spaced. Therefore, the main objective of this works is to construct a WiFi signal fingerprinting database that consist of 64 columns from 17 reference locations that could minimize the RSS error as well as mobile robot positioning

error. By using this approach, the fingerprinting database could be automatically constructed which requires only 27% recording time compared to total time needed to record at all 64 locations.

Figure 5.16 on the other hand shows the effect of selection probability $p(s)$ to the interpolation errors. This error can be simply calculated as $E = \sum_i^N \left\| (\hat{z}_i - z_i) \right\| / N$ where N is the total number of locations (database), $\hat{z}_i$ and z_i are the interpolated and the original RSS data, respectively. The values z_i can be obtained from the 'removed' data accordingly to $p(s)$ earlier. In the smaller $p(s)$, only a few number of RL is selected. In this sense, the smaller RL may affect the radii of influence of the SP-MSM. Therefore, the computation of the nodal function may also be affected which resulting the larger interpolation error. However, from $p(s) = 0.15$ and onwards, the interpolation error of the SP-MSM outperforms both IDW and Kriging algorithm. The famous Kriging method is also keeping its reputation where the interpolation error is also better than the conventional IDW interpolation method.

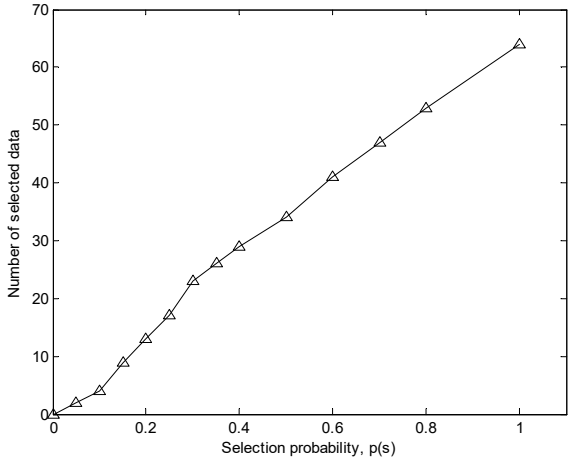

Figure 5.15: Relation between $p(s)$ and number of selected data

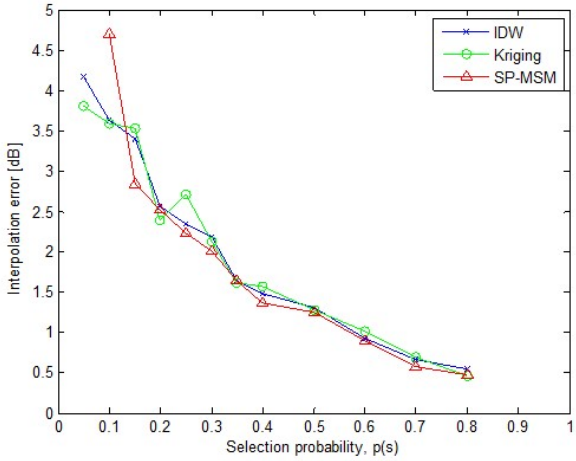

Figure 5.16: Comparison of interpolation errors of IDW, Kriging algorithm, and the proposed SP-MSM with respect to $p(s)$

5.7.2 Positioning Errors

While having a generous database made from all three interpolation methods i.e. IDW, Kriging and SP-MSM, the ground truth database is also available. Ground truth database can be defined as the original hard-labored data that was manually recorded. That being said, these 64 original data can be also pre-processed by the LPF, and being treated as a complete fingerprint database as well. The 64 locations are also assigned as the 64 test locations with individual Location Identification number (Location ID #) shown explicitly in Figure 5.13. Later, the computation of positioning error of the interpolated will be compared to the ground truth database. Since the low pass filter is used, comparisons between unfiltered and filtered RSS are discussed. Table 5.6 presents the positioning error result evaluated at all 64 locations in the form of $\mu \pm \sigma$, where μ is the average positioning error and σ is the error standard deviation. The evaluation is made on four difference signal fingerprint databases which are the ground truth database as well as the databases from the IDW, Kriging, and the proposed SP-MSM interpolation methods. As expected the error of filtered signal is improved regardless the method used. This fact has ensured that filtering the raw signal is a sensible option to apply.

The IDW method has the highest positioning error among all methods for both unfiltered and filtered signals. The Kriging algorithm has improved the positioning error to the more conventional IDW method. The proposed method however on the other hand scored much better compared to the other two. This is because the SP-MSM is a local interpolant, for which the interpolation is only taking place within the radius of influence while neglecting the effect of far-off neighbors. Moreover, the addition information from the signal propagation parameter has improved the computation of the nodal function Q of the MSM interpolations.

Table 5.6: Average of positioning error on difference signal fingerprint databases

Fingerprint Database	**Average Positioning Error [m]**	
	Unfiltered RSS (signal average)	Filtered RSS (weighted histogram)
Ground truth	3.18 ± 1.11	2.72 ± 1.12
IDW	3.60 ± 1.24	3.26 ± 1.49
Kriging algorithm	3.56 ± 1.25	3.21 ± 1.51
SP-MSM	3.53 ± 1.23	3.06 ± 1.54

Table 5.7: Average of positioning error on using filtered RSS with difference fingerprint databases.

Test position ID [#]	Average positioning error [m]					Test position ID [#]	Average positioning error [m]				
	Ground truth	IDW	Kriging	SP-MSM	Winning Method		Ground truth	IDW	Kriging	SP-MSM	Winning Method
#1	4.78	4.22	4.77	3.71	SP-MSM	#33	2.89	2.31	2.26	1.57	SP-MSM
#2	2.60	2.75	2.91	2.79	IDW	#34	2.23	2.59	2.33	2.41	Kriging
#3	2.87	1.32	1.14	1.32	Kriging	#35	2.73	3.63	3.31	3.69	Kriging
#4	2.07	2.55	2.51	2.00	SP-MSM	#36	3.18	4.16	3.62	3.51	IDW
#5	1.77	0.84	0.82	0.58	SP-MSM	#37	2.52	4.58	3.23	4.40	Kriging
#6	3.10	1.64	1.53	1.37	SP-MSM	#38	2.44	1.40	1.51	1.19	SP-MSM
#7	6.54	7.25	6.92	6.92	SP-MSM	#39	3.42	5.49	4.99	5.41	Kriging
#8	5.07	4.76	5.07	4.59	SP-MSM	#40	4.86	7.16	7.18	7.21	IDW
#9	3.99	3.99	4.14	4.08	IDW	#41	3.07	4.23	3.81	4.12	Kriging
#10	1.38	1.82	1.49	1.53	Kriging	#42	2.18	2.49	2.57	2.01	SP-MSM
#11	1.36	0.77	0.91	0.90	IDW	#43	2.04	2.24	2.05	1.83	SP-MSM
#12	2.04	2.46	2.42	2.73	Kriging	#44	2.11	2.61	3.08	2.58	SP-MSM
#13	2.19	2.47	2.55	2.84	IDW	#45	3.82	4.55	5.05	4.48	IDW
#14	1.95	2.32	2.23	2.09	SP-MSM	#46	1.47	2.38	1.80	1.07	SP-MSM
#15	2.72	3.64	3.47	3.66	Kriging	#47	2.92	3.61	3.28	3.43	Kriging
#16	3.95	2.78	2.62	2.70	Kriging	#48	1.78	3.07	2.61	3.35	Kriging
#17	2.51	2.22	3.36	2.24	SP-MSM	#49	2.24	1.78	1.76	1.68	SP-MSM
#18	1.90	2.17	2.33	2.31	IDW	#50	3.44	3.95	3.55	4.13	Kriging
#19	1.63	2.42	2.14	2.09	SP-MSM	#51	3.84	3.90	3.94	2.78	SP-MSM
#20	1.57	2.82	3.33	2.89	SP-MSM	#52	3.18	3.45	3.15	3.05	SP-MSM
#21	1.50	2.06	2.51	2.12	IDW	#53	1.76	2.71	2.46	2.23	SP-MSM
#22	4.50	4.31	3.51	4.15	Kriging	#54	3.24	4.55	4.92	5.11	IDW
#23	2.76	4.44	3.92	3.89	SP-MSM	#55	1.49	1.24	1.33	1.68	IDW
#24	4.29	3.53	3.59	3.40	SP-MSM	#56	1.73	3.41	3.41	3.04	SP-MSM
#25	2.32	1.17	1.65	1.16	SP-MSM	#57	1.76	4.12	3.93	3.13	SP-MSM
#26	2.52	2.87	2.78	2.67	SP-MSM	#58	2.76	2.50	2.43	2.36	SP-MSM
#27	0.89	3.53	4.26	2.33	SP-MSM	#59	3.25	3.17	3.49	3.31	IDW
#28	1.45	3.75	4.05	4.08	IDW	#60	1.39	1.52	1.04	1.32	Kriging
#29	1.38	4.04	3.81	3.96	Kriging	#61	1.97	2.61	1.95	1.80	SP-MSM
#30	2.84	5.49	6.63	6.31	IDW	#62	2.95	3.66	3.22	3.60	Kriging
#31	5.51	6.52	6.48	6.35	SP-MSM	#63	2.98	2.41	2.50	2.03	SP-MSM
#32	3.35	7.76	7.66	7.31	SP-MSM	#64	3.22	2.17	1.86	1.46	SP-MSM

A much details positioning error at each of 64 test locations with respect to the difference fingerprint databases are tabulated in Table 5.7 which shows the positioning error at each individual location. Among these 64 locations, there are some locations that either IDW or Kriging better than the proposed SP-MSM. Comparatively, the 'winning method' i.e. the best interpolation method at that particular test location, SP-MSM is ranked first with 52% wins, Kriging at 26% and lastly IDW with 22% wins. In addition, the observation at locations near to the wall, which is at location ID #1 to #8, #15, #16, #23, #24, #31, #32, #45, #51, #52, and #61, the proposed SP-MSM method is also a better interpolation method. This result as a matter of fact is in accordance with our initial findings where MSM is indeed the best interpolation method in the case of near-wall locations.

Figure 5.17 shows the positioning error at certain mid-space location (location ID #46) over the sampling period. The error is evaluated using WKNN positioning system where $K = 4$ is used. This commonly used constant value of K is selected such that a uniform square selection can be made while neglecting the neighbors outside this square [32]. Due to the fluctuative nature of the unfiltered raw data, the errors are also badly influenced, in this case the positioning errors regardless of databases used are in the range of 0 [m] to 8.25 [m]. Figure 5.18 on the other hand shows the positioning error of the filtered signal RSS data using the low pass filter at the same test location. The fluctuation which is occurs in the previous computation has been greatly suppressed and the positioning error ranges from 0 [m] to 4.25 [m]. The positioning errors however still the best if the ground truth database is used, but the proposed method come in second place and much better than both IDW and Kriging interpolation algorithm. Considering the time taken and the efforts required to obtain the ground truth database, it is no doubt that these database will works well. However, having the ground truth database is not practical despite having good results. Hence, in order to minimize the efforts, interpolation is needed. In such case, the proposed method i.e. SP-MSM works the best compared to other method.

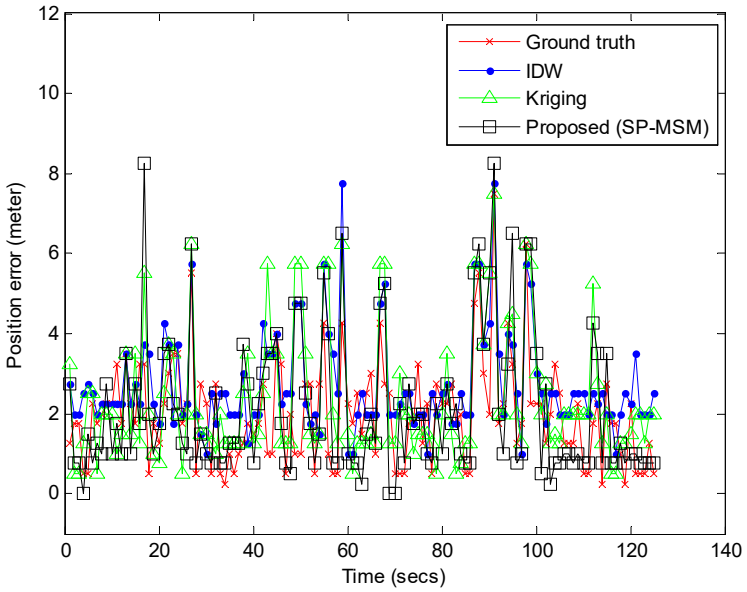

Figure 5.17:Positioning error at location #46 prior to each sampling time of the unfiltered RSS data

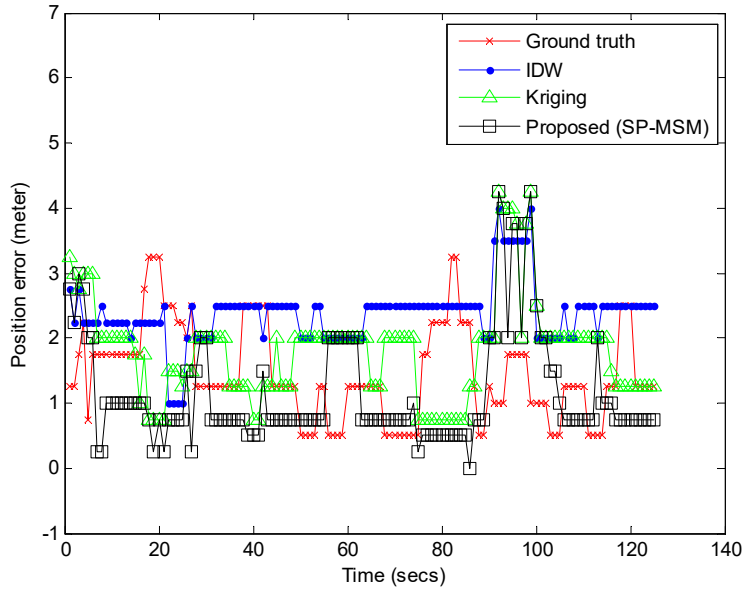

Figure 5.18: Positioning error at location #46 prior to each sampling time of the filtered RSS data

5.7.3 Distinctive Test Locations

The assessments of positioning accuracies in this works are made at four distinctive locations over the sampling period. Since three WiFi APs were used, the four distinctive locations are corresponding to the Line-Of-Sight (LOS) conditions of the three APs. Figure 5.19 to Figure 5.22 shows the four mobile robot distinctive locations, where the *central* location at ID #27 has a clear unobstructed LOS typically from all APs, while the *left* location at ID #63 has LOS with AP2, rather far from AP1 and multiple wall obstruction by AP3. The *bottom* location at ID #16 has LOS condition with AP1 and narrow LOS with both AP2 and AP3. The last distinctive location, the *right* location at ID #7 has severe multipath fading effects mainly because it location being near to two side walls, obstructed by AP3 and far from AP2. These four locations can be regarded as stimulating locations for this study. Under these circumstances, WKNN is also used in this section with similar constant value of K as in previous discussion. Consequently, the proposed SP-MSM database is used with the aid of signal filtering since they are the best method for interpolation as well as the effectiveness of the low pass filter.

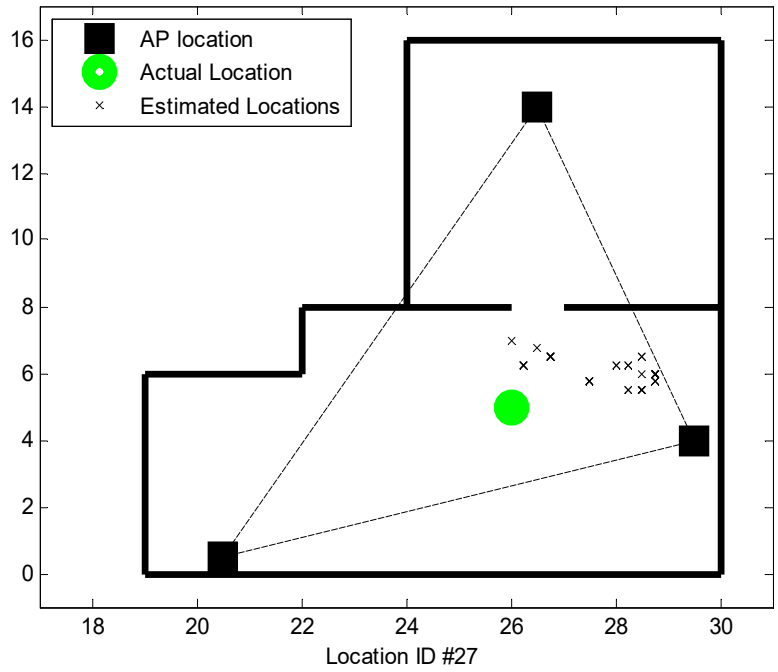

Figure 5.19: Evaluation of the positioning accuracy at the four distinctive locations (*central*)

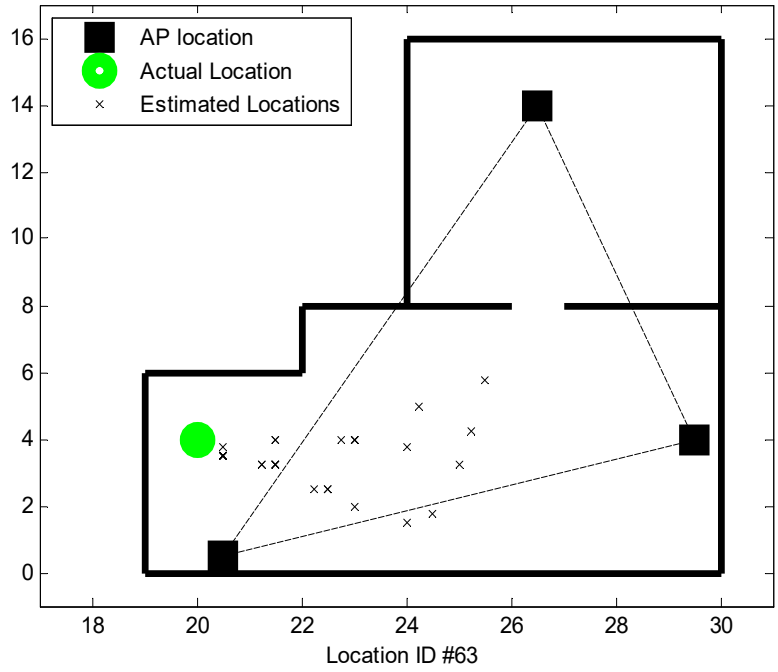

Figure 5.20: Evaluation of the positioning accuracy at the four distinctive locations (*left*)

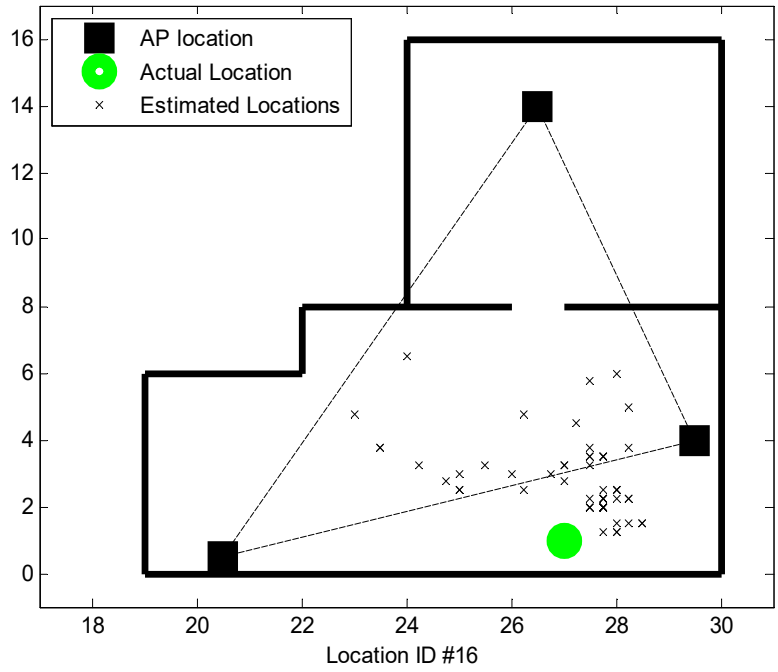

Figure 5.21: Evaluation of the positioning accuracy at the four distinctive locations (*bottom*)

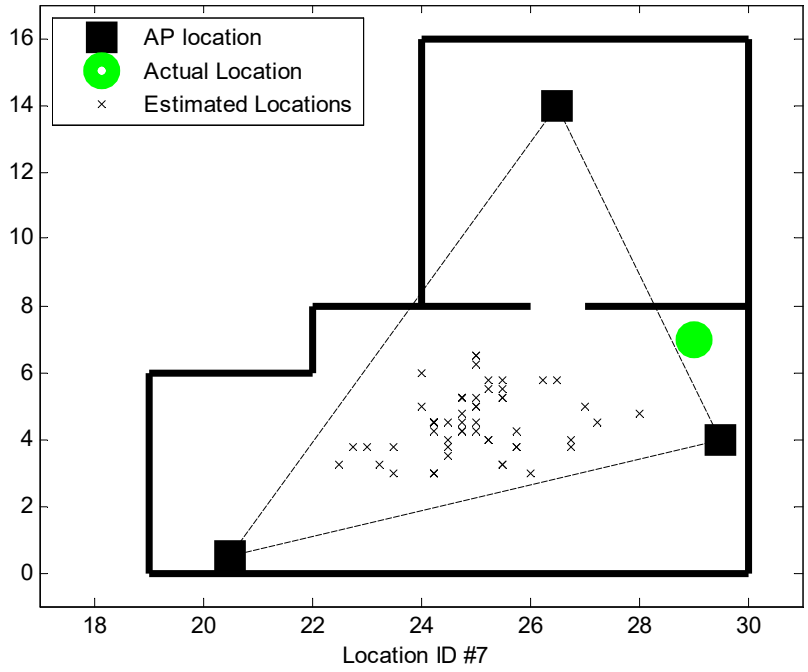

Figure 5.22: Evaluation of the positioning accuracy at the four distinctive locations (*right*)

At the *central* location #27, the positioning system works precisely with the accuracy of 2.33 ± 0.42 [m]. This is benefited from the clear and obstructed LOS between the WiFi APs and the mobile robot, which can be practical. On the *left* location #63 where there are no LOS scenario, the precision has been decreased to 2.03 ± 1.61 [m] despite the increase in the positioning error average. This is because the estimated location over sampling period are scattered away from the actual location. At the *bottom* location #16, the positioning accuracy is obtained at 2.70 ± 1.56 [m]. While most of the estimated locations are somewhat located near to the actual locations, there are also some of the data distributed away from the actual location, hence contributing to the high standard deviation. This may be resulting from multipath fading since the actual location is located near to the wall. Similarly at the *right* location #7, the multipath fading from the two side walls has affected the system accuracy with 6.92 ± 1.14 [m], with literally no estimated locations near to the actual location.

As a summary from these four distinctive test locations, the positioning system works best when there are a clear unobstructed LOS between the mobile robot and the WiFi AP transmitter. Positioning at wall, especially at multiple side walls may affect the positioning system badly. In this case, the use of robust filter is needed in order to obtain better positioning accuracies.

5.8 Summary

This section discussed the use of fingerprinting method for Wireless Positioning System (WPS). The main problem of this technique is that a considerable amount of effort in the domain of workload and time consumption is required in order to construct the fingerprinting database. This is because the fingerprinting database is constructed in such a way that an average of WiFi RSS is computed from a series of manual measurement in a location. Since a higher number of reference locations i.e. higher granularity levels are needed to obtain the reasonable accuracy, then the effort problem is getting worst. Hence, this research proposes to automatically construct the database by means of database interpolation.

In the initial experiments, three different interpolation schemes are introduced which are the Inverse Distance Weighting (IDW), the stochastic Kriging algorithm and the proposed method i.e. the Modified Shepard's Method (MSM). In summary, the proposed method MSM has outperformed both the IDW and Kriging algorithm especially in the case of near-to-wall test location using the WKNN matching algorithm.

Due to inexistence of ground truth data, another experiment is conducted and a new novel interpolation method known as the Signal-Propagated Modified Shepard's Method (SP-MSM) is proposed where it is dedicated for the wireless signal interpolation. A total of 64 reference locations are defined for data collection and act as the ground truth data. To infer the interpolation methodologies, some of the data are removed using the random Bernoulli selection process. Again the proposed method i.e. the SP-MSM performs better than the other two methods with 52% wins compared to IDW (22%) and Kriging algorithm (27%) wins from the total of 64 test locations. Moreover, the use of low-pass-filter (LPF) has improved the accuracies of the positioning system. In addition, four distinctive stationary test locations accordingly to the Line-Of-Sight (LOS) have been introduced.

Chapter 6 IMPROVING POSITIONING ACCURACY

"*Without continual growth and progress, such words as improvement, achievement, and success have no meaning*"

- Benjamin Franklin, 1700s

6.1 Introduction

In the stationary positioning system, the mobile robot stays in a particular location while the wireless receiver device kept on obtaining the wireless data i.e. the WiFi RSS. Then the resulting signal is matched to those signal recorded earlier in order to estimate the location of the mobile robot. However, as has been discussed previously in Chapter 2, the wireless signal especially those of IEEE 802.11 WiFi signal suffers fluctuation problem due to the complex signal propagation mechanism and more severely multipath effects. Moreover the nature of the wireless signal is non-deterministic and prone to noise causes by signal interferences, arrangement of the indoors furniture and the passing by humans. Therefore, at the same location the mobile robot may record RSS that differs significantly with the fingerprinting database.

The database is made by averaging the RSS signal over some period of time. Since the online signal suffers from fluctuation problem, then the positioning error will be also partaking bad variations. Hence there is a need of signal filtering method that could eliminate the noisy signals.

This chapter describes the filtering methods that are taken to eliminate the fluctuation problems in the effort of improving the positioning system accuracy.

6.2 Stationary Positioning Problem

The WPS system employing fingerprinting technique has been exhaustively described in previous chapters. The fingerprinting technique has been proved better than the trilateraion technique [95]. The fingerprinting technique such depicted in Figure 1.3 and Figure 5.1 generally consists of two phases. In the training phase, as explained previously the multiple WiFi signals radiated from AP_1 to AP_k are recorded and the average signal strength is stored in the database. In the positioning phase, the signal measured by the mobile robot is matched to those in database and the result is later returned in the form of estimated location, usually in Cartesian spatial space [42].

As simple it might sound, yet such positioning technique have challenges due to the fluctuative behaviour of the wireless signal. Taking an example of using deterministic database matching such as the nearest neighbour (NN) and a stationary mobile robot with the measured WiFi RSS vary unexpectedly as shown in Figure 6.1, then the online signal is matched to the fingerprint database at each sampling time. Theoretically the positioning system using such signal will yield different locations due to the differences with the average signal stored in the database. Computation the average of these locations is not so beneficial since the 'true' location is unknown. Hence it is perplexing.

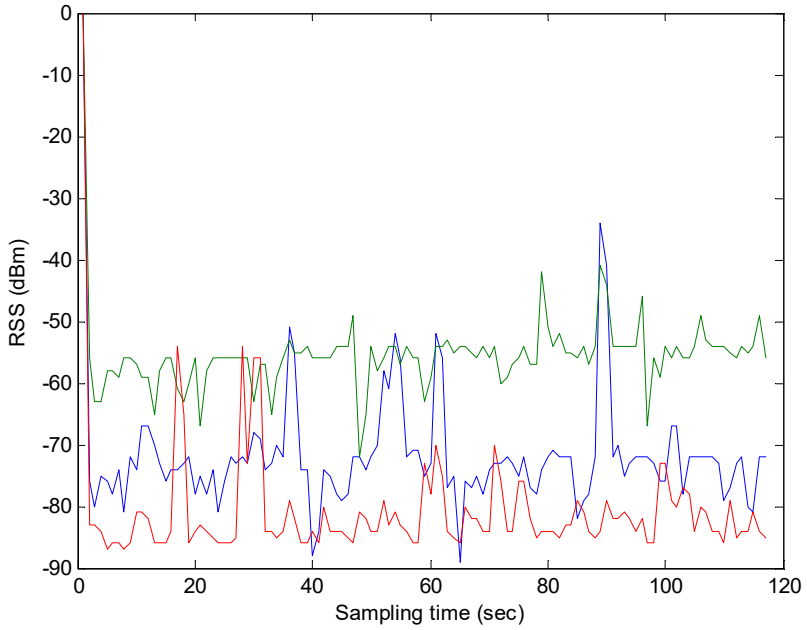

Figure 6.1: An example of the WiFi signal fluctuation received from three WiFi Access Point where the mobile robot stays stationary over some period of time

Therefore, it is natural to filter in the sense of predicting the incoming signal to the mobile robot. A correct prediction will yield in accurate positioning result of the mobile robot. In this chapter, several notable filters such as the Moving Average Digital Filter, Low Pass Filter and Linear Kalman Filter are used to filter and predict the WiFi signal in the online phase. As a rule of thumb, the signal fingerprint database has been constructed beforehand having the tuple of reference location coordinate and the average RSS over some sampling period. In addition, the result is also compared with the original WiFi data to observe the effectiveness of the filtering algorithms.

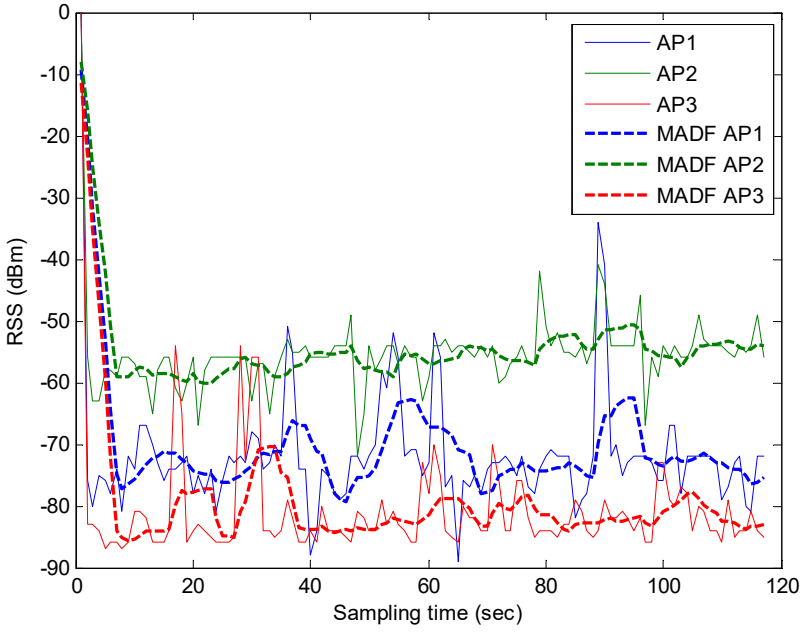

Figure 6.2: The filtering of the fluctuative WiFi signal using Moving Average Digital Filter with $KS = 5$

6.2.1 Moving Average Digital Filter

The Moving Average Digital Filter (MADF) is commonly used Digital Signal Processing (DSP) research field, mainly because it is the easier filter to understand and use. As the name implies, the MADF operates by averaging a number of points from the input signal to produce each point in the output signal. The term averaging number of points is typically described by the Kernal Size (*KS*), which is given as (Eq. 6-1),

$$y(n) = \frac{1}{KS}\{x(n) + x(n-1) + x(n-2) + \ldots + x(\mathrm{n}-(KS-1))\} \quad , \qquad \text{(Eq. 6-1)}$$

where $y(n)$ is the resulting filtered signal and $x(n)$ is the online WiFi RSS data at sampling time n. From (Eq. 6-1), one can observe that filtering at n is made such a way that the previous signal depending on KS is used. Hence, MADF is a recursive-type filter that takes advantage of current and previous measurements.

Figure 6.2 shows the result of filtering the same fluctuative WiFi signal using the MADF at $KS = 5$. Generally the obvious peaks such as shown by AP1 at about sampling time 90 sec has been suppressed considerably by the MADF. The accuracy of using such filter from positioning point of view will be discussed in later section.

6.2.2 Low Pass Filter

The Low Pass Filter (LPF) can be considered as conventional filter since the usage of LPF can be generally applied in many fields. The SP-MSM interpolation method presented in Section 5.6 also uses LPF for filtering both fingerprinting database and online RSS signal. LPF as a matter of fact works very well in the case of analog signal. The WiFi RSS signal however, is a digital filter. Therefore, a conversion is required. In this dissertation, the bilinear transformation is used to discretize the first-order LPF.

A first order low pass filter (LPF) can be described in continuous-time function as

$$H(s) = \frac{1}{T_c s + 1} \qquad \text{(Eq. 6-2)}$$

,where $H(s)$ and T_c is the transfer function and the time constant of the filter in Laplace domain, respectively. Since the WiFi RSS observation is in discrete time, then the bilinear transformation is used to discretize the continuous-time function, defining

$$s = \frac{2}{\Delta t}\frac{1 - z^{-1}}{1 + z^{-1}} \qquad \text{(Eq. 6-3)}$$

,where Δt is the sampling time in discrete system z. Substituting equation (4.2) into (4.1) will resulting into

$$H(z) = \frac{\Delta t(1+z^{-1})}{(\Delta t + 2T_c) + (\Delta t + 2T_c)z^{-1}} \quad \text{(Eq. 6-4)}$$

which shows the general transfer function of a first order discrete-time system. Subsequently, solving for input-output relation of this transfer function, the filtering of the raw signal x at time step k can be computed by

$$y_k = -\frac{\Delta t - 2T_c}{\Delta t + 2T_c} y_{k-1} + \frac{\Delta t}{\Delta t + 2T_c}(x_k + x_{k-1}). \quad \text{(Eq. 6-5)}$$

Similarly as MADF, LPF is also the recursive-type filter where the current and previous measurements are taken into consideration. Figure 6.3 presents the filtering of the WiFi RSS signal using the LPF at cut-off frequency, $f_c = 0.2$ sec. It can be seen that the fluctuative signal from all three WiFi AP have been successfully suppressed.

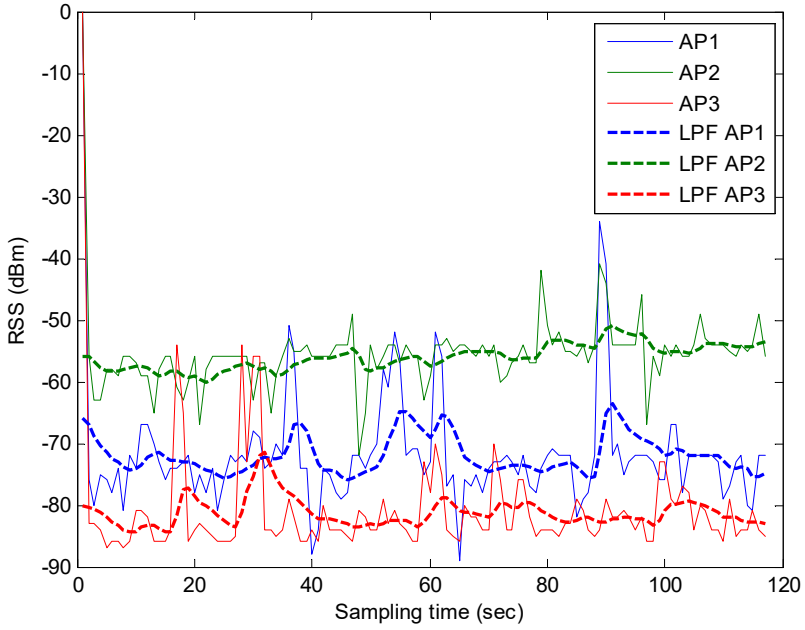

Figure 6.3: The filtering of the fluctuative WiFi signal using Low Pass Filter at $f_c = 0.2$ sec

6.2.3 Linear Kalman Filter

In the 60s, Kalman proposed the Kalman filter as a recursive filter to determine the random values of linear and nonlinear system from lousy and noisy signals [96]. Kalman filter uses the knowledge of current and previous states to track or predict and thus revise the past, present and future states. Kalman filter can plot the system's trajectory, making it suitable to model systems such as radars that anticipate and estimate the next state [97]. Kalman filter has been tremendously successful filter and prediction algorithm that almost all field are using them in large-scale with many variations and improvements, even in WPS systems [30][76][98].

This dissertation employs the classical approach of the Linear Kalman Filter (LKF) in order to predict the online WiFi RSS signal with the goal of improving the stationary positioning system. If we consider the discrete-time system:

$$\begin{aligned} &\text{Initial state} && : x_0 \\ &\text{State model} && : \hat{x}_k = Ax_{k-1} + Bu_{k-1} + w_k \\ &\text{Measurement model} && : z_k = Hx_k + v_k \end{aligned} \qquad \text{(Eq. 6-6)}$$

, where the state variable x, u and w represents the original WiFi signal, the control input and the noise at time k, and the measurement model also pertain the noise variable v. The control input is however cannot be controlled due to the fact that the WiFi AP are limited by the built manufacturers. Hence, we will assume it as unity. Intuitively, (Eq. 6-6) will becomes

$$\begin{aligned} \hat{x}_k &= Ax_{k-1} + w_k \\ z_k &= Hx_k + v_k \end{aligned} . \qquad \text{(Eq. 6-7)}$$

Since the LKF is an iterative method, it is easier to illustrate the computation in graphical manner. Figure 6.4 shows the algorithm of the LKF employed in this works.

The Linear Kalman Filter (LKF) operates by taking the measurement value (z_k) as input and outputs a priori state estimates ($\hat{x}_k$) of the next process. It is a repetition of prediction and correction processes.

(i). The prediction process inputs a former posteriori state estimates ($\hat{x}_{k-1}$) and a posteriori error covariance (P_{k-1}), calculating a posteriori state estimate and a priori estimate error covariance ($\hat{x}_k^-, P_k^-$) as the end result. These values are later forwarded to the correction process. The

system model variables used is the prediction process is the state transition matrix (A) and the process noise covariance (Q).

(ii). The output of the correction process is a posteriori state estimate ($\hat{x}_k$) and the posteriori estimate error covariance (P_k). The values used for input are not only the posteriori estimate and the priori estimate error covariance from the prediction process ($\hat{x}_k^-$, P_k^-), but also the measurement (z_k). The system model variables used in the correction process is the measurement prediction matrix (H) and the measurement error covariance matrix (R).

The prediction of the WiFi RSS can be accurately forecasted by using the measured value of the current state as well as the value reflecting the prediction from the current state by means of recursive algorithm and adaptive Kalman Gain. Moreover, the more we trust our measurement i.e. smaller value of error covariance estimate, then the system will converge into meaningful value in short period of time. In this research, a heuristic value of error standard deviation of about 3 dB is used resulting in convergence in considerable amount of time. Figure 6.5 shows the application of LKF towards the fluctuative WiFi sample signals retrieved from three different AP where the mobile robot stays stationary over some period of time. The constant straight line over y-axis represent the average computation of the RSS signals respective to the APs. By trusting the measurement at aforementioned standard deviation, we can observe that the resulting filtered signals are converged to respective signal average at about 20 sec.

Since the fingerprinting database is made from the signal average, we expect that the positioning error of the mobile robot stationary location will improved significantly compared to MADF and LPF.

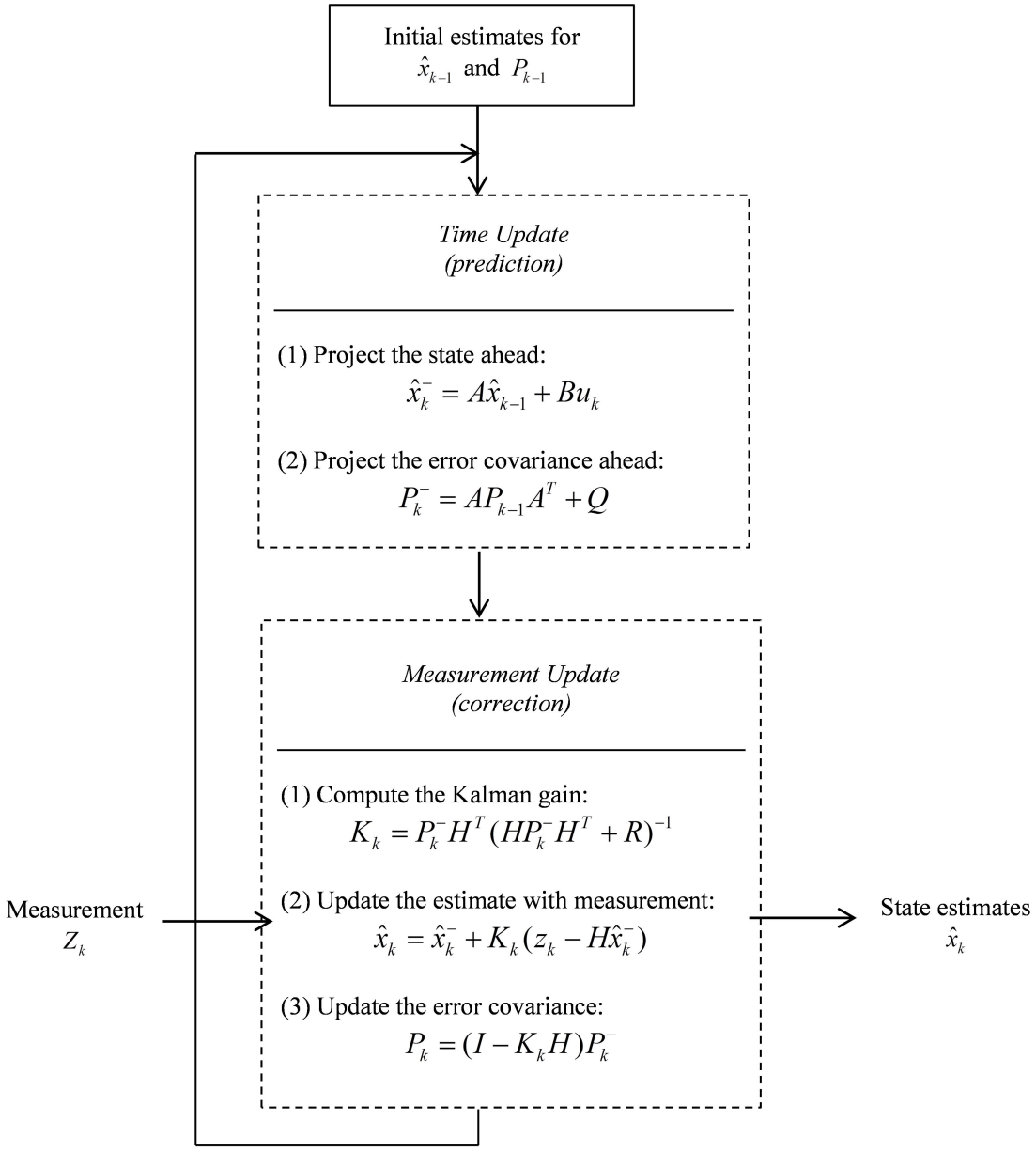

Figure 6.4: The Linear Kalman Filter algorithm

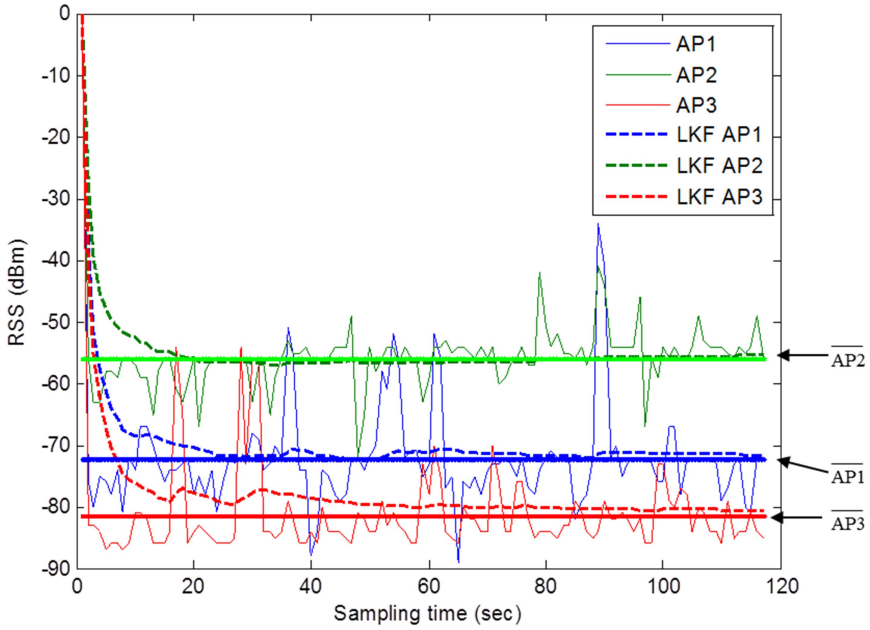

Figure 6.5: The filtering of the fluctuative WiFi signal using the Linear Kalman Filter

6.2.4 Filters Comparison

This section presents the result of positioning system using the three filtering method described previously which are the MADF, LPF and LKF. The comparison will also be made with the unfiltered raw signal in order to comprehend the effectiveness of the filtering system. Fingerprinting technique with WKNN matching algorithm is used to evaluate the positioning errors and accuracies. In addition, four distinctive stationary test positions as described in Section 5.7.3 are used for similarity observations. The four distinctive locations are:

(i). *central* position at Location ID #27

(ii). *bottom* position at Location ID #2

(iii). *right* position at Location ID #7

(iv). *left* position at Location ID #63

Table 6.1: The positioning error and accuracy of the positioning system on using raw data

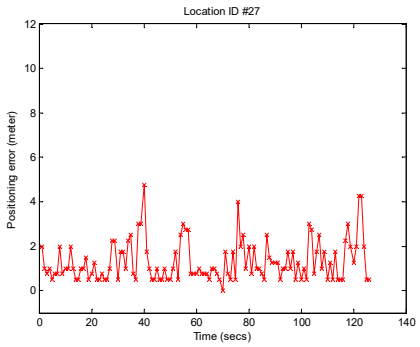 *central* position (Loc. ID #27)	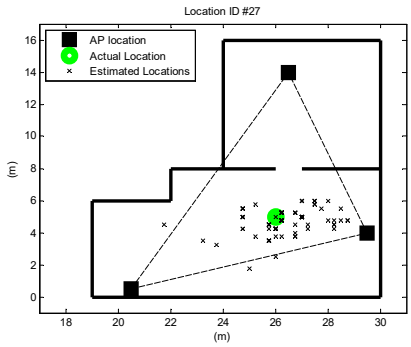 $\bar{E} = 1.3095 \pm 0.9178\,[\mathrm{m}]$
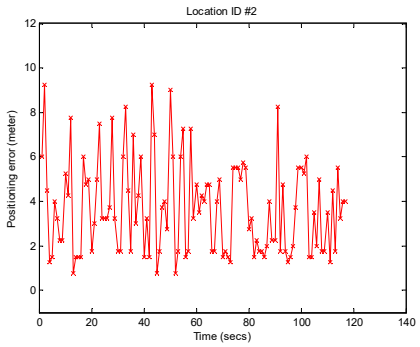 *bottom* position (Loc. ID #2)	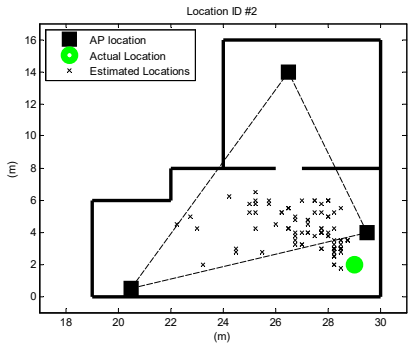 $\bar{E} = 3.7009 \pm 2.1130\,[\mathrm{m}]$
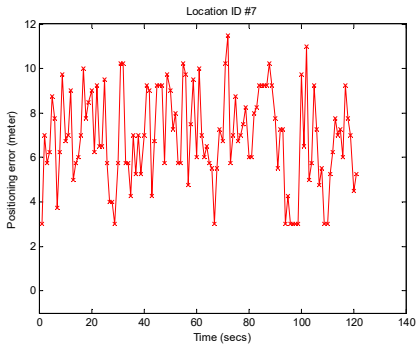 *right* position (Loc. ID #7)	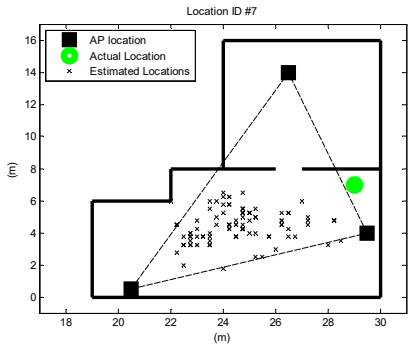 $\bar{E} = 6.9091 \pm 2.0974\,[\mathrm{m}]$
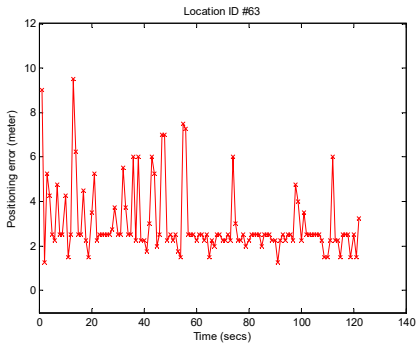 *left* position (Loc. ID #63)	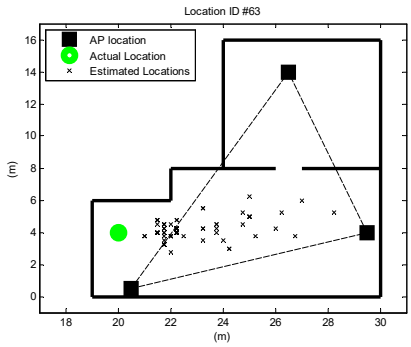 $\bar{E} = 3.0000 \pm 1.5759\,[\mathrm{m}]$

Table 6.2: The positioning error and accuracy of the positioning system on using MADF data

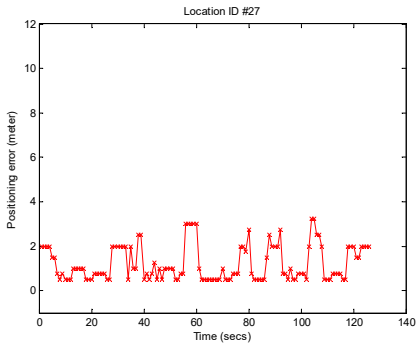 *central* position (Loc. ID #27)	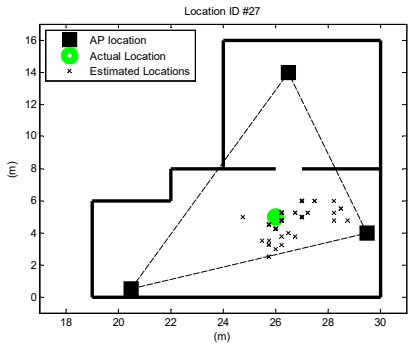 $\bar{E} = 1.2183 \pm 0.8006\,[\mathrm{m}]$
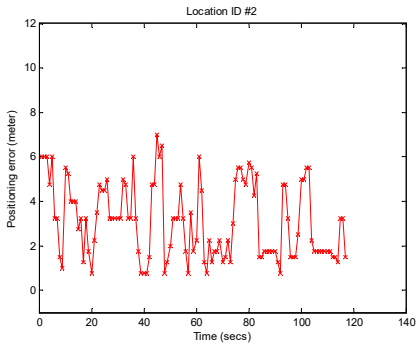 *bottom* position (Loc. ID #2)	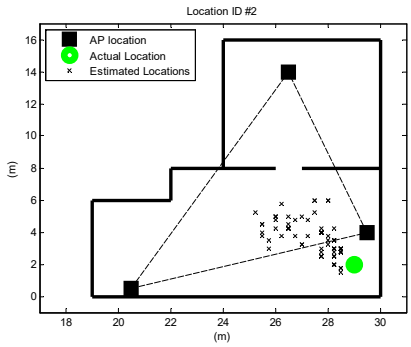 $\bar{E} = 3.1175 \pm 1.7018\,[\mathrm{m}]$
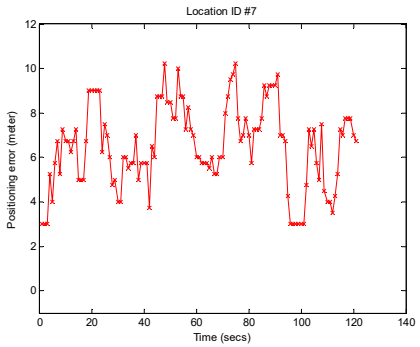 *right* position (Loc. ID #7)	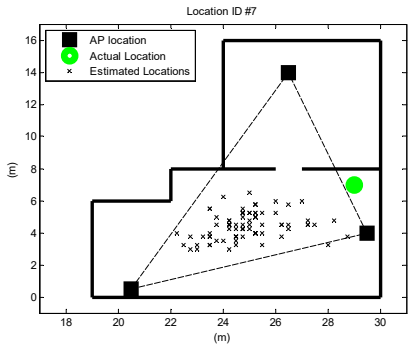 $\bar{E} = 6.5227 \pm 1.8569\,[\mathrm{m}]$
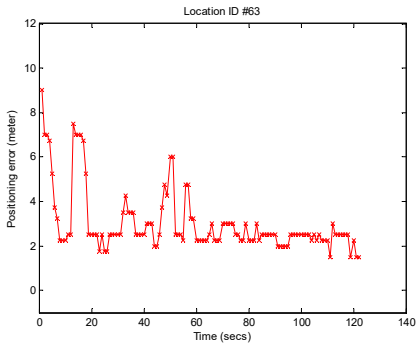 *left* position (Loc. ID #63)	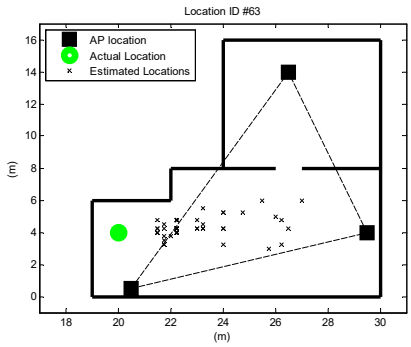 $\bar{E} = 3.0266 \pm 1.4445\,[\mathrm{m}]$

Table 6.3: The positioning error and accuracy of the positioning system on using LPF data

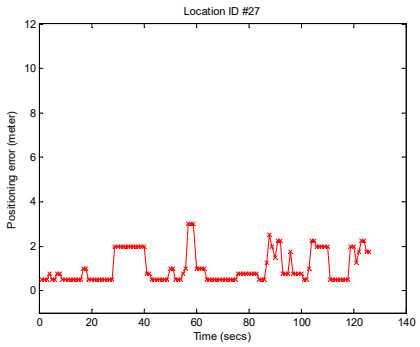 *central* position (Loc. ID #27)	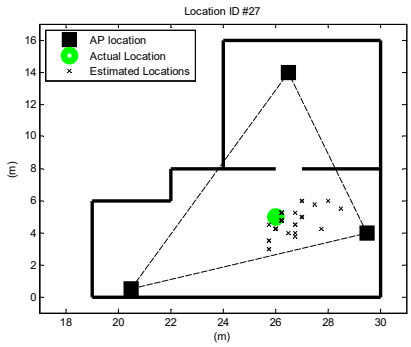 $\bar{E} = 1.0377 \pm 0.7036\,[\mathrm{m}]$
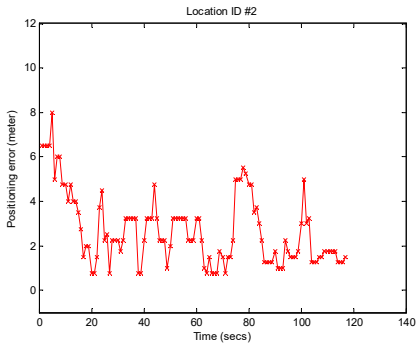 *bottom* position (Loc. ID #2)	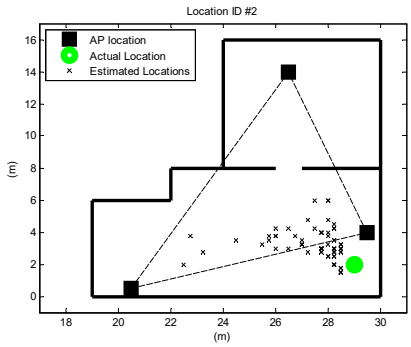 $\bar{E} = 2.7051 \pm 1.5966\,[\mathrm{m}]$
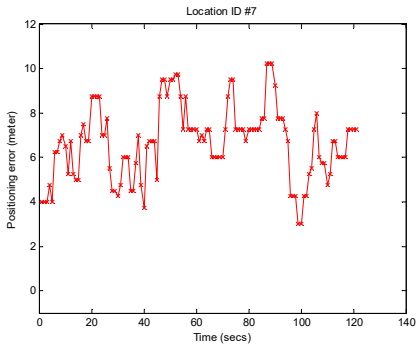 *right* position (Loc. ID #7)	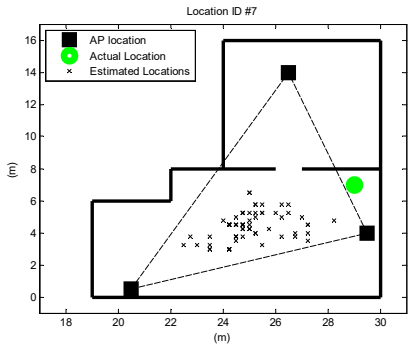 $\bar{E} = 6.6921 \pm 1.6573\,[\mathrm{m}]$
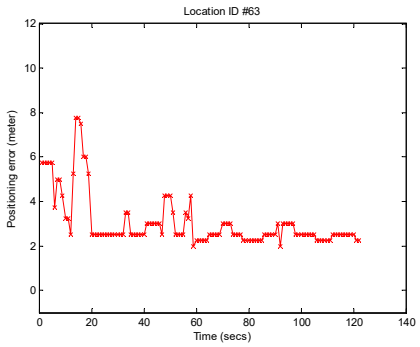 *left* position (Loc. ID #63)	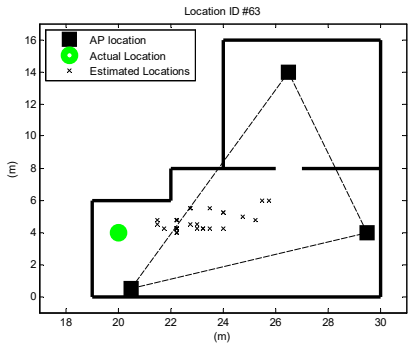 $\bar{E} = 3.0512 \pm 1.2073\,[\mathrm{m}]$

Table 6.4: The positioning error and accuracy of the positioning system on using LKF data

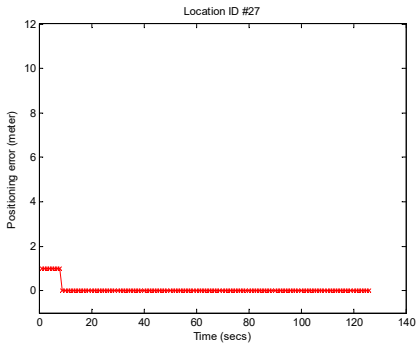 *central* position (Loc. ID #27)	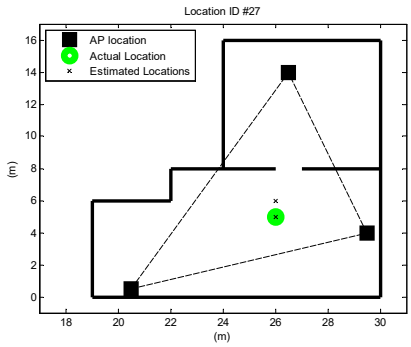 $\overline{E} = 0.0635 \pm 0.2448\,[\mathrm{m}]$
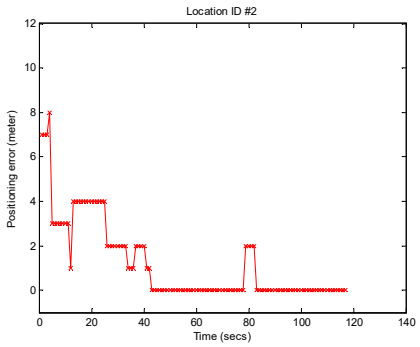 *bottom* position (Loc. ID #2)	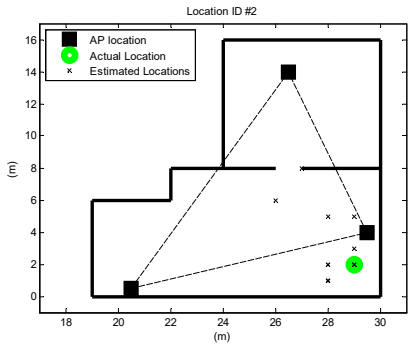 $\overline{E} = 1.1966 \pm 1.8206\,[\mathrm{m}]$
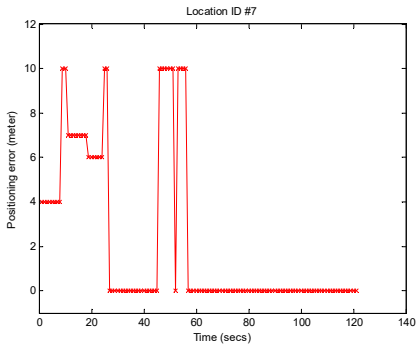 *right* position (Loc. ID #7)	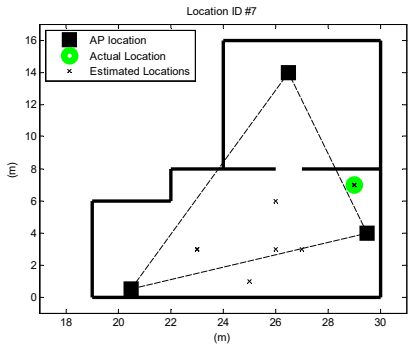 $\overline{E} = 2.1818 \pm 3.6056[\mathrm{m}]$
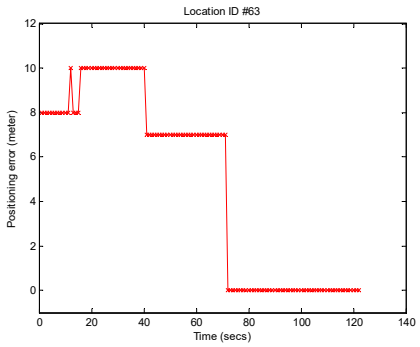 *left* position (Loc. ID #63)	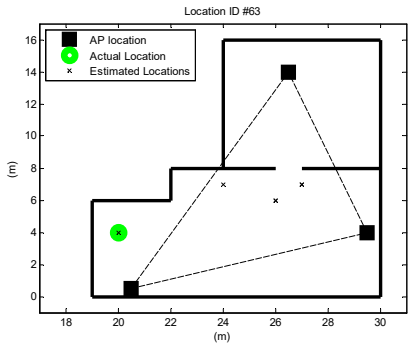 $\overline{E} = 4.8279 \pm 4.2362\,[\mathrm{m}]$

Table 6.1, Table 6.2, Table 6.3 and Table 6.4 tabulated the positioning error and their accuracy with respect to the four distinctive test positions using the WiFi RSS unfiltered raw data, filtered using Moving Average Digital Filter (MADF) with kernel size of 5, filtered data using Low Pass Filter (LPF) with cut-off frequency of 0.2 sec, and Linear Kalman Filter with noise covariance of 3 dB, respectively. Generally, both positioning error and accuracies are bad when the original data is used even in the *central* position with LOS condition between all three WiFi AP. This finding suggests that using the raw data only for stationary positioning is a really bad idea.

On the other hand, using the MADF and LPF suppressed the noise of the raw data successfully, but the positioning system is not so improved. Even though the positioning error and accuracies are improved of those using raw data, the error larger than 2 meter still cannot be tolerated by the mobile robot, especially Terapio with 0.5 meter base size. Hence, these two filters can be discarded.

The Linear Kalman Filter has performed amazingly especially in the case of *central* test position. The average error of this test location has improved dramatically from 1.3095 meter of raw data into 0.0635 meter, which is a 95% improvement. Moreover, the errors are relatively at correct location at about 10 seconds onwards. This is resulting from the adaptive Kalman gain that recursively update at each iterative computation and the corrective processes. Figure 6.6 summarizes the performance of the filters at the *central* position conducted in this research.

On the four distinctive test locations, it can be observed that the positioning error and accuracies regardless of filtering system is better at *central* test position. This is because at this particular location, the receiver i.e. the mobile robot Terapio has a clear LOS between all transmitting WiFi Access Points. Hence, the noise levels are still in acceptable range. However, in the test positions such as *bottom* and *left* where the mobile robot is encapsulated to more than one wall, the receiver is badly affected by the signal propagation mechanism such as the reflection and refraction, which causes severe multipath effect to the received signal.

Therefore, it can be concluded that the positioning system works best when there is LOS between the robot and the WiFi AP. A further research considering such factor can be made to improve the WiFi AP placement. In addition, positioning near to two or more walls can be rather challenging for a mobile robot application.

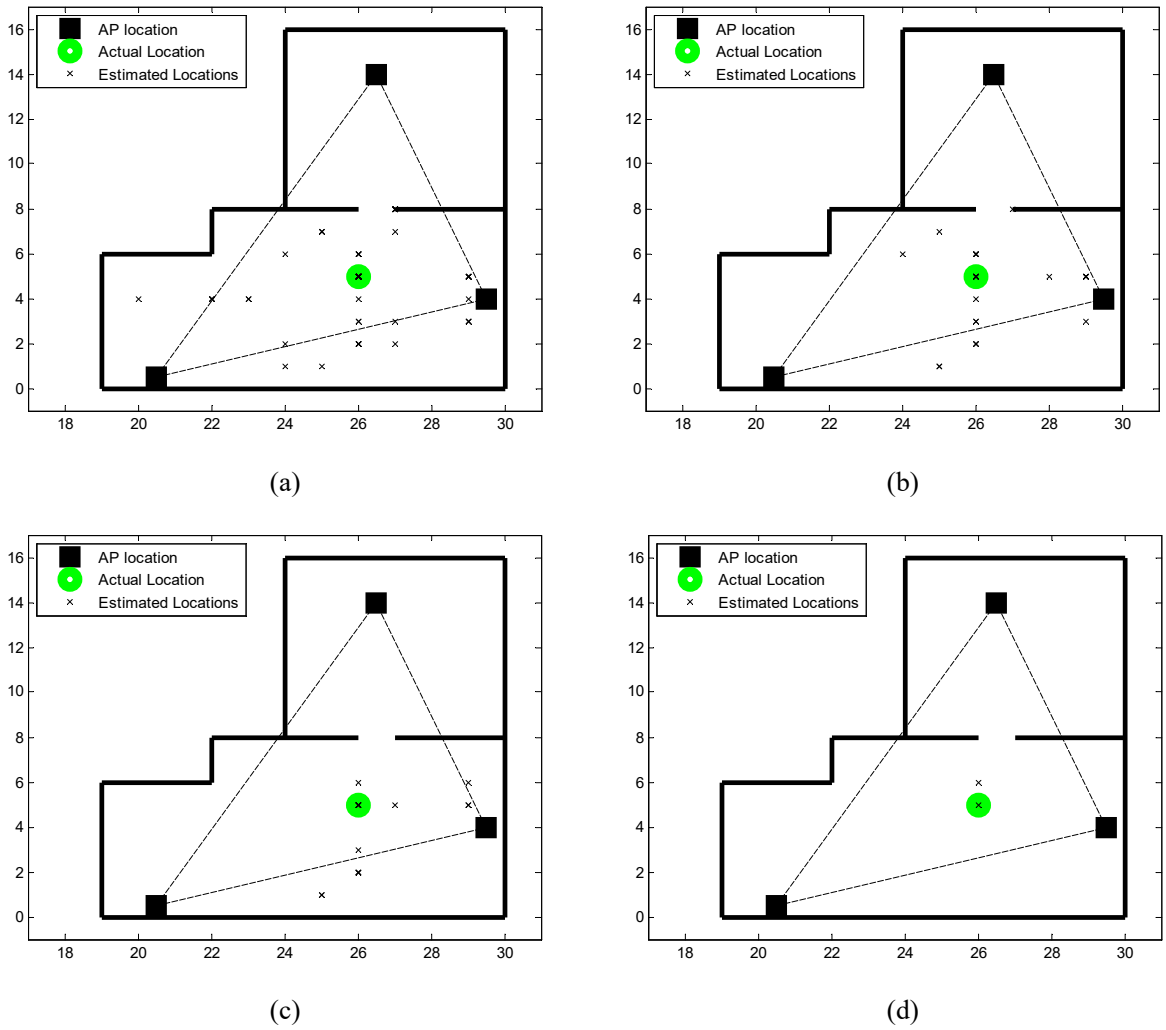

Figure 6.6: The performance of the filters at *central* test location; (a) on using the raw data, (b) on using the MADF filter, (c) on using the LPF, and (d) on using the LKF.

6.3 Comparison with Trilateration Positioning Technique

This dissertation has described the use of fingerprinting technique to position a mobile robot in an indoor environment. However, as mentioned earlier in Section 1.1.2, there are two general techniques for wireless positioning system, the triangulation or trilateration technique being the other one. The triangulation technique requires modification to the WiFi AP in order to output the angular information. The triangulation technique on the other hand, does not require such modification, only the locations of transmitting devices are needed. This information can be provided when the optimization of AP placement described in Chapter 3 is conducted. This section compares the positioning accuracy between the fingerprinting technique and the trilateration technique. The mathematical expression of trilateration technique is also derived.

6.3.1 Path Loss Models

Figure 6.7 shows the concept of geometrical location estimation based on trilateration technique. This technique requires the knowledge of the transmitting devices such as the WiFi Access Points which can be easily obtained from the information management entity. In such requirement therefore, the nomadic transmitting devices such as ad-hoc hotspots are rather impractical to utilize this technique.

The trilateration technique is basically works by forming triangle between the mobile robot and a transmitter. Therefore, trilateration method requires at least three transmitters in range in order to form the triangle. The distance between the mobile robot and the transmitters, represents by the variables r_1, r_2 and r_3 can be reverse-found by the signal propagation model. However, as has been rigorously discussed, there is no generic model of signal propagation and the signal is prone to noises caused by the complex signal mechanisms, interferences, etc. Hence, the accuracy of this technique might be debatable. Nevertheless, positioning can still be achieved by this technique and thus, comparison can be made.

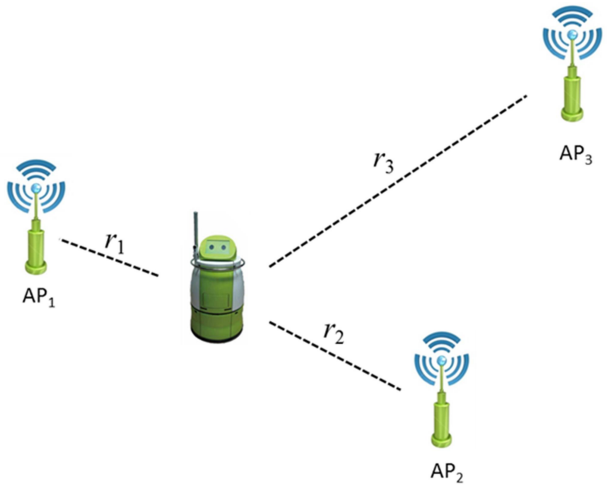

Figure 6.7: Location estimation using trilateration technique

The mathematical derivation of the trilateration technique is as following;

If the mobile robot at an unknown location in Cartesian space represent by (x_u,y_u), then the WiFi signal is received from three or more AP given as $P(r)$. Taking the wireless signal propagation model such as the Log Distance Path Loss model given as [46]

$$P(r) = P(r_0) - 10n\log_{10}(r/r_0), \quad \text{(Eq. 6-8)}$$

where r is the separation distance between the mobile robot and the WiFi AP, $P(r_0)$ is the close-in reference power distance typically at 1 meter, and n is the path loss exponent. Reversing this equation could yield in r, which will be used for later trilateration.

In a triangle, the square of the hypotenuse is equal to the sum of square of its left and right side lines, which is given as

$$(x_i - x_u)^2 + (y_i - y_u)^2 = r_i^2 \quad \text{(Eq. 6-9)}$$

, where (x_i,y_i) is the location of the WiFi AP. Deriving for three WiFi AP will yield in

$$\begin{aligned} r_1^2 &= (x_1 - x_u)^2 + (y_1 - y_u)^2 \\ r_2^2 &= (x_2 - x_u)^2 + (y_2 - y_u)^2 \\ r_3^2 &= (x_3 - x_u)^2 + (y_3 - y_u)^2 \end{aligned} . \quad \text{(Eq. 6-10)}$$

Taking the difference of the triangles,

$$\begin{aligned} r_1^2 - r_3^2 &= (x_1 - x_u)^2 - (x_3 - x_u)^2 + (y_1 - y_u)^2 - (y_3 - y_u)^2 \\ r_2^2 - r_3^2 &= (x_2 - x_u)^2 - (x_3 - x_u)^2 + (y_2 - y_u)^2 - (y_3 - y_u)^2 \end{aligned} \quad \text{(Eq. 6-11)}$$

which can be further expanded into

$$\begin{aligned} 2(x_3 - x_1)x_u + 2(y_3 - y_1)y_u &= (r_1^2 - r_3^2) - (x_1^2 - x_3^2) - (y_1^2 - y_3^2) \\ 2(x_3 - x_2)x_u + 2(y_3 - y_2)y_u &= (r_2^2 - r_3^2) - (x_2^2 - x_3^2) - (y_2^2 - y_3^2) \end{aligned} . \quad \text{(Eq. 6-12)}$$

Rearranging (Eq. 6-12) into matrix form

$$2\begin{bmatrix} (x_3 - x_1) & (y_3 - y_1) \\ (x_3 - x_2) & (y_3 - y_2) \end{bmatrix}\begin{bmatrix} x_u \\ y_u \end{bmatrix} = \begin{bmatrix} (r_1^2 - r_3^2) - (x_1^2 - x_3^2) - (y_1^2 - y_3^2) \\ (r_2^2 - r_3^2) - (x_2^2 - x_3^2) - (y_2^2 - y_3^2) \end{bmatrix} \quad \text{(Eq. 6-13)}$$

Then, the unknown location (x_u, y_u) can be found in

$$\begin{bmatrix} x_u \\ y_u \end{bmatrix} = 2\begin{bmatrix} (x_3 - x_1) & (y_3 - y_1) \\ (x_3 - x_2) & (y_3 - y_2) \end{bmatrix}^{-1} \times \begin{bmatrix} (r_1^2 - r_3^2) - (x_1^2 - x_3^2) - (y_1^2 - y_3^2) \\ (r_2^2 - r_3^2) - (x_2^2 - x_3^2) - (y_2^2 - y_3^2) \end{bmatrix}. \quad \text{(Eq. 6-14)}$$

In this works, (Eq. 6-14) is used to estimate the location of a mobile robot when the robot stays stationary at the *central* location (in this case, Loc. ID #27). Then the separation distance between the robot and the transmitters are deduced using the LDPL model. Figure 6.8 shows the result when such technique is used. As has been expected, the positioning errors are indeed impractical where the average error is at 48.81 ± 56.62 meter, which is larger than the experimental area itself. Hence, the trilateration technique by deducing the distance from path loss models can be taken out of league. A more vibrant site-specific model can be developed to improve this accuracy.

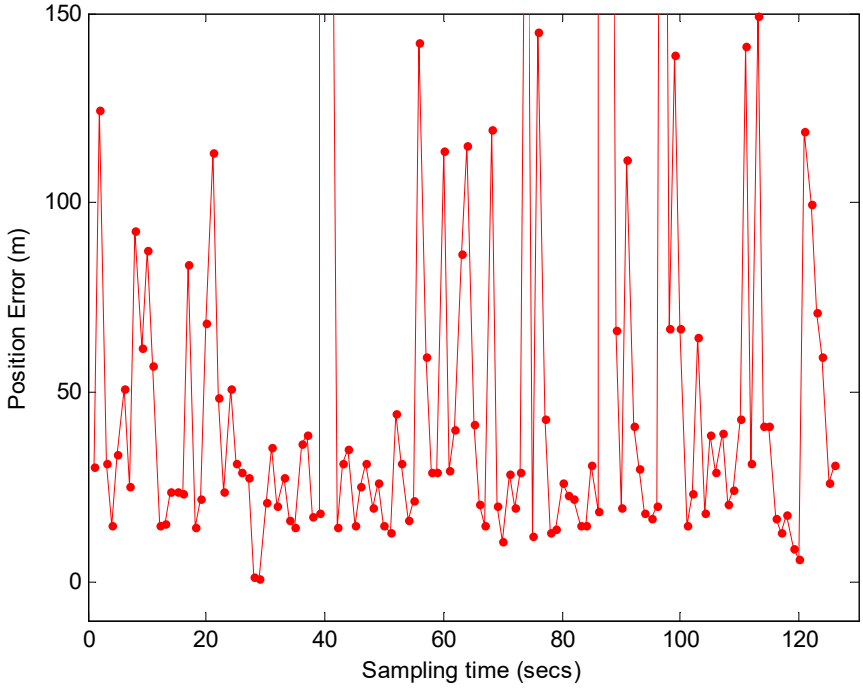

Figure 6.8: Positioning error at stationary location (Location ID #27) using trilateration technique where the separation distance is deduced from path loss model

6.3.2 Site-Specific Models

A site-specific modeling is a better option for trilateration technique when the locations of the transmitting devices are known. An experiment to measure the WiFi RSS data similar to the fingerprinting technique is required. Then, the mathematical fit to the WiFi RSS measurements can be made. In order to estimate the mobile robot location in the real-time, the online measurement signal is correlated with the mathematical fit in order to interpolate the distance measures. Afterwards, the location is computed similarly using (Eq. 6-14).

In this research, a comprehensive site surveys in the experimental area has been made for the fingerprinting technique earlier from Location ID #1 to Location ID #64. These data can also be used for fitting the signal models received from AP1, AP2 and AP3. In order to obtain the most realistic model, the LOS condition should be taken into consideration. Hence, a small number of the sampling locations are selected, From AP1, the selected Location IDs are #4, #12, #19, #28, #35, #42, #48, #54, #59 and #63. The Location ID #46, #32, #31, #16, #15 and #1 are selected for AP2 and lastly for AP3, the Location ID #23, #22, #21, #20, #19, #18, #17 and #16 are carefully selected as reference signal data. Then, the mathematical fitting to these selected locations corresponding to the WiFi AP are given by

$$\begin{aligned} RSS_{AP1} &= 15d_1^{-0.3728} - 79.12 \\ RSS_{AP2} &= -10.26d_2^{-0.553} - 37.77\,. \\ RSS_{AP1} &= -48.27d_3^{0.1619} \end{aligned} \qquad \text{(Eq. 6-15)}$$

Figure 6.9 shows the respective models derived from fitting the WiFi signal data in the corresponding Location IDs with respect to the functions given in (Eq. 6-14), where the average of WiFi RSS measurements in the stationary locations are the reference data. In such situations, one can observe that the fluctuations that concur with the logarithmic relationship between the signal strength and the separation distance between the transmitter and the receiver.

Figure 6.10 on the other hand shows the positioning error at the *central* test position (Loc. ID #27) where (Eq. 6-14) is used to compute the position. The separation distance between the robot and the transmitters are deduced using the relation described in (Eq. 6-15). Using this technique, the accuracy of the positioning error is at 7.34 ± 8.26 meter which is a significant improvement compared when the separation distance is deduced using LDPL model. It is however is no better compared to fingerprinting technique especially when Linear Kalman Filter is used.

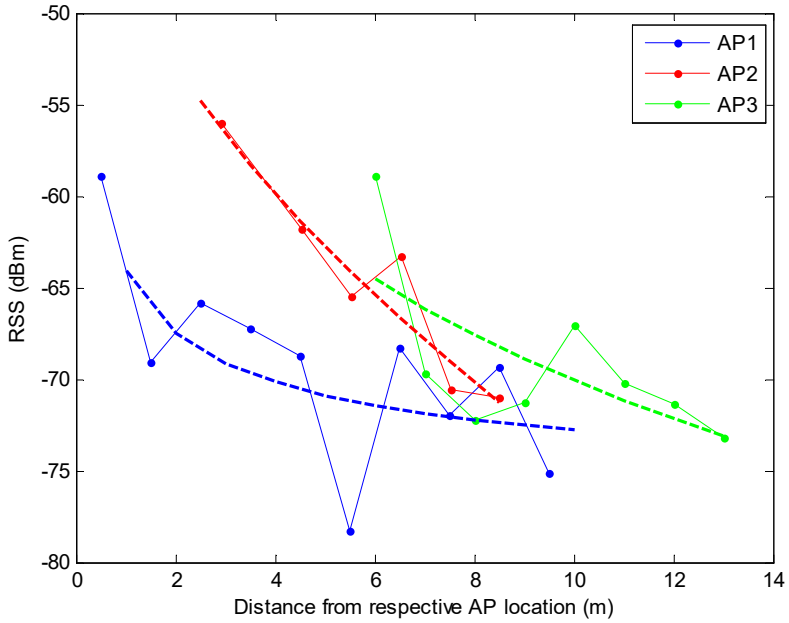

Figure 6.9: The fitting models of the RSS with respect to the separation distance from the WiFi AP. The straight lines are the measurement values and the dotted lines are the fitting values.

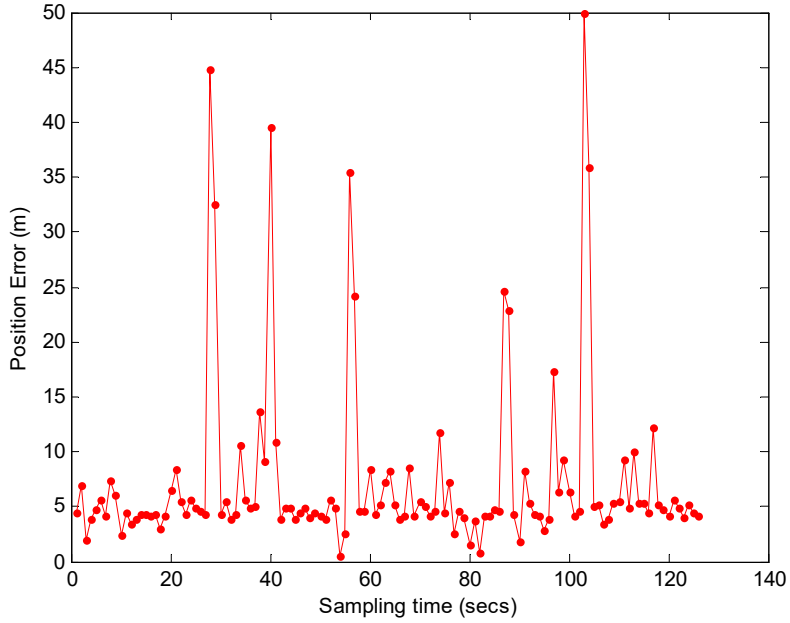

Figure 6.10: Positioning error at stationary location (Location ID #27) using trilateration technique where the separation distance is computed from the site-specific model.

6.4 Summary

The stationary positioning system with the use of raw WiFi RSS data may cause bad variation of positioning results due to the signal fluctuation problems. The signal fluctuation caused by complex signal propagation and mechanism is non-deterministic thus controlling them is an ambitious effort. Hence the signal filtering approach is highly desired.

In this works, three signal filtering methods have been applied, namely the Moving Average Digital Filter (MADF), the Low Pass Filter (LPF) and the Linear Kalman Filter (LKF). At all four distinctive test positions, the LKF has proven to be the best filtering method. With a proper choice of noise standard deviation, the online signal is likely to converge to the signal average which is the reference values in the fingerprinting database. In such cases, the lower noise standard deviation means that the WiFi RSS measurement is much more trustfulness.

By using the LKF with an appropriate choice of standard deviation, the accuracies of the positioning system is improved as well as in term of precisions and therefore solved the stationary positioning problem.

The positioning employing trilateration technique where distance is computed from (1) path loss model and (2) measurement fitting has also been experimented. The measurement fitting as a result of site-specific survey is better than the path loss model, but their results are no better than fingerprinting technique.

Chapter 7 CONCLUSION AND FUTURE PERSPECTIVES

"*One worthwhile task carried to a successful conclusion is better than 50 half-finished tasks*"

- B.C. Forbes, 1900s

7.1 General Conclusions

This dissertation presents the research works related to the design and analysis of the Wireless Positioning System (WPS), typically using the ubiquitous 2.4GHz Wireless Fidelity (WiFi) Received Signal Strength (RSS) data to estimate the location of a mobile client i.e. the mobile robot in this case, in a known indoor environment. The mobile robot in this context is aimed for the medical service and support round robot Terapio developed by Toyohashi University of Technology, Japan. The proposed WPS system could enhance the functionality of Terapio in the sense of self-localization especially in a stationary location without using any conventional localization sensor such as the laser range finder LIDAR or the need of have computation of camera-based image processing or any odometry information such as the dead reckoning method. Moreover, the use of wireless system could also be used for later multi-robot communication as well as adaptation to the multi-agent systems.

This research proposed the WPS system for mobile robot application in several frameworks;

(1) the optimization of the WiFi Access Point (AP) placement, where the optimization problem is solve using a modified brute search namely the Grid Greedy Logic Search (GGLS) and the combination of the Tree Hierarch and a cost function. The final result concludes that the placements of the wireless nodes are not necessary to be in symmetrical patterns as suggested by many other literatures,

(2) the assessments of WiFi signal using the Design of Experiment (DoE) method, where two parameters for positioning system i.e. the antenna heights of the transmitters and the separation distance between the receiver and the transmitter. DoE by means of randomized measurement and ANOVA analysis proved that the antenna heights were not a significant parameter for positioning system,

(3) the interpolation of the fingerprinting database, where the main problem of costly efforts during data collection to create the WiFi signal fingerprint database is solved. The proposed method namely the Modified Shepard's Method (MSM) has performed better than the Kriging algorithm and the conventional Inverse Distance Weighting (IDW) methods. Later, a novel method namely the Signal-Propagated Modified Shepard Method (SP-MSM) is proposed where extensive experiments and data collections were conducted resulting in much trustful yields. In overall 64 stationary test locations, SP-MSM methods has the better positioning result at 52% more test locations compared to other methods, and

(4) the improvisation of stationary positioning using filtering methods, where three different methods are experimented which are the Moving Average Digital Filter (MADF), the Low Pass Filter (LPF), and the Linear Kalman Filter (LKF). The LKF is proven to be the best filtering methods compared to the other two. In addition, the trilateration technique is also demonstrated where the separation distance between the mobile robot and the WiFi AP are computed using two methods i.e. the signal models (Log-Distance Path Loss model) and the site-specific model by fitting the WiFi data to a specific mathematical models. In any cases, both trilateration methods are outperformed by the fingerprinting technique with major positioning error.

Table 7.1 tabulated the overall methods and techniques of the stationary positioning system that has been employed and experimented in this research works focusing on the *central* test location. In general, there are two positioning techniques which are the fingerprinting technique and trilateration technique. The trilateration technique is a simple method, but proven to be ineffective. This is due to the reason of the complex signal propagation and mechanism that made the computation of the transmitter-receiver separation distance is unreliable. Hence, bad accuracy.

Table 7.1: Comparison of stationary positioning error employed in this dissertation

Method	Description	Average Error [meter]
Fingerprinting (raw data)	Database is generated using SP-MSM, WKNN at 4.	1.309 ± 0.918
Fingerprinting (moving average filter)	Database is generated using SP-MSM. WKNN at 4. Kernel size is 5.	1.218 ± 0.800
Fingerprinting (low pass filter)	Database is generated using SP-MSM. WKNN at 4. Cut-off freq at 0.2 sec.	1.038 ± 0.704
Fingerprinting (Kalman filter	Database is generated using SP-MSM. WKNN at 1. SD is set to 3dB.	0.064 ± 0.245
Trilateration (path loss model)	Log-distance path loss model is used. Model variables are estimated using SP method.	48.81 ± 56.62
Trilateration (site-specific model)	Distance is obtained from the fitted functions.	7.34 ± 8.26

The fingerprinting techniques on the other hand are extensively experimented using the fingerprinting database generated by the SP-MSM interpolation method, and the positioning is estimated using the Weighted K-Nearest Neighbor (WKNN) algorithm. Using the raw data for positioning is not a good idea too since the signal is affected by the fluctuation problems. Therefore, the filtering is needed. Overall, the LKF with the choice of 3 dB noise standard deviation has the best result with the outstanding positioning errors and accuracies.

In summary, the wireless positioning system for the mobile robot Terapio in any indoor environment can be made on the following procedures;

(i). find the optimal location to install the WiFi AP according to the GGLS algorithm,
(ii). set the antenna heights of the transmitters at least to the equal heights of the Terapio wireless antenna,
(iii). construct the WiFi fingerprinting database by using the SP-MSM method,
(iv). estimate Terapio stationary location using the WKNN positioning algorithm, and lastly
(v). update and improve the stationary location using the Kalman Filter.

7.2 Research Contribution

The contribution of the dissertation among many is the milestone works for Terapio. Current Terapio relies on the heavy computation of the SLAM algorithm to estimate its position. By using the wireless approach, this computation can be reduced. Moreover, the floor plan has been also digitized in Terapio memory, thus could be used to improve its localization algorithm. A fusioning of SLAM and WPS could be also experimented to obtain a much reliable positioning and navigation system.

The WiFi AP placement can be used for networking management entities in order to deploy the wireless nodes in an environment. This approach could yield in maximum signal coverage with minimum number of required WiFi AP. The placement of the wireless nodes specifically for positioning system can be further studied with respect to the four distinctive locations i.e. the *central*, *bottom*, *left* and *right* test locations.

Statistical evidence that antenna heights are not a significant parameter for positioning system in an indoor environment, with the specified conditions has been presented. It has been later validated by actual experiments.

Interpolation methods can save the data collection stage for creating the database. Moreover, the 64 location of database at 1 meter spacing granularity generated by the interpolation systems can be further used for experiments by other interested parties. These 64 locations could also serve as a benchmark for further works. The Linear Kalman Filter is proven to be the best filtering algorithm to the incoming online signal so that the wireless fluctuation problems can be solved.

An application of the proposed WPS can be use immediately used by Terapio. The fingerprinting scheme including the LKF application can be used to determine and correct the final positioning of Terapio where the navigation error is cause by the odometry error. This immediate application is illustrated in Figure 7.1 where the navigation of the mobile robot is developed by internal sensing element. There will be position error at the final position that resulting from the odometry error such as the wheel slippage, contact point of the wheel as well as unequal floor contacts. Moreover, the odometry error is cumulative over time thus affecting the final position. Therefore, the final position can be particularly variate from the targeted goal position. By employing the proposed WPS system, the final position can be determine automatically especially with the use of Linear Kalman Filter to predict the online WiFi signal. This is because at the final position, the mobile robot stays stationary for some period of time similarly to the condition demonstrated in this dissertation.

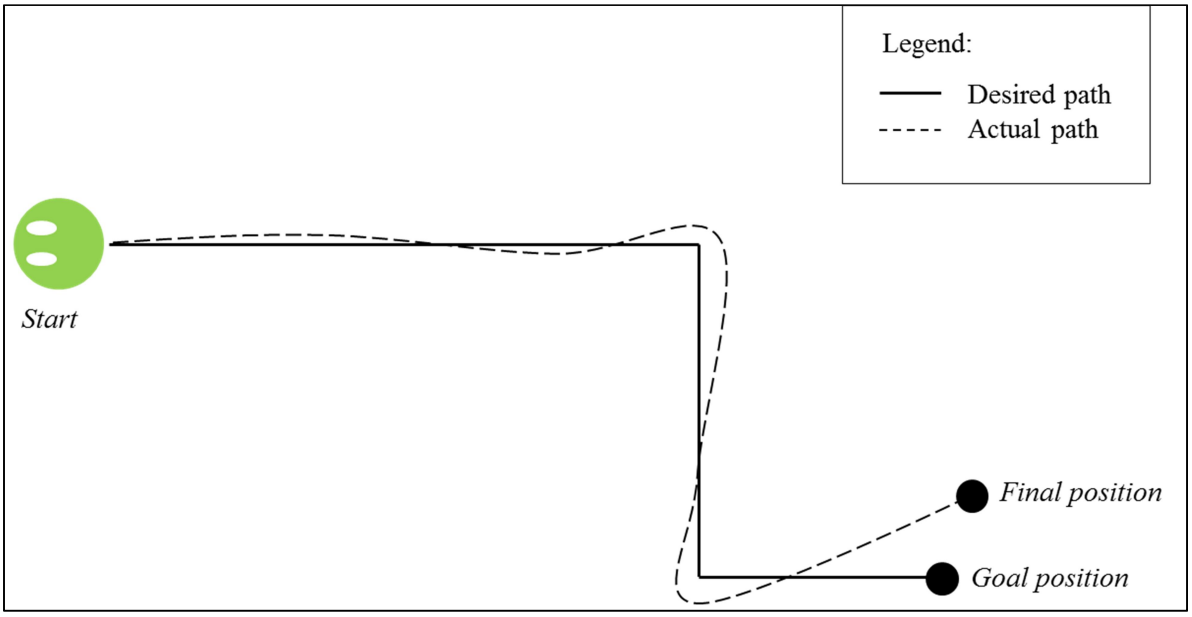

Figure 7.1: An illustration of immediate application of the WPS for determining the final position of the mobile robot where the position error is caused by odometry error.

7.3 Challenges and Limitations

The sampling time of the WiFi signal is limited, since the signal is firstly transmitted by the AP, then it has to wait for receiver respond before transmitting signals again. Hence, the delay is big. This problem however can be solved using Zero-Order-Hold (ZOH) method [99] where the sampling time can be reduced with timely synchronization.

The Radio Frequency signal such as WiFi signal is inherently unstable, which means that the todays signal may not be similar to yesterday's signal. The radio map collected earlier may deviate from the current one. In addition, the WiFi signal also decays over life time. Therefore, these lucrative factors may cause the instability of the fingerprinting database that makes such methods very challengeable. The research works in [100] describes an interesting technique where each reference locations is marked and assigned with the RFID tags in order to observe any changes in the fingerprinting database.

In this dissertation, using the WiFi alone for positioning on a stationary location could yield in good result, but when the receivers start to move (mobility), positioning can become challenging. Therefore, fusioning with other motion-sensitive sensors may be required, such as the gyroscope, digital compass for orientation as well as odometry information. In addition, the frontal obstacles faced by the mobile robot cannot be detected by outside sensing element such as WiFi signal, hence for practical implementation, the integration with other sensors such as infrared is required to detect the obstacles.

7.4 Future Perspectives

In this dissertation, the positioning systems are focus on stationary location where the mobile robot stays in a same location for a period of time. Such approach is not much practical especially when dealing with mobile robot where mobility is expected. The WiFi signal can be extended from stationary positioning into mobility tracking, and ultimately for navigational system. One possible approach is to consider the spatio-temporal information of the fingerprinting database. Figure 7.2 shows an ideal spatio-temporal WiFi signal pattern when a user is walking passing through a WiFi AP in a pathway [101]. The signal is weak when the user is far from the AP and stronger when the user is near the AP as the user is walking in the pathway. This characteristic can be utilizes by means of probabilistic and likelihood estimation.

The fingerprinting database can also be simplify by depicting the spatio-temporal pattern, which means that a cluster of database can be made according to the strongest signal received by the mobile robot. Figure 7.3 depicted the spatio-temporal patterns of the WiFi RSS in the Terapio experimental area from the 64 reference locations. The WiFi APs are marked with three different colors to represent the strongest signal received from the mobile robot. That being said, the strong RSS transmitted by AP3 could be measured at the locations near to AP3 (which is in red), similarly to the other two APs. Therefore, when the mobile robot has the RSS for which the AP3 signal is the strongest, then the fingerprinting database can be clustered to the locations marked in red. Hence, this method will improve the processing time as well as positioning accuracy.

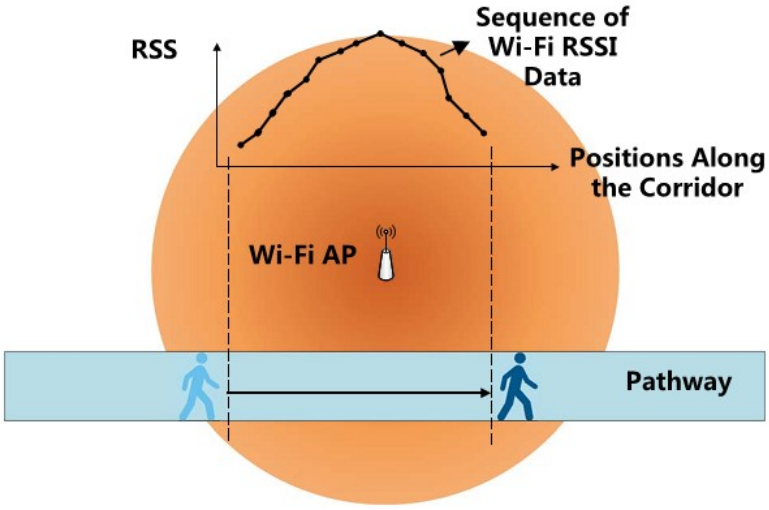

Figure 7.2: An ideal WiFi spatio-temporal signal patterns [101]

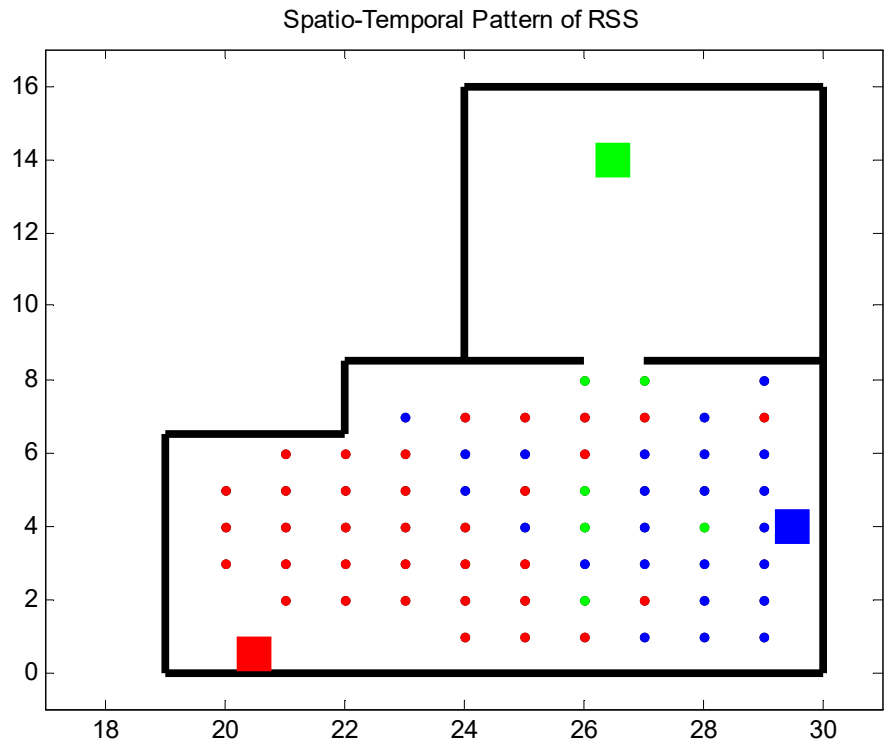

Figure 7.3: The spatio-temporal patterns in the experimental area with respect to the three WiFi APs

Multiple Terapio operating on the same environment depicted earlier in Figure 1.5 is also a good perspective especially in the case of multi-agents system with emphasize on inter-robot communication, self-position, as well as updating and reporting individual location to the server. In addition, in order to improve the accuracy, the fingerprinting database can be also updated whenever any individual robot detects abnormal changes in the fingerprint database, and then update the new database. This new updated database can also be collaboratively used by the multiple Terapio. Such method is known as fingerprinting *crowdsourcing.* Recent works have reported that the use of such technique could maintained the database as well as providing enough data for user localization, which also known as the Organic Indoor Positioning System (OIPS) [102][103].

Figure 7.4 illustrate the concept of the OIPS in the practical application of multiple mobile robots Terapio. In the beginning time t_o, if we assume there is only one Terapio working on the area, then the database crowdsourcing is not so influenced since only one robot is around and so, only the neighboring areas are updated. Over the time noted by t_p, more and more Terapios are working on the environment, and therefore the data crowdsourcing are much feasible when multiple mobile robots are uploading their data respective of the signal strength and its corresponding location. At later time t_q, the signal fingerprint and its

database are well updated and maintained with the crowdsourced by more mobile robot Terapios. Indeed, we can observed that as more mobile robots participate in updating the signal strength and the locations, the colors of the area becomes darker, which literally means that the database 'organically' developed with data input. Such technique however, is prone to noise since the wireless signal exhibit non-deterministic behavior. Moreover, more open problems available such as the fusioning of signal uploaded by multiple robots at the same position, the validity (correct or incorrect) of the uploaded data and the interruption of routine procedures of the mobile robot.

The future perspective described in this section numerate some of most potential research perspective in the field of wireless positioning system and its application to mobile robot(s). As of this writing, this field is now about 15 years old of research. It still can be considered young and hence, this wireless positioning system field has a bright future for extending relevant research works.

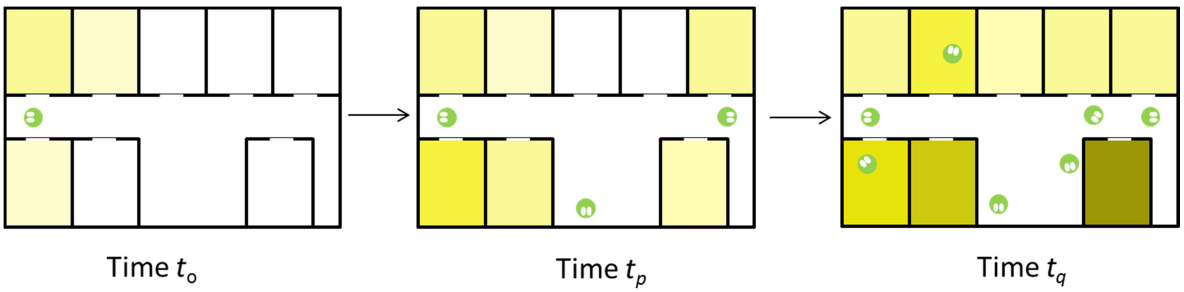

Figure 7.4: An illustration of maintaining the fingerprinting database through multiple Terapio *crowdsourcing*. The depth of the color represents the density of the WiFi RSS as the robots upload their received data corresponding to the exact location.

References

[1] K. Capek, *Rossum's Universal Robots*. 1920.

[2] W. G. Walter, "An Imitation of Life," *Scientific American*, vol. 182, no. 2. pp. 42–45, 1950.

[3] W. G. Walter, "A Machine That Learns," *Scientific American*, vol. 185, no. 2. pp. 60–63, 1951.

[4] R. A. Lindemann, D. B. Bickler, B. D. Harrington, G. M. Ortiz, and C. J. Voothees, "Mars exploration rover mobility development," *IEEE Robot. Autom. Mag.*, vol. 13, no. 2, pp. 19–26, 2006.

[5] R. Tasaki, M. Kitazaki, J. Miura, and K. Terashima, "Prototype design of medical round supporting robot 'Terapio,'" in *2015 IEEE International Conference on Robotics and Automation (ICRA)*, 2015, pp. 829–834.

[6] K. Terashima, S. Takenoshita, J. Miura, R. Tasaki, M. Kitazaki, R. Saegusa, T. Miyoshi, N. Uchiyama, S. Sano, J. Satake, R. Ohmura, T. Fukushima, K. Kakihara, H. Kawamura, and M. Takahashi, "Medical round robot - Terapio -," *J. Robot. Mechatronics*, vol. 26, no. 1, pp. 112–114, 2014.

[7] Y. Ueno, K. Kitagawa, and K. Terashima, "Development of the Differential Drive Steering System Using Spur Gear for Omni-Directional Mobile Robot," *日本機械学会論文集（C編）*, vol. 78, no. 789, pp. 568–581, 2012.

[8] Y. Ueno, T. Ohno, K. Terashima, and H. Kitagawa, "The development of driving system with differential drive steering system for omni-directional mobile robot," *2009 IEEE Int. Conf. Mechatronics Autom. ICMA 2009*, pp. 1089–1094, 2009.

[9] H. Brook, *Artificial Intelligence*. Usborne Publishing Ltd., 2016.

[10] W. M. Y. W. Bejuri, M. M. Mohamad, and M. Sapri, "Ubiquitous Positioning: A Taxonomy for Location Determination on Mobile Navigation System," *arXiv Prepr. arXiv1103.5035*, vol. 2, no. 1, p. 15, Mar. 2011.

[11] R. Angeles, "RFID Technologies: Supply-Chain Applications and Implementation Issues," *Inf. Syst. Manag.*, vol. 22, no. 1, pp. 51–65, Dec. 2005.

[12] C.-C. Lin, M.-J. Chiu, C.-C. Hsiao, R.-G. Lee, and Y.-S. Tsai, "Wireless Health Care Service System for Elderly With Dementia," *IEEE Trans. Inf. Technol. Biomed.*, vol. 10, no. 4, pp. 696–704, Oct. 2006.

[13] L. a. Guerrero, F. Vasquez, and S. F. Ochoa, "An Indoor Navigation System for the Visually Impaired," *Sensors*, vol. 12, no. 6, pp. 8236–8258, 2012.

[14] G. Borriello, V. Stanford, C. Narayanaswami, and W. Menning, "Guest Editors' Introduction: Pervasive Computing in Healthcare," *IEEE Pervasive Comput.*, vol. 6, no. 1, pp. 17–19, Jan. 2007.

[15] K. Sayrafian-Pour and J. Perez, "Robust Indoor Positioning Based on Received Signal Strength," *2007 2nd Int. Conf. Pervasive Comput. Appl.*, pp. 693–698, 2007.

[16] M. Li and Y. Liu, "Underground coal mine monitoring with wireless sensor networks," *ACM Trans. Sens. Networks*, vol. 5, no. 2, pp. 1–29, Mar. 2009.

[17] L. Mo, Y. He, Y. Liu, J. Zhao, S.-J. Tang, X.-Y. Li, and G. Dai, "Canopy closure estimates with GreenOrbs: sustainable sensing in the forest," in *Proceedings of the 7th ACM Conference on Embedded Networked Sensor Systems - SenSys '09*, 2009, p. 99.

[18] Z. Yang, M. Li, and Y. Liu, "Sea Depth Measurement with Restricted Floating Sensors," in *28th IEEE International Real-Time Systems Symposium (RTSS 2007)*, 2007, pp. 469–478.

[19] S. Fu, Z. Hou, and G. Yang, "An indoor navigation system for autonomous mobile robot using wireless sensor network," in *2009 International Conference on Networking, Sensing and Control*, 2009, pp. 227–232.

[20] C. Röhrig and F. Künemund, "Mobile robot localization using WLAN signal strengths," *2007 4th IEEE Work. Intell. Data Acquis. Adv. Comput. Syst. Technol. Appl. IDAACS*, vol. 7, no. 2, pp. 704–709, 2007.

[21] X. Kuai, K. Yang, S. Fu, R. Zheng, and G. Yang, "Simultaneous localization and mapping (SLAM) for indoor autonomous mobile robot navigation in wireless sensor networks," *2010 Int. Conf. Netw.*

Sens. Control ICNSC, pp. 128–132, 2010.
[22] S. Hara, "Localization," *Osaka City University*, 2008.
[23] P. Connolly and D. Boone, "Indoor Location in Retail: Where is the Money," 2013.
[24] C. Ververidis and G. C. Polyzos, "Mobile Marketing Using a Location Based Service," *Communication*. 2002.
[25] J. Steenstra, A. Gantman, K. Taylor, and L. Chen, "Location based service (LBS) system and method for targeted advertising." Google Patents, 2004.
[26] S. He and S. G. Chan, "Wi-Fi Fingerprint-Based Indoor Positioning : Recent Advances and Comparisons," vol. 18, no. 1, pp. 466–490, 2016.
[27] H. Liu, H. Darabi, P. Banerjee, and J. Liu, "Survey of Wireless Indoor Positioning Techniques and Systems," *IEEE Trans. Syst. Man Cybern. Part C (Applications Rev.*, vol. 37, no. 6, pp. 1067–1080, Nov. 2007.
[28] Y. Gu, A. Lo, and I. Niemegeers, "A survey of indoor positioning systems for wireless personal networks," *IEEE Commun. Surv. Tutorials*, vol. 11, no. 1, pp. 13–32, 2009.
[29] B. T. Fang, "Simple solutions for hyperbolic and related position fixes," *IEEE Trans. Aerosp. Electron. Syst.*, vol. 26, no. 5, pp. 748–753, 1990.
[30] A. S. Paul and E. A. Wan, "RSSI-Based indoor localization and tracking using sigma-point kalman smoothers," *IEEE J. Sel. Top. Signal Process.*, vol. 3, no. 5, pp. 860–873, 2009.
[31] P. Bahl and V. N. Padmanabhan, "RADAR: an in-building RF-based user location and tracking system," in *Proceedings IEEE INFOCOM 2000. Conference on Computer Communications. Nineteenth Annual Joint Conference of the IEEE Computer and Communications Societies (Cat. No.00CH37064)*, 2000, vol. 2, pp. 775–784.
[32] B. Li, J. Salter, A. Dempster, and C. Rizos, "Indoor positioning techniques based on wireless LAN," in *First IEEE International Conference on Wireless Broadband and Ultra Wideband Communications*, 2006, pp. 13–16.
[33] J. Borenstein, H. R. Everett, L. Feng, and D. Wehe, "Mobile robot positioning: Sensors and techniques," *J. Robot. Syst.*, vol. 14, no. 4, pp. 231–249, 1997.
[34] a. Mandal, C. V. Lopes, T. Givargis, a. Haghighat, R. Jurdak, and P. Baldi, "Beep: 3D indoor positioning using audible sound," *Second IEEE Consum. Commun. Netw. Conf. 2005. CCNC. 2005*, pp. 348–353, 2005.
[35] V. Moghtadaiee, A. G. Dempster, and S. Lim, "Indoor localization using FM radio signals: A fingerprinting approach," in *2011 International Conference on Indoor Positioning and Indoor Navigation, IPIN 2011*, 2011.
[36] S. S. Saad and Z. S. Nakad, "A standalone RFID indoor positioning system using passive tags," *IEEE Trans. Ind. Electron.*, vol. 58, no. 5, pp. 1961–1970, 2011.
[37] S. Feldmann, K. Kyamakya, A. Zapater, and Z. Lue, "An indoor Bluetooth-based positioning system : concept , Implementation and experimental evaluation," *Int. Conf. Wirel. Networks*, pp. 109–113, 2003.
[38] S. Y. Jung, S. Hann, and C. S. Park, "TDOA-based optical wireless indoor localization using LED ceiling lamps," *IEEE Trans. Consum. Electron.*, vol. 57, no. 4, pp. 1592–1597, 2011.
[39] J. Hsu, "What's Next After 25 Years of Wi-Fi?," *IEEE Spectrum Magazine*. [Online]. Available: http://spectrum.ieee.org/tech-talk/telecom/wireless/whats-next-after-25-years-of-wifi.
[40] D. SCHNEIDER, "New Indoor Navigation Technologies Work Where GPS Can't," *IEEE Spectrum Magazine*. [Online]. Available: http://spectrum.ieee.org/telecom/wireless/new-indoor-navigation-technologies-work-where-gps-cant.
[41] F. Herranz, Á. Llamazares, E. Molinos, M. Ocaña, and M. Á. Sotelo, "WiFi SLAM algorithms: an experimental comparison," *Robotica*, vol. 34, no. 4, pp. 837–858, Apr. 2016.
[42] J. Biswas and M. Veloso, "WiFi localization and navigation for autonomous indoor mobile robots," *Proc. - IEEE Int. Conf. Robot. Autom.*, pp. 4379–4384, 2010.
[43] National Aeronautics and Space Administration, "Imagine The Universe!" [Online]. Available: http://imagine.gsfc.nasa.gov/.
[44] N. Lamn, "What If You Could See WiFi?," 2013. [Online]. Available: http://nickolaylamm.com/art-for-clients/what-if-you-could-see-wifi/.

[45] I. T. U. (ITU), “Documents of the International Radio Conference (Atlantic City, 1947).”
[46] T. Rappaport, *Wireless Communications: Principles and Practice*, 2nd ed. Upper Saddle River, NJ, USA: Prentice Hall PTR, 2001.
[47] M. Hidayab, A. H. Ali, and K. B. A. Azmi, “Wifi signal propagation at 2.4 GHz,” *APMC 2009 - Asia Pacific Microw. Conf. 2009*, pp. 528–531, 2009.
[48] D. Tummala, “Indoor Propagation Modeling at 2.4 GHz for IEEE 802.11 Networks,” University of North Texas, 2005.
[49] M. Lott and I. Forkel, “A multi-wall-and-floor model for indoor radio propagation,” in *IEEE VTS 53rd Vehicular Technology Conference, Spring 2001. Proceedings (Cat. No.01CH37202)*, vol. 1, pp. 464–468.
[50] Recommendation ITU-R P.1238-1 Data, “P.1238 : Propagation data and prediction methods for the planning of indoor radiocommunication systems and radio local area networks in the frequency range 300 MHz to 100 GHz,” 2015.
[51] D. B. Green and A. S. Obaidat, “An accurate line of sight propagation performance model for ad-hoc 802.11 wireless LAN (WLAN) devices,” in *2002 IEEE International Conference on Communications. Conference Proceedings. ICC 2002 (Cat. No.02CH37333)*, vol. 5, pp. 3424–3428.
[52] Z. Xiang, S. Song, J. Chen, H. Wang, J. Huang, and X. Gao, “A Wireless LAN-based Indoor Positioning Technology,” *IBM J. Res. Dev.*, vol. 48, no. 5/6, pp. 617–626, 2004.
[53] V. Erceg, L. J. Greenstein, S. Y. Tjandra, S. R. Parkoff, A. Gupta, B. Kulic, A. A. Julius, and R. Bianchi, “An empirically based path loss model for wireless channels in suburban environments,” *IEEE J. Sel. Areas Commun.*, vol. 17, no. 7, pp. 1205–1211, Jul. 1999.
[54] L. E. Miller, “Propagation Model Sensitivity Study,” *Contract Report, JS Lee Assoc., Inc*, 1992.
[55] Mathuranathan, “Log Distance Path Loss or Log Normal Shadowing Model,” 2013. [Online]. Available: http://www.gaussianwaves.com/2013/09/log-distance-path-loss-or-log-normal-shadowing-model/.
[56] L. Liao, W. Chen, C. Zhang, L. Zhang, D. Xuan, and W. Jia, “Two birds with one stone: Wireless access point deployment for both coverage and localization,” *IEEE Trans. Veh. Technol.*, vol. 60, no. 5, pp. 2239–2252, 2011.
[57] A. J. Nicholson, Y. Chawathe, M. Y. Chen, B. D. Noble, and D. Wetherall, “Improved access point selection,” *Proc. 4th Int. Conf. Mob. Syst. Appl. Serv. - MobiSys 2006*, p. 233, 2006.
[58] A. Akella, G. Judd, S. Seshan, and P. Steenkiste, “Self-management in chaotic wireless deployments,” *Wirel. Networks*, vol. 13, no. 6, pp. 737–755, 2007.
[59] O. Baala, Y. Zheng, and A. Caminada, “The Impact of AP Placement in WLAN-Based Indoor Positioning System,” *2009 Eighth Int. Conf. Networks*, pp. 12–17, 2009.
[60] Y. Chen and J. Francisco, “A practical approach to landmark deployment for indoor localization,” *Sens. Ad Hoc …*, vol. 11, 2006.
[61] S.-H. Fang and T.-N. Lin, “A Novel Access Point Placement Approach for WLAN-Based Location Systems,” *2010 IEEE Wirel. Commun. Netw. Conf.*, pp. 1–4, Apr. 2010.
[62] Y. Zhao, H. Zhou, and M. Li, “Indoor Access Points Location Optimization Using Differential Evolution,” in *2008 International Conference on Computer Science and Software Engineering*, 2008, vol. 1, pp. 382–385.
[63] Á. Huszák, G. Gódor, and K. Farkas, “Investigation of WLAN Access Point Placement for Indoor Positioning,” in *Meeting of the European Network of Universities and Companies in Information and Communication Engineering*, 2012, pp. 350–361.
[64] K. Farkas, Á. Huszák, and G. Gódor, “Optimization of Wi-Fi Access Point Placement for Indoor Localization,” *J. IIT (Informatics IT Today)*, vol. 1, no. 1, pp. 28–33, 2013.
[65] Ying He, Weixiao Meng, Lin Ma, and Zhian Deng, “Rapid deployment of APs in WLAN indoor positioning system,” in *2011 6th International ICST Conference on Communications and Networking in China (CHINACOM)*, 2011, pp. 268–273.
[66] B. Li, Y. Wang, H. K. Lee, A. Dempster, and C. Rizos, “Method for yielding a database of location fingerprints in WLAN,” *IEE Proc. - Commun.*, vol. 152, no. 5, p. 580, 2005.
[67] A. Jashua, Bardwell; Devin, *CWNA: Certified Wireless Network Administrator : Official Study Guide : (exam PWO-100)*. McGraw-Hill/Osborne, 2005.

[68] A. Chella, G. Lo~Re, I. Macaluso, M. Ortolani, and D. Peri, "A Networking Framework for Multi-Robot Coordination," *Recent Adv. Multi Robot Syst.*, no. May, pp. 1–14, 2008.
[69] Recommendation ITU-R P.1238-1, P. Data, P. Methods, F. O. R. The, P. Of, I. R. Systems, and R. L. Area, "Propagation Data And Prediction Methods for the Planning of Indoor Radiocommunication systems and Radio Local Area networks in the Frequency Range 900 MHz to 100 GHz," *Dermatol. Surg.*, vol. 39, no. 3 Pt 2, pp. I–III, 1999.
[70] S. Sen and B. Radunovic, "You are facing the mona lisa: spot localization using phy layer information," *Mobisys*, pp. 183–196, 2012.
[71] N. Marques, F. Meneses, and A. Moreira, "Combining similarity functions and majority rules for multi-building, multi-floor, WiFi positioning," *2012 Int. Conf. Indoor Position. Indoor Navig. IPIN 2012 - Conf. Proc.*, no. November, pp. 13–15, 2012.
[72] A. Bose and H. F. Chuan, "A practical path loss model for indoor WiFi positioning enhancement," *2007 6th Int. Conf. Information, Commun. Signal Process. ICICS*, pp. 0–4, 2007.
[73] T. S. Development, "Homedale::Wi-Fi/WLAN Monitor." [Online]. Available: http://www.the-sz.com/products/homedale/.
[74] D. C. Montgomery, *Design and Analysis of Experiments*. John Wiley & Sons, 2006.
[75] B. S. -, J. H. L. -, T. L. -, and H. S. K. -, "Enhanced Weighted K-Nearest Neighbor Algorithm for Indoor Wi-Fi Positioning Systems," *Int. J. Networked Comput. Adv. Inf. Manag.*, vol. 2, no. 2, pp. 15–21, 2012.
[76] S. Ali-Löytty, Tommi Perälä, V. Honkavirta, and R. Piché, "Fingerprint Kalman Filter in indoor positioning applications," *Proc. IEEE Int. Conf. Control Appl.*, vol. 1683, no. c, pp. 1678–1683, 2009.
[77] O. Costilla-reyes, "Dynamic Wi-Fi Fingerprinting Indoor Positioning System," no. October, 2014.
[78] N. Bhatia and C. Author, "Survey of Nearest Neighbor Techniques," *IJCSIS) Int. J. Comput. Sci. Inf. Secur.*, vol. 8, no. 2, pp. 302–305, 2010.
[79] M. Lee and D. Han, "Voronoi tessellation based interpolation method for Wi-Fi radio map construction," *IEEE Commun. Lett.*, vol. 16, no. 3, pp. 404–407, 2012.
[80] T. C. Tsai, C. L. Li, and T. M. Lin, "Reducing calibration effort for WLAN location and tracking system using segment technique," *Proc. - IEEE Int. Conf. Sens. Networks, Ubiquitous, Trust. Comput.*, vol. 2006 I, pp. 46–51, 2006.
[81] J. Krumm and J. Platt, "Minimizing Calibration Efforts for an Indoor 802.11 Device Location Measurement System," *Measurement*, pp. 1–9, 2003.
[82] W. Bong and Y. C. Kim, "Fingerprint Wi-Fi radio map interpolated by discontinuity preserving smoothing," *Lect. Notes Comput. Sci. (including Subser. Lect. Notes Artif. Intell. Lect. Notes Bioinformatics)*, vol. 7425 LNCS, no. 1, pp. 138–145, 2012.
[83] K. Arai and H. Tolle, "Color Radiomap Interpolation for Efficient Fingerprint WiFi-based Indoor Location Estimation," vol. 2, no. 3, pp. 10–15, 2013.
[84] S. S. Jan, S. J. Yeh, and Y. W. Liu, "Received signal strength database interpolation by Kriging for a Wi-Fi indoor positioning system," *Sensors (Switzerland)*, vol. 15, no. 9, pp. 21377–21393, 2015.
[85] C. Liu, A. Kiring, N. Salman, L. Mihaylova, and I. Esnaola, "A Kriging algorithm for location fingerprinting based on received signal strength," *2015 Work. Sens. Data Fusion Trends, Solut. Appl. SDF 2015*, 2015.
[86] J. Li and A. D. Heap, "A review of comparative studies of spatial interpolation methods in environmental sciences: Performance and impact factors," *Ecological Informatics*, vol. 6, no. 3–4. pp. 228–241, 2011.
[87] D. Shepard, "A two-dimensional interpolation function for irregularly-spaced data," *23rd ACM Natl. Conf.*, pp. 517–524, 1968.
[88] G. Matheron, "Principles of geostatistics," *Econ. Geol.*, vol. 58, no. 8, pp. 1246–1266, 1963.
[89] R. J. Renka, "Multivariate interpolation of large sets of scattered data," *ACM Trans. Math. Softw.*, vol. 14, no. 2, pp. 139–148, 1988.
[90] K. Basso, P. R. D. A. Zingano, and C. M. D. S. Freitas, "Interpolation of scattered data: investigating alternatives for the\nmodified Shepard method," *XII Brazilian Symp. Comput. Graph. Image Process. (Cat. No.PR00481)*, 1999.

[91] M. Angjelicinoski, V. Atanasovski, and L. Gavrilovska, “Comparative analysis of spatial interpolation methods for creating radio environment maps,” in *2011 19th Telecommunications Forum, TELFOR 2011 - Proceedings of Papers*, 2011, pp. 334–337.
[92] W. Schwanghart and N. J. Kuhn, “TopoToolbox: A set of Matlab functions for topographic analysis,” *Environ. Model. Softw.*, vol. 25, no. 6, pp. 770–781, 2010.
[93] J. Koo and H. Cha, “Localizing WiFi access points using signal strength,” *IEEE Commun. Lett.*, vol. 15, no. 2, pp. 187–189, 2011.
[94] J. A. Nelder and R. Mead, “A simplex-method for function minimization,” *Comput. J.*, vol. 7, no. 4, pp. 308–313, 1965.
[95] E. Mok and G. Retscher, “Location determination using WiFi fingerprinting versus WiFi trilateration,” *J. Locat. Based Serv.*, vol. 1, no. 2, pp. 145–159, 2007.
[96] R. E. Kalman, “A New Approach to Linear Filtering and Prediction Problems,” *J. Basic Eng.*, vol. 82, no. 1, p. 35, 1960.
[97] S.-H. Lee, I.-K. Lim, and J.-K. Lee, “Method for Improving Indoor Positioning Accuracy Using Extended Kalman Filter,” *Mob. Inf. Syst.*, vol. 2016, pp. 1–15, 2016.
[98] J. Yim, C. Park, J. Joo, and S. Jeong, “Extended Kalman Filter for wireless LAN based indoor positioning,” *Decis. Support Syst.*, vol. 45, no. 4, pp. 960–971, 2008.
[99] G. J. L. Naus, R. P. A. Vugts, J. Ploeg, M. J. G. Van De Molengraft, and M. Steinbuch, “Cooperative adaptive cruise control, design and experiments,” *2010 Am. Control Conf.*, vol. 1, no. 1, pp. 6145–6150, 2010.
[100] L. W. Yeh, M. S. Hsu, Y. F. Lee, and Y. C. Tseng, “Indoor localization: Automatically constructing today’s radio map by iRobot and RFIDs,” *Proc. IEEE Sensors*, pp. 1463–1466, 2009.
[101] G. Shen, Z. Chen, P. Zhang, T. Moscibroda, and Y. Zhang, “Walkie-markie: Indoor pathway mapping made easy,” *Proc. 10th USENIX Conf. Networked Syst. Des. Implement.*, pp. 85–98, 2013.
[102] J. Park, B. Charrow, D. Curtis, J. Battat, E. Minkov, J. Hicks, S. Teller, and J. Ledlie, “Growing an organic indoor location system,” *Proc. 8th Int. Conf. Mob. Syst. Appl. Serv. MobiSys 10*, no. June, p. 271, 2010.
[103] B. Wang, Q. Chen, L. T. Yang, and H. C. Chao, “Indoor smartphone localization via fingerprint crowdsourcing: Challenges and approaches,” *IEEE Wirel. Commun.*, vol. 23, no. 3, pp. 82–89, 2016.

List of Publications

Journals:

1. Abdul Halim Ismail, Ryosuke Tasaki, Hideo Kitagawa, and Kazuhiko Terashima, "*Optimum Placement of Wireless Access Point for Mobile Robot Positioning in an Indoor Environment*", Journal of Robotics and Mechatronic (JRM), Volume 28, No. 2, Pages 162-172, April 2016.
2. Abdul Halim Ismail, Yuki Mizushiri, Ryosuke Tasaki, Hideo Kitagawa, Takanori Miyoshi and Kazuhiko Terashima, "*A Novel Automated Construction Method of Signal Fingerprint Database for Mobile Robot Wireless Positioning System*", International Journal of Automation Technology (IJAT), May 2017.

International Refereed Conferences:

1. Ismail, A.H. and Terashima, K., "*Optimization of Wireless Nodes Placement for Mobile Robot Indoor Localization*", in Proceeding of International Conference on Advanced Technology in Experimental Mechanics (ATEM), October 4-8, 2015, Toyohashi, Japan.
2. T. Thewan, A.H. Ismail, M. Panya, and and K. Terashima, "*Assessment of WiFi RSS using Design of Experiment for Mobile Robot Wireless Positioning System*", ISIF/IEEE International Conference on Information Fusion (Fusion 2016), July 5-8, 2016, Heidelberg, Germany.
3. Abdul Halim Ismail, Ryosuke Tasaki, Hideo Kitagawa, and Kazuhiko Terashima, "*WiFi RSS Fingerprint Database Construction for Mobile Robot Indoor Positioning System*", IEEE International Conference on Systems, Man, and Cybernetics (SMC2016), October 9-12, 2016, Budapest, Hungary.

Poster Presentation:

1. Abdul Halim Ismail, Ryosuke Tasaki, Hideo Kitagawa, and Kazuhiko Terashima, "3.1 Wireless Positioning Framework for Mobile Robot", at 平成２７年度成果報告会　デモンストレーションの部, July 14th, 2016, 2F Human-Robot Symbiosis Center, Toyohashi University of Technology.

Appendix A **Map and Floor Plan**

The raw blueprint of the 2nd floor of Human-Robot Symbiosis Research Center, Toyohashi University of Technology, Japan

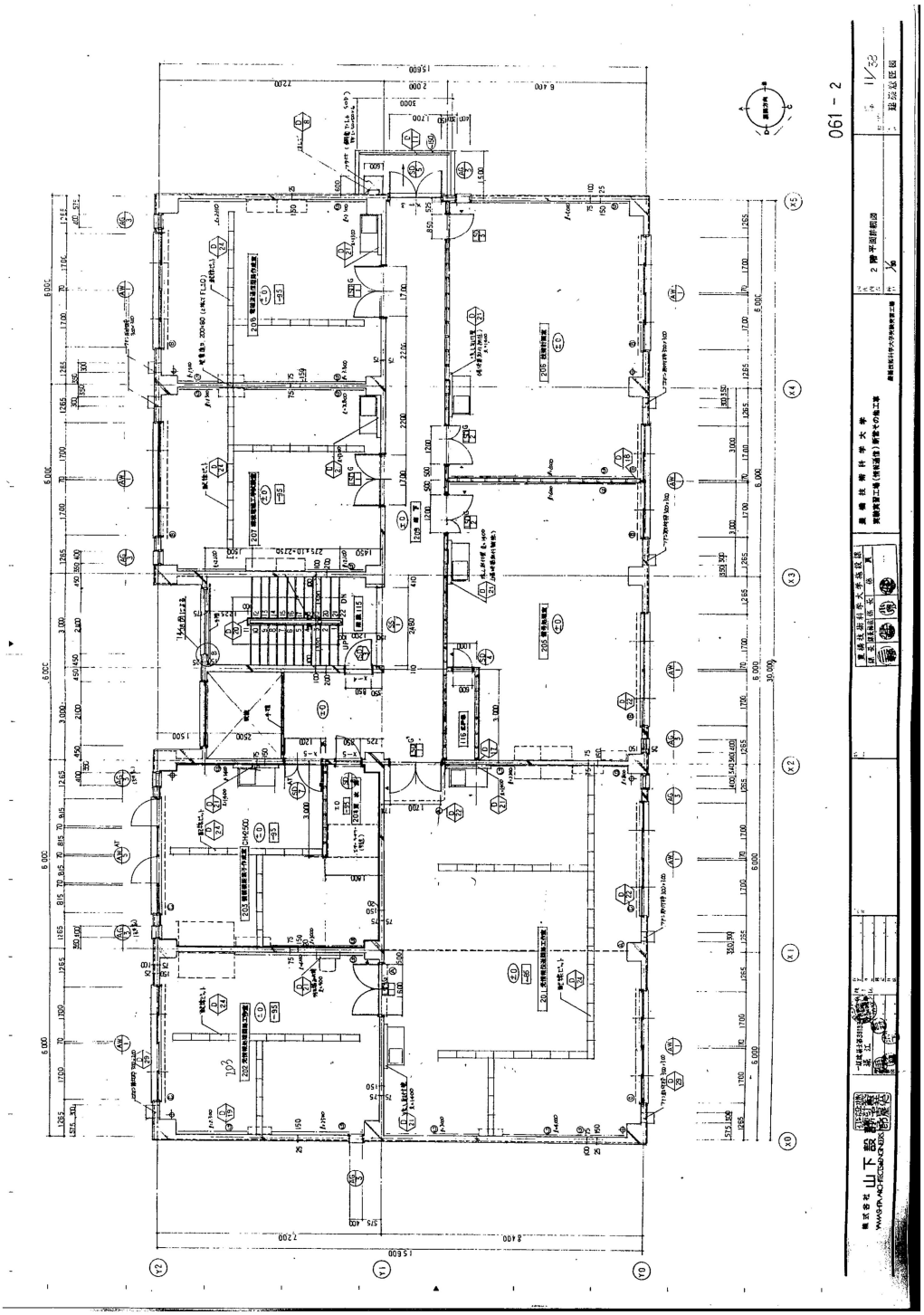

Appendix B **Mathematical Derivation**

B-1 Derivation of Free Space Path Loss Model and Its Unit

Consider the free space propagation model shown on the right to derive the free space path loss formula. Assuming that the transmitted power at the source as P_t whose gain in that particular direction is G_t, then the radiated power density at a given distance d is given by

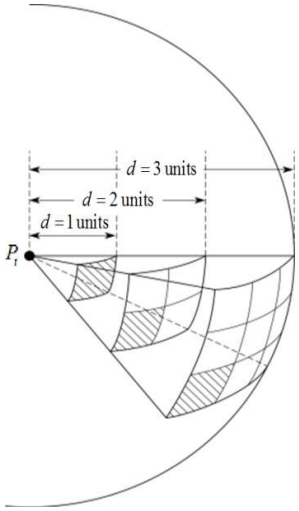

$$\rho = \frac{P_t G_t}{4\pi d^2} \text{ watts/m}^2.$$

If the receiving antenna located at the distance d, whose gain is G_r and the effective area is A, where

$$A = G_r \frac{\lambda^2}{4\pi},$$

then the received power P_r at the terminal of the received antenna is given as

$$P_r = \rho A = P_t G_t G_r \left(\frac{\lambda}{4\pi d}\right)^2.$$

In the above equation, the signal is found to attenuate per square of the distance. The path loss is the quantity measured by the ratio of the transmitted power to the received power. Assuming unity gain of both transmitter and receiver,

$$PL = \left(\frac{4\pi d}{\lambda}\right)^2.$$

Taking logarithmic function to the equation

$$PL(dB) = 10\log\left[\left(\frac{4\pi d}{\lambda}\right)^2\right], \text{ where } \lambda = {}^{c}\!/_{f}$$

Then it becomes

$$PL(dB) = 10\log\left[\left(\frac{4\pi d \cdot f}{c}\right)^2\right].$$

For d in meters, f in GigaHertz and $c = 3\times10^8$ ms^{-1}

$$\begin{aligned} PL(dB) &= 10\log\left[\left(\frac{4\pi d\cdot f\times1\times10^9}{3\times10^8}\right)^2\right] \\ &= 20\log(d)+20\log(f)+20\log\left(\frac{4\pi\times10}{3}\right) \\ &= 20\log(d)+20\log(f)+32.45 \end{aligned}$$

For d in meters and f in Herts

$$\begin{aligned} PL(dB) &= 10\log\left[\left(\frac{4\pi d\cdot f}{3\times10^8}\right)^2\right] \\ &= 20\log(d)+20\log(f)+20\log\left(\frac{4\pi}{3\times10^8}\right) \\ &= 20\log(d)+20\log(f)-147.55 \end{aligned}$$

For d in meters and f in KiloHerts

$$\begin{aligned} PL(dB) &= 10\log\left[\left(\frac{4\pi d\cdot f\times1\times10^3}{3\times10^8}\right)^2\right] \\ &= 20\log(d)+20\log(f)+20\log\left(\frac{4\pi}{3\times10^5}\right) \\ &= 20\log(d)+20\log(f)-87.55 \end{aligned}$$

And finally, for d in Kilometers and f in GigaHerts

$$\begin{aligned} PL(dB) &= 10\log\left[\left(\frac{4\pi d\cdot f\times1\times10^9}{3\times10^8}\right)^2\right] \\ &= 20\log(d)+20\log(f)+20\log\left(\frac{4\pi\times1\times10^9}{3\times10^5}\right) \\ &= 20\log(d)+20\log(f)+92.45 \end{aligned}$$

B-2 Derivation of Kriging Weight [85]

Under the intrinsic stationary assumption, a sufficient condition for unbiasedness can be given as

$$\sum_{i=1}^{k}\lambda_i - 1 = 0\,.$$

Taking the advantage of unbiasedness, the Kriging estimator error variance can be derived as

$$\begin{aligned}
&Var\left(\bar{z}_u^* - \bar{z}_u\right)\\
&= \mathbb{E}\left[\bar{z}_u^* - \bar{z}_u\right]^2 = \mathbb{E}\left[\sum_{i=1}^{k}\lambda_i\left(\bar{z}_i - \bar{z}_u\right)\right]^2\\
&= \sum_{i=1}^{k}\sum_{j=1}^{k}\lambda_i\lambda_j\cdot\frac{1}{2}\mathbb{E}\left[\bar{z}_i - \bar{z}_u\right]^2 + \sum_{i=1}^{k}\sum_{j=1}^{k}\lambda_i\lambda_j\cdot\frac{1}{2}\mathbb{E}\left[\bar{z}_j - \bar{z}_u\right]^2 - \sum_{i=1}^{k}\sum_{j=1}^{k}\lambda_i\lambda_j\cdot\frac{1}{2}\mathbb{E}\left[\bar{z}_i - \bar{z}_j\right]^2\\
&= 2\sum_{i=1}^{k}\lambda_i\gamma_{i,u} - \sum_{i=1}^{k}\sum_{j=1}^{k}\lambda_i\lambda_j\gamma_{i,u}
\end{aligned}$$

To minimize this expression, under the unbiasedness condition, the *Lagrange multiplier L* is introduced. Thus, the aim now is

$$\min_{\lambda_k\in\mathbb{R}} 2\sum_{i=1}^{k}\lambda_i\gamma_{i,j} - \sum_{i=1}^{k}\sum_{j=1}^{k}\lambda_i\lambda_j\gamma_{i,u} + 2L\cdot\left(1 - \sum_{i=1}^{k}\lambda_i\right).$$

The Kriging error variance can be differentiate with respect to a weight λ_i and let it equal to 0, that is

$$\sum_{j=1}^{k}\lambda_j\gamma_{i,j} + L = \gamma_{i,u}\,.$$

And so, the Kriging weights that minimize the error variance can be obtained by solving the equation set:

$$\begin{cases}
\sum_{j=1}^{k}\lambda_j\gamma_{i,j} + L = \gamma_{i,u}, \quad i = 1\ldots k\\
\sum_{i=1}^{k}\lambda_i = 1.
\end{cases}$$

which can be re-arranged in matric form,

$$\begin{pmatrix}
\gamma_{1,1} & \cdots & \gamma_{1,k} & 1\\
\vdots & \ddots & \vdots & 1\\
\gamma_{k,1} & \cdots & \gamma_{k,k} & \vdots\\
1 & \cdots & 1 & 0
\end{pmatrix}
\begin{pmatrix}
\lambda_1\\ \vdots\\ \lambda_k\\ L
\end{pmatrix}
=
\begin{pmatrix}
\gamma_{1,u}\\ \vdots\\ \gamma_{k,u}\\ 1
\end{pmatrix}.$$

Thus, the Kriging weights can be computed as,

$$\begin{pmatrix} \lambda_1 \\ \vdots \\ \lambda_k \\ L \end{pmatrix} = \begin{pmatrix} \gamma_{1,1} & \cdots & \gamma_{1,k} & 1 \\ \vdots & \ddots & \vdots & 1 \\ \gamma_{k,1} & \cdots & \gamma_{k,k} & \vdots \\ 1 & \cdots & 1 & 0 \end{pmatrix}^{-1} \begin{pmatrix} \gamma_{1,u} \\ \vdots \\ \gamma_{k,u} \\ 1 \end{pmatrix}.$$